Molecular mechanism of regulation of iron transport across placenta

Thesis submitted by

Rumeza Hanif

For the Degree of

Doctor of Philosophy in Biochemistry

Research Department of Structural and Molecular Biology

University College London

Gower Street, London, WC1E 6BT, UK

London

2011

Declaration

I, **Rumeza Hanif**, declare that all work presented in this thesis is the result of my own work. Where information has been derived from other sources, I confirm that this has been mentioned in the thesis. The work herein was carried out while I was a graduate student at the University College London, Research Department of Structural and Molecular Biology under the supervision of Professor Kaila Srai.

Abstract

During the third trimester of pregnancy, iron transport from mother to the foetus against a concentration gradient determines the iron endowment in foetal and neonatal life. Hfe functions as an upstream regulator of liver hepcidin which has been demonstrated to be a negative regulator of intestinal absorption of dietary iron and macrophage efflux of recycled iron. Hepcidin has also been proposed to be a negative regulator of iron efflux from the placenta, however it is not known if hepcidin is of maternal or foetal origin during pregnancy. The exact mechanism and molecules involved in the regulation of iron transport across the placenta are not well understood.

In this study the effects of *Hfe* and dietary iron levels on transfer of iron from mother to foetus was investigated in order to determine the importance of maternal and foetal *Hfe* status on iron transport. The effect of maternal hepcidin on placental iron transport in WT and *Hfe* KO dams was also studied. The molecular mechanism of iron transport across placenta was elucidated by using BeWo cells as a model for iron uptake, transport and efflux.

This study has shown that the mechanism regulating iron metabolism during pregnancy is dependent on the iron status of the mother and its genotype. A clear link could be seen between the maternal iron status and foetal body iron stores. The lack of *Hfe* in both dams and pups increased iron absorption in the body and raised serum iron levels but the effect of *Hfe* was diet dependent.

However, foetal genotype seems to affect liver iron accumulation and certain iron transporter gene expression only with low and normal iron diets.

In this study BeWo cells were utilised to model the placental syncytiotrophoblasts. The insensitivity of iron transporter proteins in BeWo cells to hepcidin treatment might be due to the cell-specific response of hepcidin. TfR1, DMT1 and FPN1 were localised in these cells to understand the molecular mechanism of iron transport across placenta. Finally, the presence of ZIP14 and its response to hepcidin treatment in mice may indicate the presence of an alternative pathway of iron transport across placenta.

To

My parents, Eman and Eshaal

Acknowledgements

''There is nothing like returning to a place that remains unchanged to find the ways in which you yourself have altered''. Nelson Mandela

I am deeply grateful to my supervisor, Professor Kaila Srai Singh for his detailed review, constructive criticism and excellent advice during the preparation of this thesis. I have also learned silence from his talkative nature.

I offer my regards and blessings to all the members of our research group who supported me in any respect during the completion of this project. In particular, I would like to thank Dr. Sara Balesaria for helping me in the laboratory and providing me with mice tissue samples, Dr. Henry Bayele and Dr. Mohammad Salama for their wise advice, moral support and good company during PhD. I am grateful to Dr. Vernon Skinner for his help in the laboratory. I would also like to thank Dr. Mina Edwards for her help in the tissue culture facility and Dr. Maud Dumoux for teaching me immunostaining and confocal microscopy.

How can I forget my lovely and lively friends in the department who became my extended family. Depali, Qing, Helene, Marillia, Nazia and Batoul are worth mentioning who kept reminding me about the existence of real, colourful

and attractive universe outside the world of PCR and western blotting. Together we laughed, cried and ate a lot during these four years.

I owe my loving thanks to my brother Dr. Wasib Hanif and his wife Wajeeha for giving us two beautiful daughters who have filled our world with joy and beauty.

Lastly, and most importantly, I wish to thank my dear parents, Mrs. Fozia Rana and Dr. Khalid Hanif. They bore me, raised me, supported me, taught me, missed me and loved me. To them I dedicate this thesis.

Contents

14

List of Figures

List of Tables

Abbreviations

µM	Micro mole
BeWo	Human choriocarcinoma cells
Ca^{2+}	Calcium ion
Cd^{2+}	Cadmium ion
Co^{2+}	Cobalt ion
Cp	Ceruloplasmin
C-terminal	Carboxy terminal
Cu^{2+}	Copper ion
cDNA	Complementary deoxyribo nucleic acid
DCT1	Divalent cation transporter 1
Dcytb	Duodenal cytochrome b
DEPC	Diethylpyrocarbonate
DFO	Desferrioxamine
DMEM	Dulbecco's Minimal Essential Medium
DMSO	Dimethylsulphoxide
DMT1	Divalent metal transporter 1
DMT1+IRE	Divalent metal transporter 1 with an iron responsive element
DMT1-IRE	Divalent metal transporter 1 without an iron responsive element
DNA	Deoxyribo nucleic acid
DPBS	Dulbecco's Phosphate Buffer Saline
DTT	Dithiothreitol
FACs	Fluorescence activated cell sorting
FBS	Foetal bovine serum
Fe	Iron
Fe^{2+}	Ferrous iron
Fe^{3+}	Ferric iron
Fe-NTA	Ferric nitriloacetic acid
FPN1	Ferroportin 1
g	Gram
GFP	Green Fluorescent Protein
HAMP	The hepcidin gene
HCl	Hydrochloric acid
HCP1	Haem Carrier Protein-1

HEK 293	Human embryonic kidney cells
Heph	Hephaestin
HET	Heterozygote
HFE	Haemochromatosis protein
Hfe **KO**	*Hfe* knockouts
Hfe	HFE mouse gene
HFE	HFE human gene
H-Ferritin	Heavy chain ferritin
HO	Haem oxygenase
HRP-1	Rat labyrinth syncytial cells
IRE	Iron-responsive element
IREG1	Iron regulated gene 1
kDa	Kilo Dalton
L	Litre
LEAP-1	Liver expressed Antimicrobial Peptide-1
LZT	LIV-1 subfamily of ZIP zinc transporters
M	Molar
MCF	Multicopper ferroxidases
MHC	Major histocompatibility complex
min	Minute
ml	Millilitre
mRNA	Messenger ribonucleic acid
MTP1	Metal transporter 1
Ni^{2+}	Nickel ion
Nramp2	Natural resistance associated macrophage protein 2
NTBI	Non-tranferrin bound iron
N-terminal	Amino terminal
PAGE	Polyacrylamide gel electrophoresis
PVDF	Polyvinylidene Fluoride
R$_{true\ cell}$	True cell monolayer resistance
R$_{blank}$	Blank reading/ resistance
Rch0-1	Rat trophoblastic Giant cells
RIPA buffer	Radioimmunoprecipitation assay buffer
RNA	Ribonucleic acid
rpm	Revolution per minute
R$_{total}$	Total resistance reading
RT-PCR	Real time-polymerase chain reaction

SDS	Sodium dodecyl sulphate
SEM	Standard error of mean
SLC40A1	Solute carrier family 40 (iron-regulated transporters), membrane 1
STEAP3	Six-transmembrane epithelial antigen of prostate protein 3
TEER	Transepithelial electrical resistance measurements
Tf	Transferrin
TfR1	Transferrin receptor 1
TfR2	Transferrin receptor 2
TFS	Transferrin saturation
v/v	Volume by volume
WT	Wild type
ZIP14	Zrt-, Irt-like proteins 14
Zp	Zyklopen
ZO	Zonula Occludin

Chapter 1

General Introduction

1.1 Biological importance of iron

Iron serves as an important catalytic centre in many enzymes as either nonhaem iron-containing proteins or haemoproteins, which makes it crucial for life. Haemoproteins are involved in wide ranging biological functions, including oxygen binding (haemoglobins), electron transfer such as the electron transport chain of mitochondria (cytochromes), and oxygen metabolism (oxidases, peroxidases, catalases, etc.) (Winfield 1965). Nonhaem iron-containing proteins like mitochondrial aconitase and iron-sulphur proteins of the electron transport chain are involved in energy metabolism (Jordanov et al. 1992), whereas ribonucleotide reductase is vital for DNA synthesis (Uppsten et al. 2004). Iron-containing proteins are also required for the metabolism of catecholamines, collagen, and tyrosine.

Iron exists in solution in two oxidative states, ferrous (Fe^{2+}) and ferric form (Fe^{3+}), which can donate and accept electrons, respectively. In order to prevent these redox reactions becoming hazardous for the organism, iron must be either bound to protein or kept in the trivalent redox state (McCord 1998). Therefore absorption, concentration, and the redox state of iron must be carefully regulated to supply the appropriate amount of iron for growth and survival while preventing iron deficiency or iron excess.

1.2 Distribution of iron in the body

A normal adult male (70 kg) has a total body iron of about 4 grams, which remains almost constant throughout adult life. Iron homeostasis in the body is largely maintained by regulation of its absorption in the duodenum. After absorption, it enters the circulation by binding to a serum protein, transferrin. About 2.5 g of iron circulates in the red blood cells as haemoglobin which is formed in bone marrow. A large part of iron is conserved by recycling from haemoglobin of aged erythrocytes by reticuloendothelial macrophages. Liver predominantly stores about 1 g of excess iron in the parenchymal tissue as ferritin and hemosiderin. Approximately 0.3 g is integrated into respiratory enzymes and myoglobin. 1 to 2 mg of iron is lost daily from an adult due to minor bleeding, exfoliation of iron-containing epithelium of skin, gastrointestinal, and urinary tract (Figure 1.1). However, women during childbearing years, lose twice that amount due to menstruation and childbirth. Therefore, to maintain normal iron balance in the body the same amount of iron from dietary sources is required to replace the lost (Bothwell et al. 1979; Crichton 1991; Conrad and Umbreith 2002).

1-2 mg per day absorbed in duodenum

Duodenum

RBCs 2300 mg

Serum Transferrin 3 mg

Bone marrow 300 mg

Muscle Myoglobin 300 mg

Reticuloendothelial macrophages 600 mg

Storage in Liver 1000 mg

1-2 mg per day of iron loss Desquamation Menstruation Minor blood loss
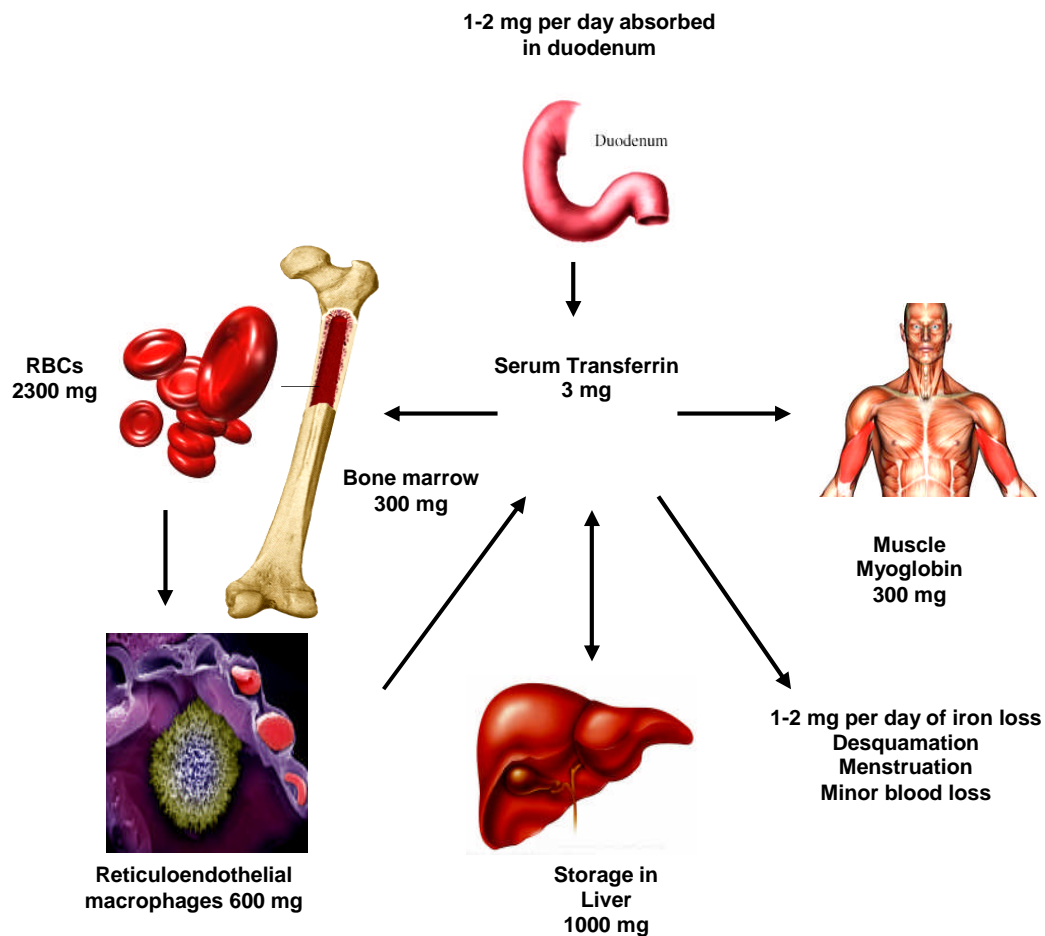
Figure 1.1 Schematic diagram showing iron distribution in the body

Iron is absorbed by the duodenum and enters the circulatory system by binding to transferrin. Iron is incorporated into haemoglobin after being taken up by the bone marrow and is recycled during the apoptosis of red blood cells by reticuloendothelial macrophages. Myoglobin and various enzymes also utilise small amounts of iron for their synthesis. Liver predominantly stores excess iron in the parenchymal tissues. 1-2 mg of iron is lost due to exfoliation of the epithelial lining of the gastrointestinal and urinary tract, hair and skin and blood loss during menstruation. The human body does not posses the physiological mechanism to excrete excess iron. Modified from Andrews, 1999.

1.3 Iron absorption, transport and storage

Iron homeostasis in the body is primarily maintained by duodenal iron uptake depending on iron stores and its bodily requirements (Hallberg et al. 1997). Dietary iron is present mostly in the Fe^{3+} form which is biologically unavailable. This iron is reduced to Fe^{2+} before entering the duodenal enterocytes through Divalent Metal Transporter 1 (DMT1) by the action of either reducing agents (ascorbic acid, cysteine and histidine) or Duodenal cytochrome b (Dcytb) (Andrew 1999; Mckie et al. 2001). Haem, present in diets from animal sources, contributes about 30% of the total iron absorbed by the body. Haem is carried into the cytosol of enterocytes through Haem Carrier Protein-1 (HCP1) and is broken down by haem oxygenase (HO), subsequently liberating Fe^{2+} and bilirubin (reviewed by Sharp and Srai 2007).

Iron is effluxed from the duodenal enterocytes into the circulation via ferroportin 1 (FPN1) and immediately oxidised to Fe^{3+} catalysed by either hephaestin in the gut or ceruloplasmin in the plasma. Iron efflux is mainly a passive transport against a concentration gradient (McGregor, 2006). In the circulation, iron is bound to serum protein transferrin (Tf). In normal conditions, Tf is about 30% iron-saturated and has a high iron-binding capacity to overcome damage caused by the accumulation of non-Tf-bound iron (NTBI). However, in some iron overload disorders like hereditary hemochromatosis, plasma iron levels exceed Tf saturation capacity which results in high NTBI levels in plasma and hepatic iron loading. The exact chemical nature of NTBI and its mechanism of uptake by the cells are not known but ZIP14, a zinc transporter, is believed to be involved in NTBI uptake (Liuzzi et al. 2006).

Hepatocytes, developing erythroids, reticuloendothelial macrophages and placental syncytiotrophoblasts acquire iron from plasma Tf. Diferric-Tf binds to transferrin receptor (TfR) at the surface of these cells. This complex is internalised via clathrin-coated pits to endosomes where iron is dissociated from Tf in an acidic environment (Van Eijk & de Jong 1992). Iron is released into the cytosol after reduction by probably six-transmembrane epithelial antigen of prostate protein 3 (STEAP3) and transport by DMT1 present on endosomal membranes. There are indications of alternative pathways of iron transport from endosomes as it has been demonstrated that *DMT1* knock out (KO) mice can transport iron across placenta (Gunshin et al. 2005). Some evidence has been found for the involvement of zinc and calcium transporters in iron transport (Luizzi et al. 2006; Oudit et al. 2006), although the role of calcium transporters is controversial (Ludwiczek et al. 2007; Mackenzie et al. 2010). Excess iron is stored in ferritin, a storage protein, in the form of Fe^{3+}.

To maintain the plasma iron range of 10 to 30 µM, iron is effluxed into the circulation via FPN1. The expression of FPN1 is confined to cells with a specific iron efflux function i.e. placental syncytiotrophoblasts, duodenum, macrophages, hepatocytes and brain endothelial cells (Rouault & Cooperman 2006). The systemic iron uptake, transport and storage are shown in Figure 1.2.
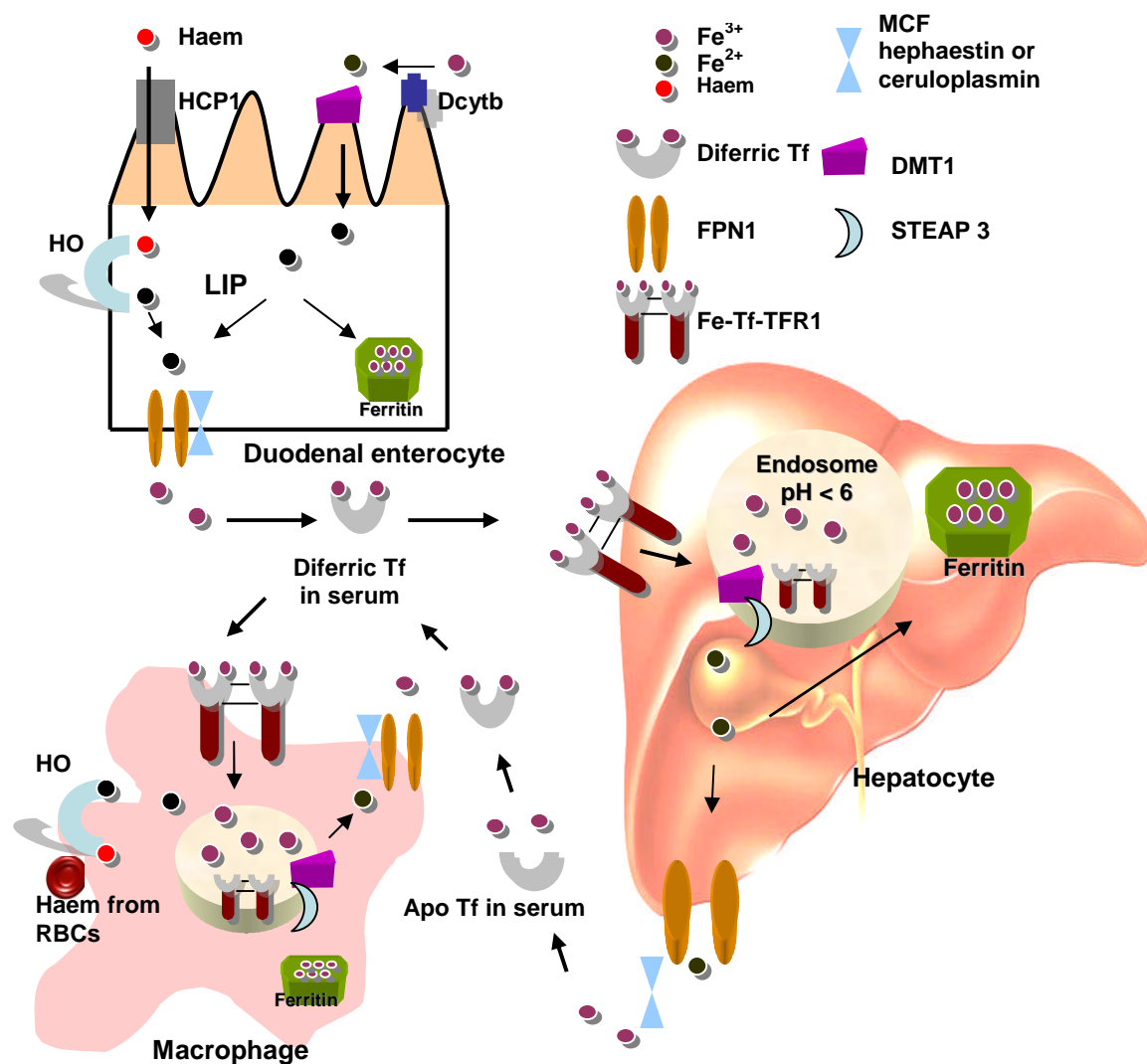
Figure 1.2 Schematic diagram showing systemic iron uptake, transport and storage

Dcytb present on the brush border membrane of duodenal enterocytes reduces iron before it enters the cells via DMT1. In an alternative pathway iron as haem is taken up by HCP1 transporter. Iron from both pathways enters the Labile Iron Pool (LIP) from where the excess iron is stored in ferritin and the remainder is effluxed into the circulation by the iron exporter FPN1 after oxidation by a MCF. Serum iron is bound to Tf which is responsible for delivering iron to various tissues including hepatocytes (major site of iron storage) and macrophages. Reticuloendothelial cells also take up iron by engulfing senescent RBCs and breaking down haemoglobin to release iron into the circulation or for storage in ferritin.

1.4 Proteins involved in iron absorption, transport and storage

1.4.1 Transferrin

Transferrin (Tf) is a 76-80 kDa plasma glycoprotein that is responsible for the transport of iron to and from various cells throughout the body (Ponka et al., 1998). Each of the two homologous lobes of Tf (one on the amino-terminal domain and the other on the carboxy-terminal domain) contains a high affinity Fe^{3+}-binding site. Diferric-Tf (also called holo-Tf) is taken up by many cells for example liver, macrophages and placenta (Trinder et al. 1986; McArdle et al. 1985)

The affinity of iron for Tf is a pH-dependent process. In plasma, where the pH is approximately 7.4, Tf binds iron very strongly, whereas virtually no binding occurs at $pH \leq 4.5$. This pH-dependent property plays an important role in the physiological mechanism of release of iron from Tf (Anderson et al. 1989).

One of the functions of Tf is to direct iron to the cells (macrophages, hepatocytes and placental syncytiotrophoblasts) that express transferrin receptor and another function is to bind iron released from the cells thus minimizing the amount of free iron in plasma and reducing the possibility of toxic oxygen radical formation. Tf production increases with iron deficiency and decreases with iron loading (McKnight et al. 1980).

1.4.2 Transferrin receptors

Tf is recognized by specific cell membrane receptors that act as gatekeepers responsible for physiological iron uptake by most cell types (Richardson and Ponka, 1997). In addition to maintaining normal homeostasis in the body, these molecules are required to sense iron concentration and communicate with the circuitry that controls the production of hepcidin (negative iron regulatory hormone). Transferrin receptor 1 (TfR1) and transferrin receptor 2 (TfR2) are the two iron sensor proteins, which are expected to sense the extracellular concentration of holo-Tf by conventional mechanisms dependent on receptor occupancy.

1.4.2.1 TfR1

TfR1 is a 180 kDa disulphide-linked transmembrane glycoprotein homodimer with each subunit (90kDa) binding one molecule of Tf (Kanevsky et al. 1997). The binding affinity of TfR1 to diferric-Tf is 10-fold higher than monoferric-Tf and 2000-fold higher than Apo-Tf (Tf without iron) at pH 7.4 (Watkins et al. 1992). The interaction of haemochromatosis-related protein, HFE with TfR1 decreases the affinity of TfR1 for Tf (Feder et al. 1998). There is a possibility that TfR1 could function as an iron sensor (rather than a Tf uptake protein) within a protein complex that includes HFE. Schmidt et al. (2008) recently demonstrated the importance of the TfR1-HFE interaction for iron regulation by introducing mutations into mice to strengthen or weaken the interaction between HFE and TfR1. A mutation that caused an increase in HFE binding to TfR1 resulted in hepcidin deficiency and iron overload. On the other hand mice

with a mutation that interferes with the TfR1-HFE interaction or mice with higher HFE content had high hepcidin and iron deficiency (Schmidt et al. 2008).

1.4.2.2 TfR2

TfR2 codes for at least 2 alternatively spliced transcripts: the alpha (α) form approximately 2.9 kbp long (AF067864) and the beta (β) form, approximately 2.5 kbp long (AF053356). TfR2-α is a type II transmembrane protein with high similarity to TfR1. TfR2-β lacks the amino terminal portion, which includes the putative transmembrane domain and part of the extracellular domain. It is therefore thought to be an intracellular form of receptor. The putative extracellular domain of the TfR2-α protein is highly homologous to TfR1 and is able to bind Tf and mediate iron uptake, although the binding affinity of holo-Tf is lower for TfR2 than TfR1 (Kawabata et al. 1999).

An interaction between HFE and TfR2 has also been found (Chen et al. 2007) but unlike the TfR1-HFE interaction, both Tf and HFE stabilise TfR2 (Johnson and Enns, 2004). Few studies have shown iron overload caused by deficiency of TfR2 in mice and humans (Fleming et al. 2002; Wallace et al. 2005). Also, tissue specific ablation of TfR2 in liver resulted in iron overload (Wallace et al. 2007). TfR2 deficiency seems to regulate systemic iron by decreasing hepcidin levels in mice (Kawabata et al. 2005; Wallace et al. 2005) and humans (Nemeth et al. 2005).

1.4.3 Divalent metal transporter 1

Ferrous iron, after reduction by Dcytb (a 286 amino acid protein with six transmembrane domains providing binding sites for ascorbate and dehydroascorbic acid which helps in reduction of ferric iron), is transported across the duodenal brush border membrane by the divalent metal transporter 1 also known as natural resistance-associated macrophage protein 2 (Nramp2), divalent cation transporter 1 (DCT1), and solute carrier family 11 membrane 2 (SLC11A2). DMT1 is a mammalian transmembrane proton-coupled metal-ion transporter which mediates the transport of various divalent metal ions including Fe^{2+}, Cd^{2+}, Co^{2+}, Ni^{2+}, Cu^{2+}, and Ca^{2+} but with its highest affinity for iron (Gunshin et al. 1997).

Studies in Belgrade rats and microcytic mice (Fleming et al. 1997, 1998) together with the ectopic expression studies (Griffiths et al. 2001) demonstrated that DMT1 plays a vital role in intestinal iron uptake and endosomal iron transport. The discovery of a DMT1 mRNA isoform with an iron-responsive element (IRE) in the 3' untranslated region accounts for its ability to maintain iron homeostasis through regulation of its expression level in response to dietary iron status, whereas the DMT1-IRE isoform, which lacks the IRE domain, lacks this function (Lee et al. 1998). DMT1+IRE and DMT1-IRE differ in their last C-terminal 18 or 25 amino acids and are found to have distinct subcellular localisation and differential cell type specificity in the adult human (Tabuchi et al. 2000). DMT1+IRE is predominantly expressed in epithelial cells of duodenum that suggests its role as apical iron transporter while the

expression of DMT1-IRE in erythroid precursor cells suggests that it is an endosomal iron transporter.

1.4.4 ZIP14

In certain physiological conditions like hereditary haemochromatosis, iron overload causes increased transferrin saturation (TFS) resulting in increased non-Tf-bound iron (NTBI) in serum which is believed to be taken up by a transmembrane protein, ZIP14 in hepatocytes (Gao et al. 2008; Liuzzi et al. 2006). Zrt-, Irt-like proteins (ZIP) are a group of protein transporters involved in bio-metal transport into the cytosol of various cells. Mostly they are responsible for zinc transport (Vallee and Falchuk 1993). Zinc transporters are divided into four subfamilies, I, II, Gufa and LIV-1 (Liuzzi and Cousins 2004; Taylor and Nicholson 2003). LIV-1 subfamily constitutes of members called LZT (LIV-1 subfamily of ZIP zinc transporters) which are part of solute carrier family 39 (slc39A) and are transmembrane proteins. It has been found that HFE decreased ZIP14 levels in HepG 2 cells which resulted in less NTBI uptake (Gao et al. 2008). The localisation of ZIP14 in iron transporter cells is not known. There is a possibility of its involvement in alternative pathways of iron uptake in cells as mice, in the absence of *DMT1,* were capable of transporting iron to their foetus (Gunshin et al. 2005).

1.4.5 Ferritin

Excess iron in the cytoplasm of cells is stored as ferritin, which is a ubiquitous protein. Mammalian ferritin can accommodate up to 4500 atoms of iron in its protein shell's internal cavity. The protein shell has a molecular mass between 430 and 460 kDa and has 24 symmetrically related subunits of two types: a light subunit (L-subunit) of approximately 19 kDa and a heavy subunit (H-subunit) of approximately 21 kDa. The entry and exit of iron may occur via channels in the protein shell. Inside the protein shell, iron is stored in the ferric oxyhydroxide phosphate of approximate composition $(FeOOH)_8$ $(FeO-OPO_3H_2)$ (Theil 1987; Harrison and Arosio, 1996). The origin and possible physiological roles of ferritin other than iron storage in the body remain indefinable.

1.4.6 Ferroportin 1

Ferroportin 1 (FPN1), a 571 amino acid membrane protein, is also known as metal transporter 1 (MTP1), iron regulated gene 1 (IREG1), solute carrier family 40 (iron-regulated transporters), membrane 1 (SLC40A1), and solute carrier family 11 (proton coupled divalent metal ion transporters), membrane 3 (SLC11A3). FPN1 has a cytoplasmic amino acid membrane terminus and 10 to 12 transmembrane domains (Abboud and Haile 2000; McKie et al. 2000; Donovan et al. 2000).

FPN1 is an iron exporter present on the basal membrane of absorptive intestinal enterocytes, hepatocytes, macrophages, and placental cells, all of which release iron into plasma (Abboud and Haile 2000; McKie et al. 2000; Donovan et al. 2000). FPN1 as an iron exporter was proved by making it

inactive in mice embryos which resulted in anaemic newborns with high iron accumulation in duodenal enterocytes, hepatocytes and macrophages (Donovan et al. 2005). This finding that FPN loss leads to severe anaemia in newborn mice confirms its important role in placental iron transport.

FPN1 internalisation via tyrosine phosphorylation followed by ubiquitination and degradation is regulated by hepcidin (Nemeth et al. 2004; De Domenico et al. 2007). Cellular iron levels also regulate FPN1 mRNA and protein expression. Changes in FPN1 expression are mediated by transcriptional and translational mechanisms. Translational regulation involves a 5' iron regulatory element (IRE) located in FPN1 mRNA (Liu et al. 2002).

1.4.7 Multicopper ferroxidases

Ceruloplasmin (Cp), Hephaestin (Heph) and the newly identified Zyklopen (Zp) are multicopper ferroxidases (MCF) (Kosman 2002; Vulpe et al. 1999; Chen et al. 2010). These MCFs are believed to be involved in maintaining iron homeostasis by oxidising it to the Fe^{3+} form, the latter is taken up by Tf as described in Section 1.4.1 (Kosman 2002; Anderson and Vulpe 2009).

An absence of Cp, has shown decreased cellular iron efflux via degradation of FPN1 in some cells (De Domenico et al. 2007). Duodenal enterocytes express Heph and its mutation has resulted in more iron accumulation in duodenum and an anaemic body (Vulpe et al. 1999). Liver predominantly produces Cp, which is a serum protein and its mutation has caused higher iron accumulation in multiple tissues leading to serious consequences (Harris et al. 1999). These

findings have confirmed the importance of MCFs in the regulation of iron transport. A recent study has proposed the presence of a novel MCF in placenta, which is structurally similar to Heph, called ZP (Chen et al. 2010). Its presence in other tissues is not known.

1.5 Iron homeostasis during pregnancy

During pregnancy duodenal iron absorption increases to compensate for the increase in foetal iron accumulation (Whittaker et al. 1991). Iron deficiency anaemia during pregnancy is one of the major causes of mortality and morbidity in pregnant women taking the lives of about half a million women each year (WHO 1991; 1992). Low maternal iron status also results in increased still births, preterm delivery, low birth weight babies, severe foetal growth retardation, long term problems including increase in blood pressure (Crowe et al. 1995), supressed immune system development (Luckwood & Sherman 1988) and diminished brain function (Soewondo 1995).

The World Health Assembly passed a resolution in 1992 urging its 90 member countries to adopt measures against iron deficiency in pregnant women by providing iron supplementations. It is surprising that sometimes these supplementations cannot overcome deficiency. A newborn infant derives 250 mg of iron from maternal iron stores via the placenta (Conrad & Umbreit 2002). During pregnancy, about 1 g of iron is lost from the mother due to expansion in maternal blood volume and transport of the metal to the foetus. The amount of iron transferred across placenta increases as gestation progresses but how this is mediated is unknown. At first, the placenta was thought to be responsible for

iron regulation during pregnancy but recent data suggested that this is a complex mechanism which might involve foetal and maternal livers. HFE and hepcidin are thought to be the central iron regulatory proteins involved in body iron homeostasis.

1.5.1 Placenta and its functions

The intimate relationship between the embryo and mother is one of the most important features of human embryonic development. During intrauterine life the survival and growth of the fertilised egg depends on the mother. The placenta surrounds the embryo and serves as the interface between the embryo and mother. The major role of the placenta is to provide nutrients and oxygen to the foetus and to eliminate foetal waste products and carbon dioxide. It synthesises and secretes hormones, growth factors, cytokines, and other bioactive molecules. It also protects the foetus against pathogens and forms an immunological barrier between mother and foetus (Pepe and Albrecht, 1995; Schneider 1991). For maintaining pregnancy and promoting normal foetal development, these comprehensive activities are essential.

1.5.2 Anatomy of the placenta

The placenta, a foetomaternal organ, consists of a foetal and a maternal part. A foetal portion develops from the chorionic sac. The chorionic sac constitutes the outermost foetal membrane in the human embryo and its villous part makes the foetal portion. On the other hand the maternal portion is derived from the endometrium, which makes the lining of the uterus. The cytotrophoblastic shell, an external layer of foetally derived trophoblastic cells, attaches the foetal and maternal portion of the placenta (Moore and Persaud 1998).

Until 20 weeks of pregnancy, the placental membrane consists of four layers: syncytiotrophoblasts, cytotrophoblasts, connective tissue of villus, and endothelium of foetal capillaries. After 20 weeks, due to histological changes, cytotrophoblast cells start disappearing over large areas of villi and leaves syncytiotrophoblasts in thin patches. At this stage the placenta consists of three layers instead of four. The placental membrane becomes markedly thin in some areas as the pregnancy progresses and syncytiotrophoblasts come in direct contact with foetal capillaries forming the vasculosyncytial placental membrane. Most of the nutrients and gases are transported from maternal serum to foetal serum through the placental membrane (Moore and Persaud 1998).

1.5.3 Comparison between human and mouse pregnancy and placentation

Established laboratory rodents such as mice, rats and rabbits have the advantage of short gestation times during pregnancy and large litters. Human and mice placental structure and pregnancy have some similar features. In mouse placenta, many cell types are analogous to those in human placenta, for example proliferating trophoblastic cells, invasive trophoblasts and cells differentiating into syncytium (Rossant and Cross 2001). Haemochorial plancenta, where maternal serum directly irrigates the foeto-placental epithelium, is common in both (Rossant and Cross 2001). A further comparison is shown in Table 1.1, taken from Carter, 2007.

Table 1.1 Comparison of human and mouse pregnancy and placentation

	Mouse	Human
Gestation	Three weeks	Nine months
Implantation	Secondarily interstitial	Primarily interstitial
Yolk sac	Inverted yolk sac placenta functions to term	Yolk sac floats free in exocoelom during first trimester
Trophoblast invasion of uterine arteries	Shallow; limited to proximal decidua	Extensive; reaching myometrial vessels
Transformation of uterine arteries	Dependent on maternal factors (uterine natural killer cells)	Dependent on trophoblast
Placental exchange area	Labyrinthine	Villous
Interhaemal barrier	Three trophoblast layers; outer one cellular, inner two syncytial	Single layer of syncytial trophoblast
Placental hormones	Placental lactogens	Chorionic gonadotropin, placental growth hormone; major source of progesterone

Taken from Carter (2007)

1.5.4 BeWo cells

To study the cellular activities and transplacental transport processes BeWo cells serve as a valid and convenient system (Taylor et al. 1991). The BeWo cell line originated from a human choriocarcinoma, a monolayer-forming trophoblast cell line with the capacity to differentiate into a syncytium (Pattillo & Gey 1968) and can be grown on filters for studying transport of iron *in vitro*. These cells differ from other polarized epithelia in that they mediate unidirectional iron transport in an apical to basal (i.e. maternal to foetal) direction via Tf and TfR1 at the apical membrane (Turkewitz & Harrison 1989).

These cells secrete placental hormones, including gonadotrophin, lactogen and steroid hormones (Cerneus & Van der 1991). These cells have been used previously as an *in vitro* model to study glucose ((Vandhana & Illsley 2002), amino acids (Eaton & Sooranna 1998; 2000) and iron (Danzeisen & McArdle 1998; Van der Ende et al. 1987) transport across placenta.

1.6 Mechanism of iron transport across placenta

Buus and Boockfor in 2004 investigated the production of TfR by several placental cell lines, Rch0-1 (rat trophoblastic Giant cells), HRP-1 (rat labyrinth syncytial cells), and BeWo cells. In species with a haemochorial placenta, it has been demonstrated that maternal iron attached to Tf binds TfR1 on the brush border membrane of the placenta which is then internalised in endosomes within the cell. Iron is subsequently released from Tf in the endosome and enters the cytoplasm while Tf and TfR1 are recycled back to the cell surface, which means Tf does not cross the multiple cell layer barrier of the placenta (McArdle et al. 1985). TfR1 is expressed more on syncytiotrophoblasts (STB) than on cytotrophoblasts. It has been localised on both the apical and basal membranes of the STB (Vanderpuye et al. 1986) but its role on the basolateral surface is not known.

HFE is also expressed in coated pits on the apical side of syncytiotrophoblasts where it is believed that it forms a complex with TfR1 and β-2-microglobulin (Parkkila et al. 1997). Contrary to this, Bastin et al. in 2006 found HFE on some parts of the basal membrane of syncytiotrophoblasts in large amounts where

FPN1 protein is strongly expressed. There is very little data on the role of HFE and hepcidin in the regulation of iron transport across the placenta.

In placental tissue, DMT1 is perceived to take part in the traffic of divalent metal ions. In human placenta at birth, DMT1 has been shown immunohistochemically to localise to the cytoplasm and basal membrane of syncytiotrophoblasts, which led to the supposition that the transport of ferrous iron from endosome to the cytoplasm, as well as across the basal membrane, is mediated by DMT1 (Georgieff et al. 2000). Gunshin et al. (2005) demonstrated that DMT1 is not essential to deliver iron to the foetus. They showed that *DMT1* KO mice were born anaemic but the total iron content in the new born pups was similar to WT. They also demonstrated that the liver in the *DMT1* KO mice had higher levels of iron than WT mice. This strongly suggests that alternative pathways of iron transfer exist in the placenta. By contrast, following birth, the *DMT1* KO mice died of iron deficiency quite rapidly, demonstrating that the protein is essential for iron absorption across gut. Whether and how it is involved in the placenta is unclear and also information regarding DMT1 expression in the placenta during early pregnancy is lacking. The proposed model of iron transport by syncytiotrophoblast is shown in Figure 1.3.

Although the proteins involved in transport of iron across the placenta have been identified, the mechanism and regulation of iron transport in response to iron deficiency, overload and genetic variations, is not well understood.

43
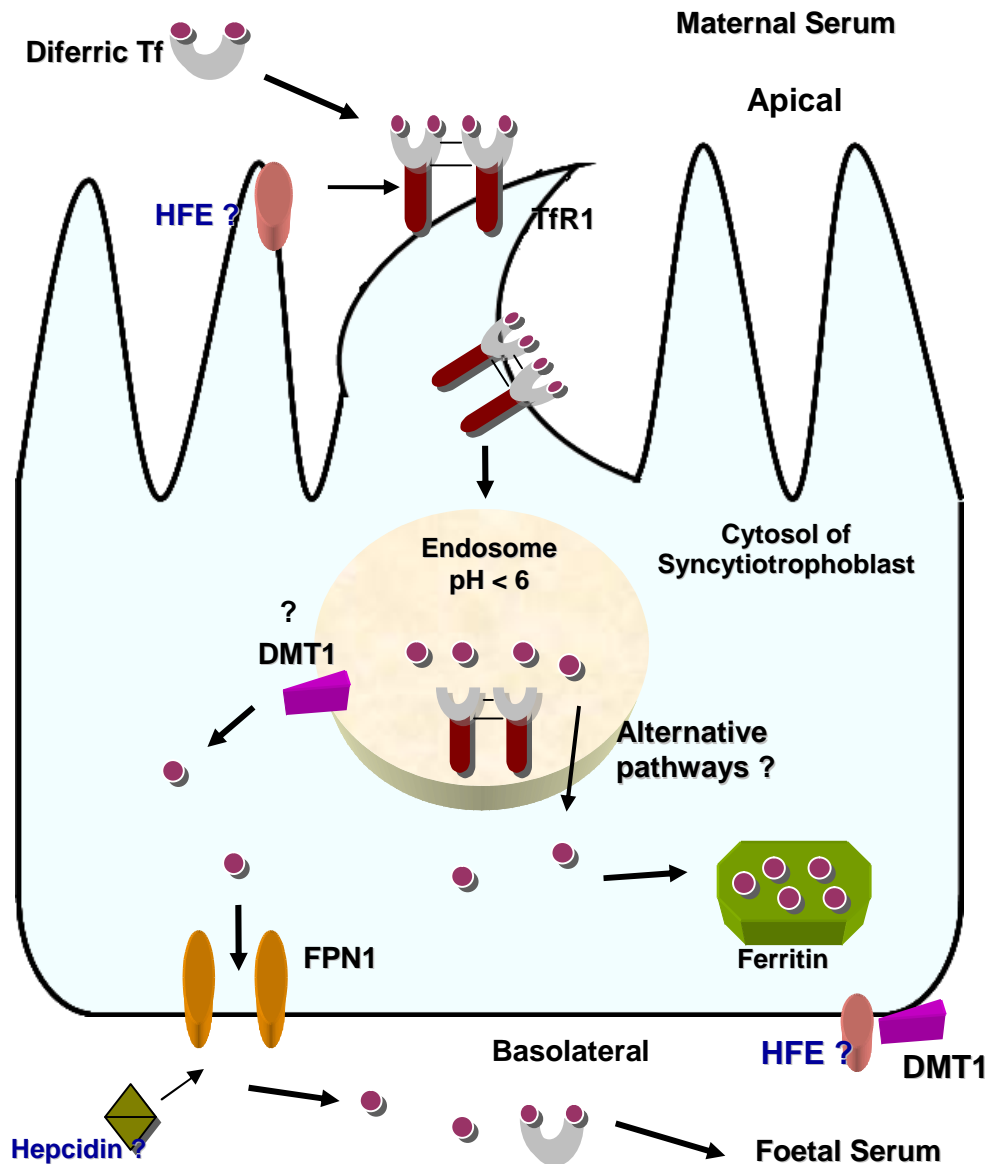
Figure 1.3 Proposed model of iron transport by human syncytiotrophoblast

TfR1 present on the apical mambrane of STB binds maternal diferric transferrin and forms a complex. This complex is internalised as an endosome which releases iron from transferrin in the acidic environment in the ferrous form. This release allows transfer of iron to the cytoplasm through DMT 1 which is localised intracellularly and on the basolateral membrane of the syncytiotrophoblast cell. The mechanism of iron release from transferrin and transfer to the cytoplasm via DMT1 is not clearly understood. From the cytoplasm, ferrous iron moves into the intracellular transfer and efflux pathway via FPN1 on or near the basolateral membrane of placenta. Before release, iron is oxidised to Fe^{3+} probably by an MCF. A few studies have shown HFE and DMT1 on the basolateral side.

1.7 Hepcidin

Human hepcidin is a 25 amino acid antimicrobial peptide belonging to the defensin family. It was first identified in human urine by Park et al. in 2001 who named it hepcidin, based on its site of synthesis (the liver, hep-) and antibacterial properties in vitro (-cidin). Krause et al. in 2000 independently isolated it from plasma and named it LEAP-1 (liver-expressed antimicrobial peptide). The main cellular sources of hepcidin are the hepatocytes but few studies have shown its synthesis at a lower level by bacteria-activated neutrophils and macrophages (Krause et al. 2000; Park et al. 2001). The hepcidin gene has also been identified in mice, rats, pigs, dogs, and several species of fish. Two other forms of this peptide are the 20- and 22- amino acid forms but only the 25- amino acid hepcidin is shown to be biologically active.

The bioactive 25-amino acid form of hepcidin has a simple hairpin structure with 8 cysteines that form 4 disulphide bonds in a ladder-like configuration. One of the disulphide bonds is an unusual vicinal bond between adjacent cysteines at the hairpin turn (Hunter et al. 2002). In a recent study, it was revealed that the N-terminus of hepcidin is essential for its bioactivity (Nemeth et al. 2006). Like other defensin peptides, it uses a relatively rigid antiparallel β-sheet constrained by disulphide bonds as the framework, around which segregated patches of cationic and hydrophobic residues are organised.

In humans, the *HAMP* gene produces hepcidin by encoding an 84-amino acid preprohepcidin. This prepropeptide is cleaved to give the 60 amino acid form of prohepcidin which is further cleaved to give the 25 amino acid form of hepcidin

that is found in blood and urine. The human *HAMP* gene comprises three exons and maps to the long arm of chromosome 19 (19q13) (Park et al. 2001).

1.7.1 Role of hepcidin in iron metabolism

Pigeon et al. in 2001 were the first to study the connection between hepcidin and iron metabolism during studies of the hepatic responses to iron overload. They showed that the mRNA for hepcidin was overexpressed by hepatocytes of experimentally iron-loaded mice. The upregulation of hepcidin was temporary and reached a plateau as early as 2 months and 1 week in carbonyl iron and iron-dextran overload model, respectively (Pigeon et al. 2001). It was proposed that the transcription factor C/EBPα is involved in this iron-mediated increase of hepcidin gene expression (Courseland et al. 2002). However, so far, the mechanisms involved in this regulation remain to be elucidated.

1.7.2 Hepcidin deficiency

The specific role of hepcidin was demonstrated by the effects of hepcidin deficiency or overload in transgenic mouse models. Mice made deficient for the transcriptional factor USF (*Usf* KO mice) were found to have haemochromatosis with iron deposition in the liver and pancreas while the spleen of these mice was relatively protected from this iron loading (Nicholas et al. 2002). This phenotype of mice indicated that hepcidin controlled intestinal iron uptake and the retention of iron in macrophages. In *Usf* KO mice, iron overload was similar to that observed in human hereditary haemochromatosis and in *Hfe* KO mice, with increased iron circulation in the blood, increased

transferrin saturation, decreased reticuloendothelial iron, and normal haematological indices (Zhou et al. 1998).

The identification of two human families with severe juvenile haemochromatosis with hepcidin deficiency managed to dispel doubts about the essential role of hepcidin in iron homeostasis (Roetto et al. 2003). Each affected family member had distinct homozygous destructive mutations in the hepcidin gene.

1.7.3 Hepcidin excess

The effects of hepcidin excess in mice that overexpressed hepcidin-1 were shown under the control of a liver-specific promoter (Nicholas et al. 2002). The newborn mice with hepcidin excess were born severely anaemic which may indicate that foetal hepcidin inhibited the placental transport of iron to the developing foetus. Excessive hepcidin also reduces intestinal iron uptake as shown by the dependence of surviving mice on parenteral iron injections. These findings are enough to indicate that hepcidin is a negative regulator of iron transport in the small intestine and in the placenta and that it induced iron retention in (mainly splenic) macrophages engaged in the recycling of iron from senescent erythrocytes by targeting FPN1. Synthetic 25-amino acid hepcidin is responsible for hypoferremia in mice, and if injected it can decrease serum iron levels up to 75% within 1 hour and the effect can persist for more than 48 hours (Rivera et al. 2005). Figure 1.4 represents the schematic diagram showing the interaction of hepcidin with FPN1 to control iron flow into the circulation.
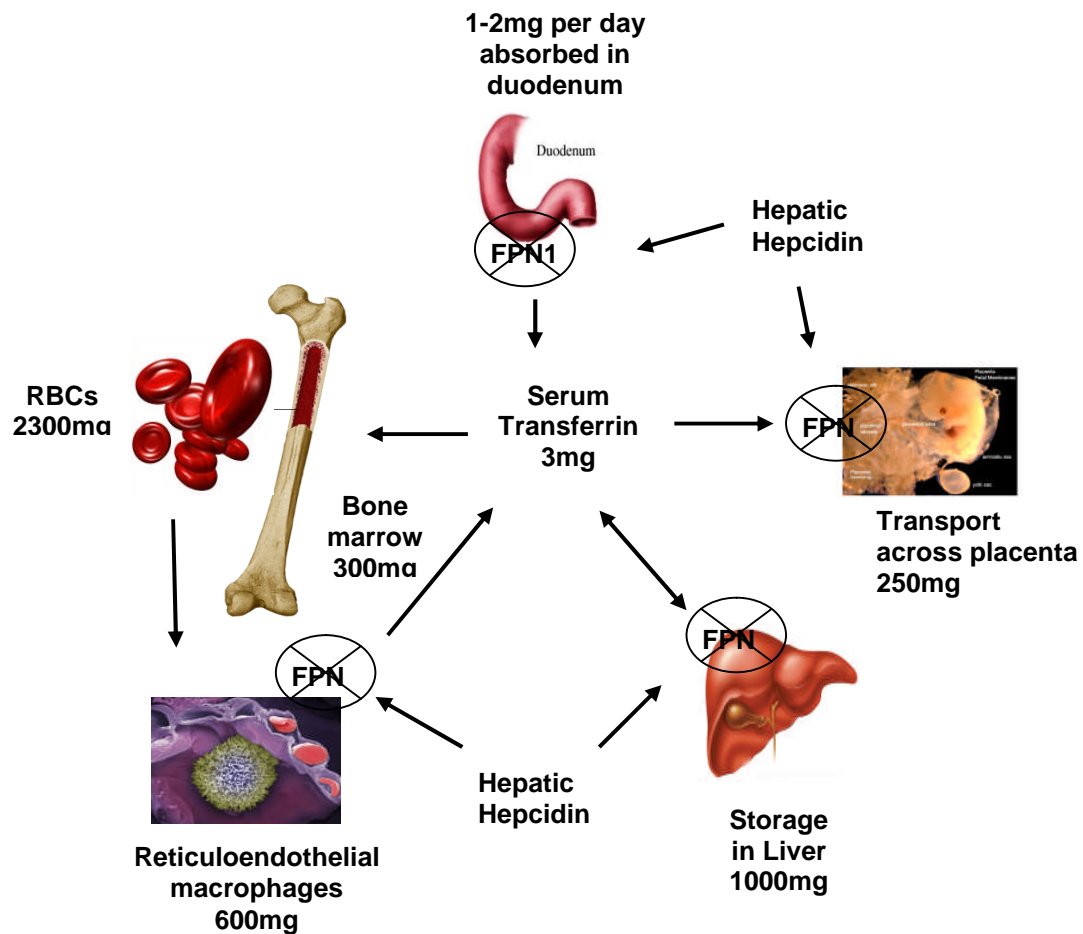
Figure 1.4 Schematic diagram showing the interaction of hepcidin with FPN1 to control iron flow into the circulation

Hepcidin controls systemic iron homeostasis by interacting with FPN1. Hepcidin targets the FPN1 present on duodenal enterocytes responsible for iron absorption, macrophages involved in the recycling of iron from dying RBCs and iron storage organ (liver). The FPN1 degradation results in less iron inflow into the circulation. During pregnancy, foetal hepcidin controls iron transport across placenta. Modified from Ganz 2011.

1.8 HFE as an iron regulator

The HFE protein is a 343 amino acid protein, homologous to the major histocompatibility complex (MHC) class I-like glycoproteins consisting of 3 extracellular loops (α1, α2, and α3), a transmembrane region and a short cytoplasmic tail (Waheed et al. 1997). This protein is predominantly expressed in liver hepatocytes and is also found in intracellular and perinuclear compartments in the enterocytes of duodenal villus crypts (Parkkila et al. 1997a). It is also highly expressed in placental syncytiotrophoblasts (Parkkila et al. 1997b). The expression of HFE has profound effects on cellular iron status.

Haemochromatosis due to mutations in the *HFE* gene is characterised by inappropriate high iron absorption and reticuloendothelial cell release that results in excess iron entering the circulation and subsequent deposition in parenchymal cells such as hepatocytes. While the precise function of the HFE protein is unknown, recent studies have shown that mutations in the *HFE* gene results in an inappropriately low level of hepcidin expression (Ahmad et al. 2002). The decrease of circulating hepcidin leads to an increased ferroportin-mediated iron efflux from reticuloendothelial cells and duodenal enterocytes resulting in increased circulating iron and eventually the saturation of Tf. Moreover, when *Hfe* KO mice were crossed with mice over-expressing hepcidin, their overload status was normalised (Nicholas et al., 2003). These studies suggest that HFE participates in the regulation of intestinal iron absorption by modulating hepcidin expression (Mura et al., 2004).

However, there are difficulties in distinguishing the primary effects of HFE on cellular iron status and its secondary effects resulting from changes in hepcidin

expression. Hepcidin mRNA measurements in patients with HFE-related haemochromatosis and *Hfe* KO mice suggest that partial hepcidin deficiency may contribute to iron overload in the most common form of haemochromatosis (mutation in *HFE* gene).

1.9 Aims

The mechanism underlying maternal-foetal iron homeostasis is not clearly defined. This study was carried out to determine the role of HFE and hepcidin in iron transport across the placenta. The aims of this study are:

(1) To determine the role of maternal and foetal *Hfe* status and its down stream modulator, hepcidin, in the transfer of iron across the placenta *in vivo*.

(2) To elucidate the molecular mechanism of iron transport across the placenta using BeWo cells as a model for iron uptake, transport and efflux.

1.10 Objectives

(1) To determine the effect of maternal *Hfe* status on iron transport across the placenta when the foetal genotype is heterozygous.

(2) To determine the effect of foetal *Hfe* status on the transport of iron across the placenta when maternal genotype is heterozygous.

(3) To determine the effect of dietary iron levels on maternal iron levels and placental protein and gene expression of iron transporters

(4) To determine the effect of synthetic hepcidin on maternal iron status and its effect on placental iron gene expression

(5) To use BeWo cells as a model of placental cells:

(i) To quantify iron transporter proteins' and regulatory genes' expression.

(ii) To determine the cellular localisation of iron transporter proteins.

Chapter 2

Materials and Methods

2.1 Mice strain, tissue collection and storage

All experimental procedures were approved and conducted in accordance with the UK Animals (Scientific Procedures) Act, 1986. Mice (129/Ola-C57BL/6 mixed background strain) with a 2kb pgk-neo gene flanked by loxP sites replacing a 2.5kb BglII fragment (for details see Bahram et al. 1999) were used as *Hfe* knockouts (KO). *Hfe* KO mice were mated with wildtype (WT) mice to produce heterozygotes (HET). For the experiments mentioned in Chapter 3, mice of all three genotypes were used.

To determine the effect of maternal and foetal *Hfe* status on iron transport across placenta mice were fed a high iron diet (150 ppm iron) for one week after weaning. After one week, mice were placed on low (12.5 ppm), normal/adequate (50 ppm) and high (150 ppm) iron diets. WT, HET and *Hfe* KO females were mated with HET males three weeks later and remained on their respective diet throughout pregnancy. Pregnancy was confirmed by detection of a vaginal plug and this day was denoted day 0.

For the experiments mentioned in Chapter 4, only WT and *Hfe* KO mice were used. After weaning, mice were fed RM1 (150 mg Fe/kg diet) for two weeks followed by mating with males of corresponding genotype (WT or *Hfe* KO). On day 14 of gestation, females were injected with either 0.15 M NaCl or 10 µg hepcidin dissolved in 0.15 M NaCl via the intraperitoneal route. They were then injected every 24 hours till day 18 of gestation.

On day 18 of gestation, dams from each group were anaesthetised with pentobarbitone. The foetuses were delivered by caesarean section and killed by decapitation. Foetuses were weighed before dissection. Mice and foetal tissues were collected by Dr. S. Balesaria, Royal Free Hospital, UK. After collection, tissues were snap frozen in liquid nitrogen and stored at -80°C until used.

2.2 Cell Biology

2.2.1 BeWo cell culture

Clone b30 of BeWo cells were incubated at 37°C with 5% CO_2 in 75 cm^2 flasks (Nunc, Roskilde, Denmark) in 20 ml of Dulbecco's Minimal Essential Medium (DMEM) with Glutamax 1 (Invitrogen, Paisley, UK) supplemented with 10% (v/v) gamma irradiated foetal bovine serum and 1% (v/v) antibiotic/antimycotic (Invitrogen, Paisley, UK). Cells were sub-cultured after every 3-5 days when they were 80% confluent and the medium was changed every 2 days.

2.2.1.1 Sub-culturing of BeWo cells

The medium was removed and the cells were washed with 10 ml prewarmed Dulbecco's Phosphate Buffer Saline (DPBS) (Invitrogen, Paisley, UK) twice. 5 ml of 1x trypsin EDTA (Invitrogen, Paisley, UK) was added to the cells and incubated for about 5 min or until the cells were detached from the surface of the flask. 10 ml of complete medium was added to resuspend the cells and deactivate the trypsin. This cell suspension was transferred to a 15 ml Falcon tube followed by centrifugation for 3 min at 2000 rpm at room temperature. The supernatant was discarded and the cell pellet was resuspended in 10 ml of the

complete medium and the aggregates were dispersed by pipetting the cell suspension up and down several times. The appropriate amount of cells was added to the fresh flask containing 15-20 ml medium (composition of medium is mentioned in Section 2.2.1).

2.2.1.2 Cryopreservation of BeWo cells

BeWo cells (80% confluent) were trypsinised by 1x trypsin-EDTA and resuspended in a complete medium at a density of 3×10^6 cells/ml. The cell suspension was first cooled on ice before dimethylsulphoxide (DMSO) (Sigma, Ayrshire, UK) was added to give a final concentration of 10% (v/v). A 1 ml aliquot of the suspension was transferred to a sterile vial. The vial was frozen at -80°C for 24 hours followed by storage in liquid nitrogen.

2.2.1.3 Recovery of frozen cells

A vial of frozen BeWo cells was taken out from the liquid nitrogen container. It was thawed in a water bath at 37°C and disinfected with 70% ethanol. The thawed cells were transferred to a tissue culture flask containing sufficient medium to dilute the DMSO at least 10 fold. Cells were incubated as mentioned in section 2.2.1 and the medium was changed after 24 hours to remove the dead cells.

2.2.2 Culture of BeWo cells stably transfected with *HFE*

BeWo cells stably transfected with *HFE* were generated by Dr. H Bayele. mRNA expression of *HFE* in these cells showed higher expression of *HFE* as compared with normal BeWo cells. These cells were cultured with complete

medium with 200 µg/ml of Zeocin and sub-cultured as explained in section 2.4.1 and its sub-sections.

2.2.3 HEK293 Tet-On and Tet-Off cell culture

HEK293 Tet-On hFPN1-Green Fluorescent Protein (GFP) cells (HEK293 with pLVX-Tight-Puro lentiviral vector) were grown in DMEM supplemented with 10% tetracycline-free foetal bovine serum (Invitrogen, Paisley, UK), 100 µg/ml G418, 0.5 µg/ml puromycin, 100 µg/ml penicillin, and 100 µg/ml streptomycin. To turn on the hFPN1-GFP expression, the cells were seeded in a 6-well plate and incubated with the supplemented medium containing 100 ng/ml of doxycycline for 24 hours. Doxycycline was removed and the cells were treated with 1 µM hepcidin for 12 to 24 hours before analysing the relative hFPN1-GFP expression by FACS.

HEK293 Tet-Off hFPN1-GFP cells (HEK293 stably transfected with pTRE-Tight vector) were grown with the supplemented medium containing doxycycline in a 6-well plate. Doxycycline was removed for 48 hours to turn on hFPN1-GFP expression followed by replacement of medium with supplemented medium containing doxycycline. The cells were treated with hepcidin for 24 hours and analysed by FACs. Both cell lines were provided by Dr T. Ganz and Dr. E. Nemeth, UCLA, USA.

2.2.4 Cell counting with haemocytometer

BeWo cells were trypsinised with 5 ml of 1x trypsin EDTA before resuspending the cell pellet in 10 ml of the medium and the aggregates were dispersed by pipetting the cell suspension up and down several times to get the homogenised cell suspension. A drop (20 µl) of cell suspension was placed on the sample introduction point on the haemocytometer. Cells were counted in four 1 mm squares grid using 400 x magnifications under inverse phase light microscope (Axiovert 25, Zeiss, Germany) using push button counter. The average value was calculated and it was multiplied by 1×10^4 to determine the number of cells per cubic millimetre.

2.2.5 Transepithelial electrical resistance measurements

A TEER voltohmmeter along with STX-2 electrodes (World Precision Instruments, Hertfordshire, UK) quantitatively assesses the confluence of a cellular monolayer by measuring the total resistance across the cell culture insert (Nunc, anopore, USA). The BeWo cells were grown on the anopore inserts and the TEER was measured daily from the 3rd day of seeding until confluence was achieved. For measuring the resistance, the inner electrode of the STX-2 electrodes was inserted carefully into the insert to avoid damage to the cell layer. The outer electrode was inserted into the cell culture well to touch the bottom of the dish containing external culture medium, as shown in Figure 2.1. The STX-2 was connected to the EVOM meter to obtain the resistance. Then the Blank reading/ resistance (R_{blank}) was subtracted from the total resistance reading (R_{total}) across the monolayer in order to obtain the true cell monolayer resistance ($R_{true\ cell}$).

$$R_{\text{(true cell)}} = R_{\text{(total)}} - R_{\text{(blank)}}$$

However, the unit area resistance was obtained by multiplying the true cell resistance with the effective surface area of the insert.

Resistance of unit area = $R_{\text{(true cell)}}$ (Ω) x Effective insert area (cm^2)

Resistance of unit area = $R_{\text{(true cell)}}$ x $\pi d^2/4$
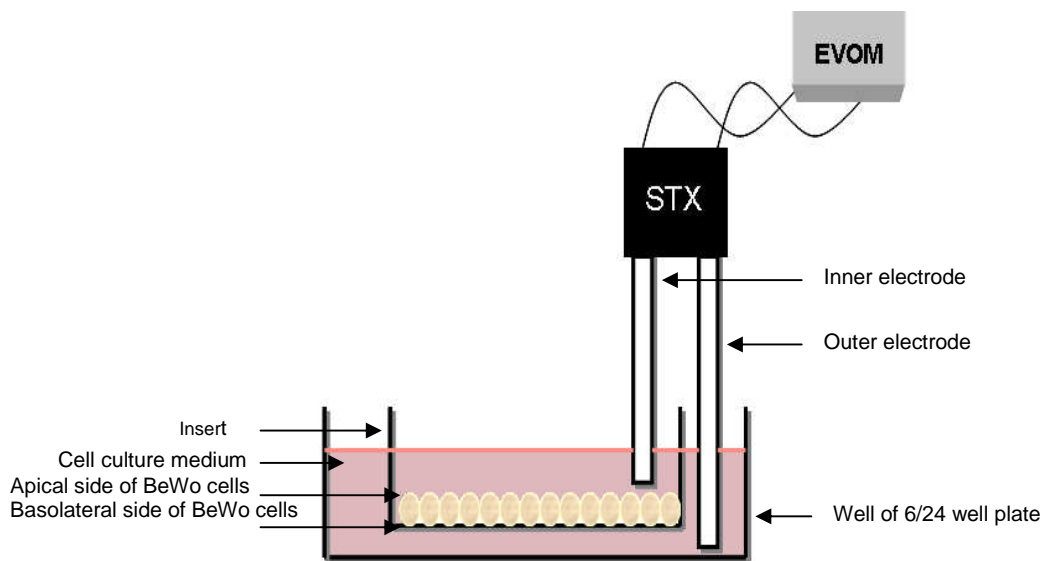
Figure 2.1 Schematic diagram showing the set-up of the STX electrode used to measure TEER of BeWo cells

BeWo cells were grown on the anopore inserts at the density of 40×10^4 cells per well. After three days post seeding, TEER was measured by electrodes and the reading was recorded on the EVOM meter. The inner electrode of the STX-2 electrodes was inserted into the insert and the outer electrode was inserted into the cell culture well to touch the bottom of the dish containing culture medium. The resistance was measured with the formula given in section 2.2.5.

2.2.6 Treatment of cells with hepcidin

BeWo cells were grown on anopore inserts at the density of 40×10^4 cells per insert for seven to ten days. The confluency of the cells was confirmed by TEER measurement. 24 hours prior to treatment, the complete medium was replaced by foetal bovine serum-free medium. Cells were treated with 1 µM commercial or in house hepcidin (structure discussed in section 2.3.5) from 2, 4, 6, 8, 12 and 48 hours. After the treatment the medium containing hepcidin was removed and the cells were washed with PBS three times and collected for RNA or protein extraction. HEK293 Tet-On and Tet-Off cells were grown in 6-well plates and treated as mentioned above.

2.2.7 Supplementation with iron (Fe-NTA)

0.024 g of $FeCl_3.6H_2O$ was dissolved in 50 ml of 10 mM NTA (0.25 g NTA in 100 ml balance salt solution). The pH was adjusted to 7.4 with HCl and the solution was sterile filtered. When the density of cells reached 70 to 80% confluence, cells were subjected to 100 µM ferric nitriloacetic acid (Fe-NTA) for 48 hours followed by washing with DPBS twice before collection for total RNA and protein extraction.

2.2.8 Induction of iron deficiency with DFO

BeWo cells were seeded in 6-well plates at a density of 40×10^4 cells until the confluency reached 70%. Cells were subjected to 20 µM desferrioxamine (DFO) for 40 hours to induce iron deficiency. Before collection for RNA extraction, cells were washed with DPBS twice after the treatment.

2.2.9 Fluorescence activated cell sorting (FACs)

HEK293 Tet-On and Tet-Off cells were cultured in 6-well plates and treated with 1 µM hepcidin as described in section 2.2.3 and 2.2.6. After the treatment, cells were washed with DPBS twice and trypsinised to detach them from the plate. The cell suspension was centrifuged at 2000 rpm for 2 min at $4^{o}C$. The cell pellet was resuspended in ice cold DPBS with the adjustment in cell suspension to a concentration of 1×10^{6} cells/ml. For the negative control, hFPN1-GFP expression was turned off in both cell lines and in the positive control it was turned on. Data was acquired by FACs using Beckman-coulter CyAn ADP Flow cytometry with Summit v4.3 software and presented as Mean$\pm$SEM in bar graph. **(a)**   **(b)**
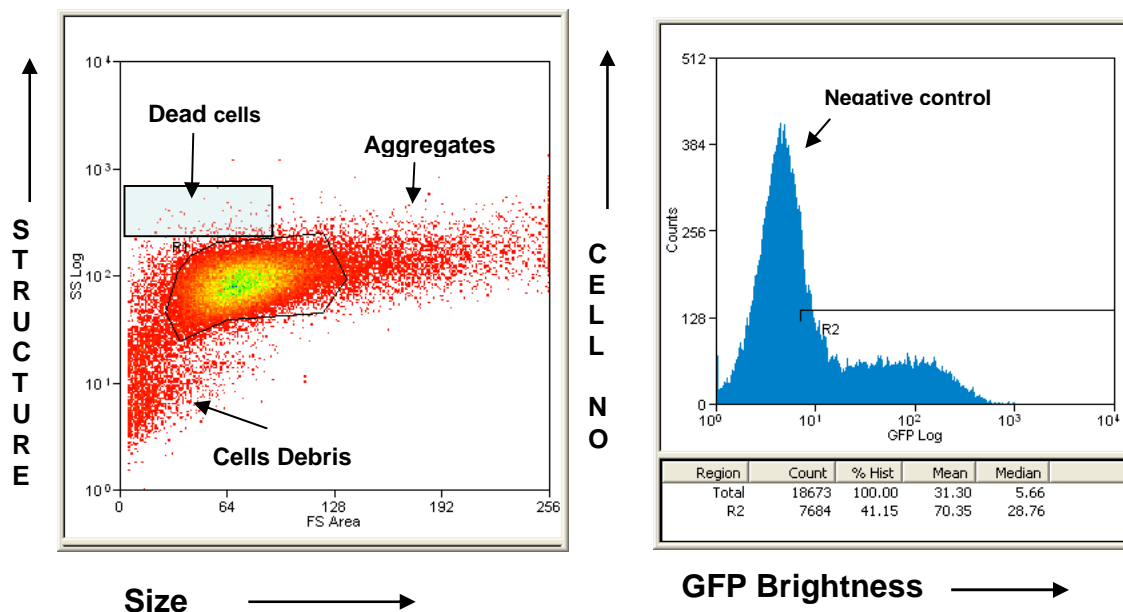
Figure 2.2 SSC vs FSC dot plot and GFP count plot of HEK293 Tet-On and Tet-Off cells

(a) represents side scatter count (SSC) vs forward scatter count (FSC) dot plot. Each dot represents a cell. Cell debris, cell aggregates and dead cells are labelled in the plot. All the dots within the enclosed area represent normal and healthy cells. (b) represents GFP count with more GFP expressed cells present in the second histogram shown under R2 region as compared with negative control cells.

2.2.10 Determination of intracellular distribution/localization of iron transporter proteins by confocal microscopy

2.2.10.1 Fixation of BeWo cells with 4% paraformaldehyde

BeWo cells were routinely cultured at the density of 40×10^4 cells per coverslip until they reached 60 to 70% confluency and fixed with freshly prepared 4% paraformaldehyde for 30 min at room temperature. After fixation cells were washed twice with PBS for 10 min by gentle shaking. Then the cells were permeabilised with ice cold methanol/ethanol (v/v) for 5 min on ice followed by two washings with PBS for 10 min and final wash with washing buffer (PBS and 0.1% BSA). Cells were incubated with blocking buffer (PBS and 1% BSA) for 20 min at 25°C. After washing with PBS twice the cells were stained with 1:100 dilution of anti-TfR1 (Santa Cruz, California, USA) for 2 hours at 25°C followed by three washings with PBS for 10 min each. Cells were incubated with 1:1000 diluted secondary antibody coupled to Alexa488 (Invitrogen, UK) for 1 hour at 25°C. To stain the cell membranes, the cells were incubated with WGA-Alexa594 (1:200 dilution) (Invitrogen, UK) for 15 min at 25°C followed by washing with PBS twice and fixing on slides with mounting solution.

The slides were observed using a confocal microscope (Leica, TCS Sp5 AOBS, Leica, Mannheim, Germany or Zeiss). For FITC and Alexa 488, a laser at 488 nm was used and emission collected from 498-548 nm. Every experiment was performed, acquired and analysed similarly and each duplicate experiment repeated three times.

2.2.10.2 Fixation of cells with methanol

BeWo cells were plated at 70% confluence on coverslips. For anti-DMT1 and anti-FPN1 staining cells were fixed with 100% methanol on ice followed by immediate incubation for 3 min at -20°C. Cells were washed twice with PBS for 10 min at 25°C with gentle shaking followed by permeabilisation with PBS and 0.025% saponin for 40 minutes at 25°C and blocking with blocking buffer (PBS, 1% BSA and 0.025% saponin) at 25°C. Cells were stained with 1:100 diluted anti-FPN1 (provided by Dr, G Anderson, Australia), anti-HFE (provided by Dr, H. Drakesmith), anti-ZIP14 (provided by Dr. Knutsen, Florida, USA), anti-DMT1 (provided by Dr, G Anderson, Australia) or double stained with 1:50 dilution anti-Nranp1 (Santa Cruz, California, USA) with anti-ZO-1, anti-Occludin or anti-E-Cadherin (1:100) overnight at 4°C in a humidified chamber. After washing twice with PBS they were stained with secondary antibodies (1:1000 dilution) coupled to Alexa488 or Alexa594 (Invitrogen, UK) and mounted on slides.

The slides were observed using a confocal microscope (Leica, TCS Sp5 AOBS, Leica, Mannheim, Germany or Zeiss). For Alexa 594, a laser at 594 nm was selected and emission was collected from 605-751 nm. Each colour was acquired sequentially. Every experiment was performed, acquired and analysed similarly and each duplicate experiment repeated three times.

2.3 Protein analysis

2.3.1 Crude membrane preparation

50 to 100 mg of tissue or cell samples were homogenised with lysis buffer using mortar and pestle. The homogenised samples were centrifuged at 2500 rpm for 15 min at 4°C to get rid of cell debris. Supernatant was transferred into a fresh tube and was centrifuged at 10,000 rpm for 45 min at 4°C. Supernatant was discarded and the membrane pellet was dissolved in sucrose buffer and stored at -80 ^{o}C. The crude membrane samples were used for western blotting or immunoprecipitation.

2.3.2 Western Blotting

2.3.2.1 Sample preparation

30 to 40 µg of protein from tissue or cell samples was mixed thoroughly with an equal volume of 2x Laemmli treatment buffer containing 0.125 M Tris-HCl buffer with pH 6.8, 4% SDS, 20% (v/v) glycerol, 0.2 M dithiothreitol DTT, and 0.02% bromophenol blue with the pH adjusted to 6.8. The mixture was heated at 95°C for 5 min then placed on ice before loading onto the gel. The SDS used in the treatment buffer is an anionic detergent that wraps around polypeptide backbone and denatures protein. In doing so, it confers a net negative charge to the polypeptide in proportion to its length.

2.3.2.2 Gel loading and transfer to the blot

The well forming comb was gently removed from the gel cassette and the wells were rinsed with 1x tank/running buffer (Sigma, St. Louis, USA). Protein marker (Biorad, USA) and samples were loaded carefully in each well. The upper and lower chambers of the electrophoresis tank were filled with tank buffer and the gel was run for approximately 90 min at 150 mA using a power pack (Biorad, USA). Meanwhile polyvinylidine difluoride (PVDF) (Biorad, USA) was soaked in 100% methanol for 10 min and after washing with phosphate buffer saline PBS-0.01% Tween (Oxoid, Hampshire, UK) the membrane and the filter paper were soaked with transfer buffer for 15 min.

The gel cassette was opened and the stacking gel was discarded. The transfer sandwich was assembled in the semi dry unit (Biorad, USA) in the following order: filter paper/ PVDF membrane/ gel/ filter paper as shown in Figure 2.3. Air bubbles were removed by rolling a clean test tube over the layers and the unit was set at 180 mA for 120 min. After transfer, the blot was stained with Ponceau S to check the successful transfer of protein. The blot was destained by washing briefly with distilled water five times and finally with PBS-Tween. It was then blocked with 20 ml of 5% non fat-dry milk in PBS-Tween for 60 min to block non-specific protein binding sites on the blot. After blocking, the immobilized proteins were probed overnight at 4°C with specific primary rabbit anti-ferroportin 1 (1:500, Alphadiagnostics, USA), mouse anti-DMT1 (1:1000, produced in house), and mouse anti-actin (1:10,000, Abcam, Cambridge, UK) followed by washing and incubation with donkey anti-rabbit secondary antibody

horseradish peroxidase conjugate (1:4000). The blot was visualised under Fujifilm LAS-1000 imager.

Cathode electrode plate $\longrightarrow$	
Filter paper, four sheets $\longrightarrow$	
Gel $\longrightarrow$	
PVDF membrane $\longrightarrow$	
Filter paper, four sheets $\longrightarrow$	
Anode electrode plate $\longrightarrow$	
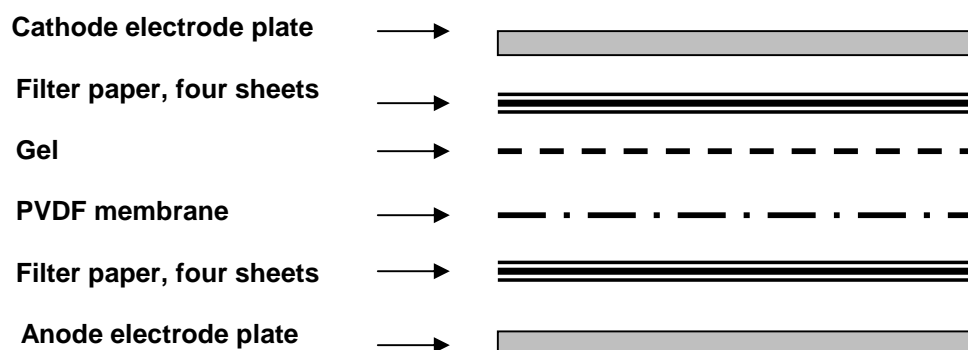
Figure 2.3 Diagram of transfer sandwich of blotter paper, PVDF membrane, and gel

The transfer sandwich was assembled to the semi dry unit in this order: filter paper/ PVDF membrane/ gel/ filter paper

2.3.2.3 Polyacrylamide gel

10% polyacrylamide resolving gel was prepared by mixing 6 ml of 30% acrylamide stock solution (Sigma, Poole, UK), 7.5 ml of distilled water, and 4.5 ml of Tris-HCl buffer with pH 8.8 (Protogel, Leicestershire, UK). 0.01 ml of TEMED (tetramethylenediamine) (Sigma, Poole, UK), and 0.08 ml of freshly made 10% (w/v) ammonium persulphate (APS) (Sigma, St. Loius, USA) were also added as initiators for polymerization reaction. The rate of formation of free radicals from persulphate is accelerated by TEMED which in turn catalyzes polymerization. The gel was cast in 1 mm plastic cassettes (Invitrogen, Carlsbad, USA) at room temperature for 60-90 min and was overlaid with 0.2-0.3 ml of isopropanol (Sigma, Poole, UK) to avoid any contact with oxygen present in the air. A 5% stacking gel containing 1.5 ml of 30% acrylamide stock solution, 1 ml of stacking Tris-HCl buffer, pH 6.8 (National Diagnostics, UK),

2.47 ml of distilled water, 0.02 ml of APS, and 0.01 ml of TEMED was overlaid on the resolving gel after discarding the isopropanol. It was then sealed with a well forming comb which was gently placed to avoid air bubble formation.

2.3.3 Immunoprecipitation

HEK293 Tet-On and Tet-Off cells seeded in 6-well plates were washed with ice-cold PBS thrice followed by addition of 0.2 ml ice-cold RIPA buffer in each well. Cells were scraped off the plate and transferred to a 1.5 ml Eppendorf tube kept on ice. Cells were sonicated four times for 5 seconds and microcentrifuged for 10 min at 4^oC. The supernatant was transferred to a new tube and protein was quantified from the cell lysate. 200 µg of cell lysate was mixed with 2 µg of rabbit anti-GFP primary antibody (Abcam, Cambridge, UK) and incubated with gentle rocking overnight at 4^oC. 20 µl of goat anti-rabbit IgG magnetic beads (New England BioLabs, UK) were added to the cell lysate after washing with 1 ml ice-cold PBS three times. The tube with the mixture was incubated at 4^oC for 1 hour with gentle rocking. The tube was then placed in a magnetic separation rack to pull beads to the side of the tube and the supernatant was discarded. The beads were washed with 1 ml ice-cold PBS for three times, 40 µl of 2x Laemmli treatment buffer was added to the beads and incubated at 4^oC for 30 min. The tube was placed in a magnetic separation rack and the supernatant was collected to run on 10% SDS-PAGE and protein was visualised after transferring to a PVDF membrane (Figure 2.4) as described in sub-section 2.3.3.2.
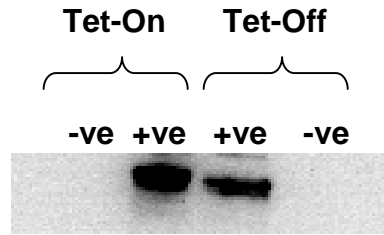
Figure 2.4 GFP protein expression in HEK293 Tet-On hFPN1-GFP cells and Tet-Off hFPN1-GFP cells

Immunoprecipitation of FPN1 tagged with GFP expression in HEK293 Tet-On hFPN1-GFP cells and Tet-Off hFPN1-GFP cells. Blot revealing protein expression of FPN1 tagged with GFP (~90kDa) in positive control (+ve) of both cell lines while no GFP expression was found in negative control when the expression was turned off.

2.3.4 Protein Quantification

Total protein was quantified from placental tissues and cell samples using the BCA protein assay kit (Pierce, Rockford, USA). The principle of this method is based on the biuret reaction when Cu^{+2} is reduced to Cu^{+1} by protein in the presence of bicinchoninic acid (BCA). Firstly, a set of albumin standards was prepared in vials with a final concentration ranging from 25 to 2000 µg/ml. Working reagent was prepared by mixing 50 parts of BCA reagent A with BCA reagent B (v/v). To 200 µl of working reagent, 10 µl of each standard, blank, and tissue or cell samples were pipetted in duplicate into the microplate well. The plate was covered and mixed thoroughly on a plate shaker for 30 seconds followed by incubation for 30 min at $37^{o}C$. After incubation the plate was cooled at room temperature and the absorbance was measured at 570 nm on a plate reader (Labsystems Multiskan MS, Finland). The average blank reading was subtracted from each standard. A standard curve was made to determine protein concentration of each sample. A standard curve is shown in Figure 2.5.

$$y = 0.0002x + 0.0035$$
$$R^2 = 0.9971$$
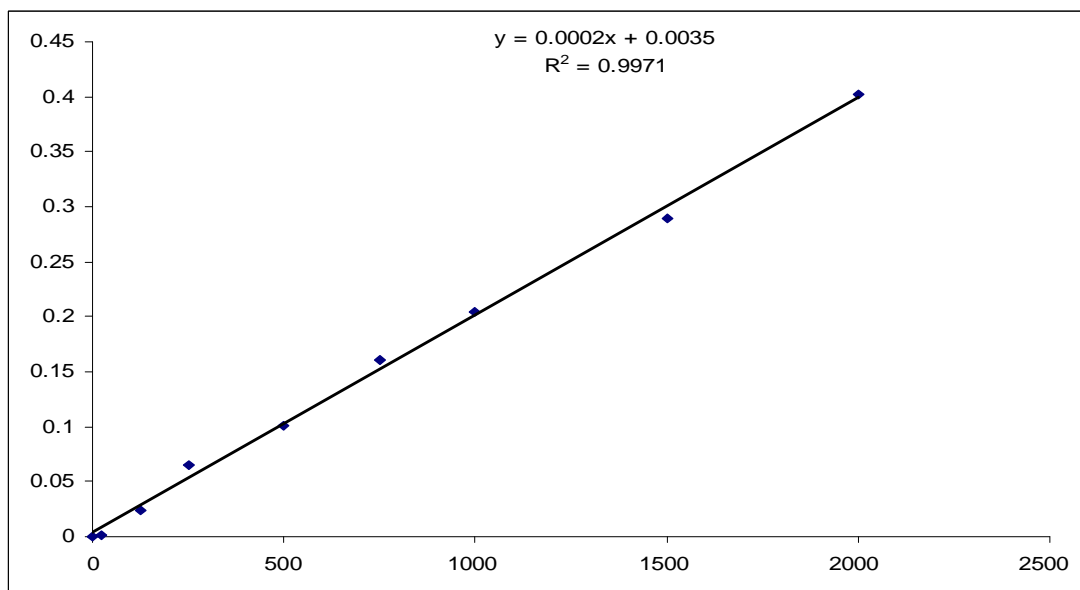
Figure 2.5 Standard curve of albumin standard with concentration ranging from 25 to 2000 µg/ml

2.3.5 Hepcidin synthesis and structural analysis

Hepcidin (H-DTHFPICIFCCGCCHRSKCGMCCKT-OH) was synthesized in house by Ms. Adams in the Dept. of Chemistry, UCL (For details see Jordan et al. 2009). The peptide mass was confirmed by electrospray mass spectrometry on a Waters Aquity UPLC-SQD MS system with an applied voltage of 60 V, the gradient used was 5 to 95% acetonitrile in water over 10 min. The calculated monoisotopic mass for hepcidin was 2787.1 Da and observed mass was 931.5 Da $[MH]^{3+}$ which deconvoluted to 2791.5 Da, Figure 2.6 (a). The commercial hepcidin (Peptide international, USA) the calculated monoisotopic mass was 2789.4 Da; observed mass, 931.42 Da $[MH]^{3+}$ which deconvoluted to 2791.26 Da, Figure 2.6 (b). To further confirm the similar composition of both peptides, the samples were run on HPLC (Dionen UltiMate 3000) using a Phenomenex Sphere Clone (5 µm particle size) and 250 x 4.60 mm column with the gradient

of acetonitrile (containing 0.1% TFA) and water (containing 0.1% TFA) over 45 min and a flow rate of 1ml/min, Figure 2.7.

(a)
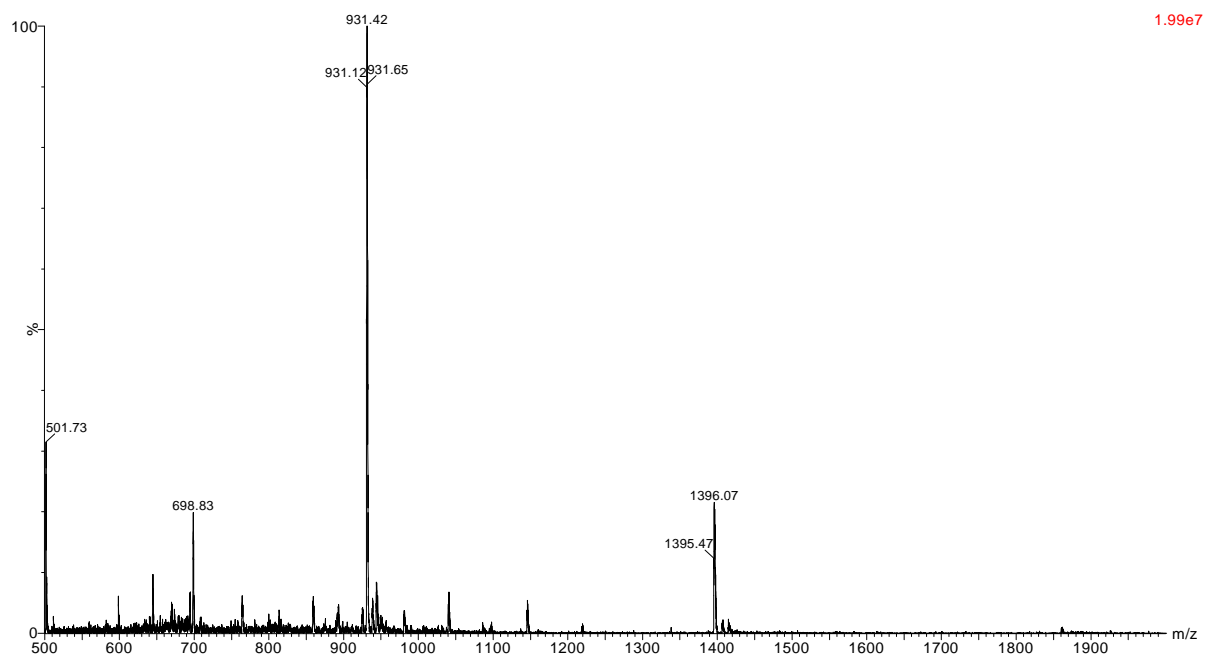
(b)
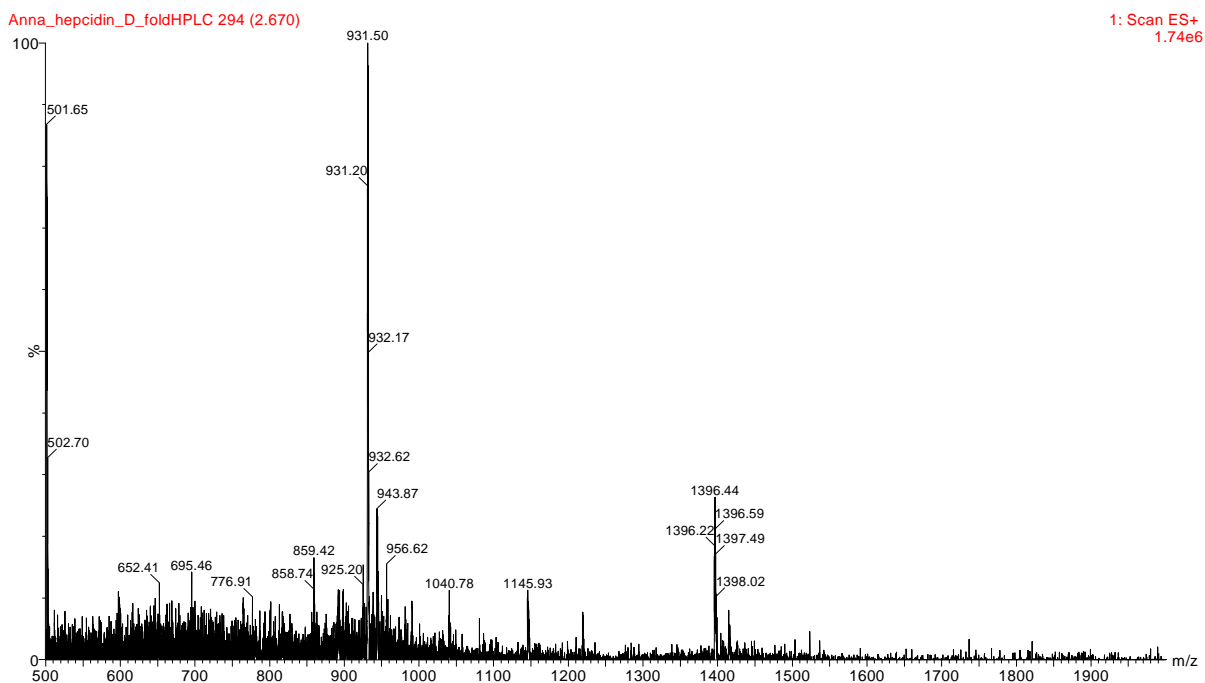
Figure 2.6 Electrospray mass spectrometry of commercial and in house hepcidin

The highest peaks in both spectra show the same deconvoluted monoisotonic mass of commercial (931.42) (a) and in house hepcidin (931.50) (b).
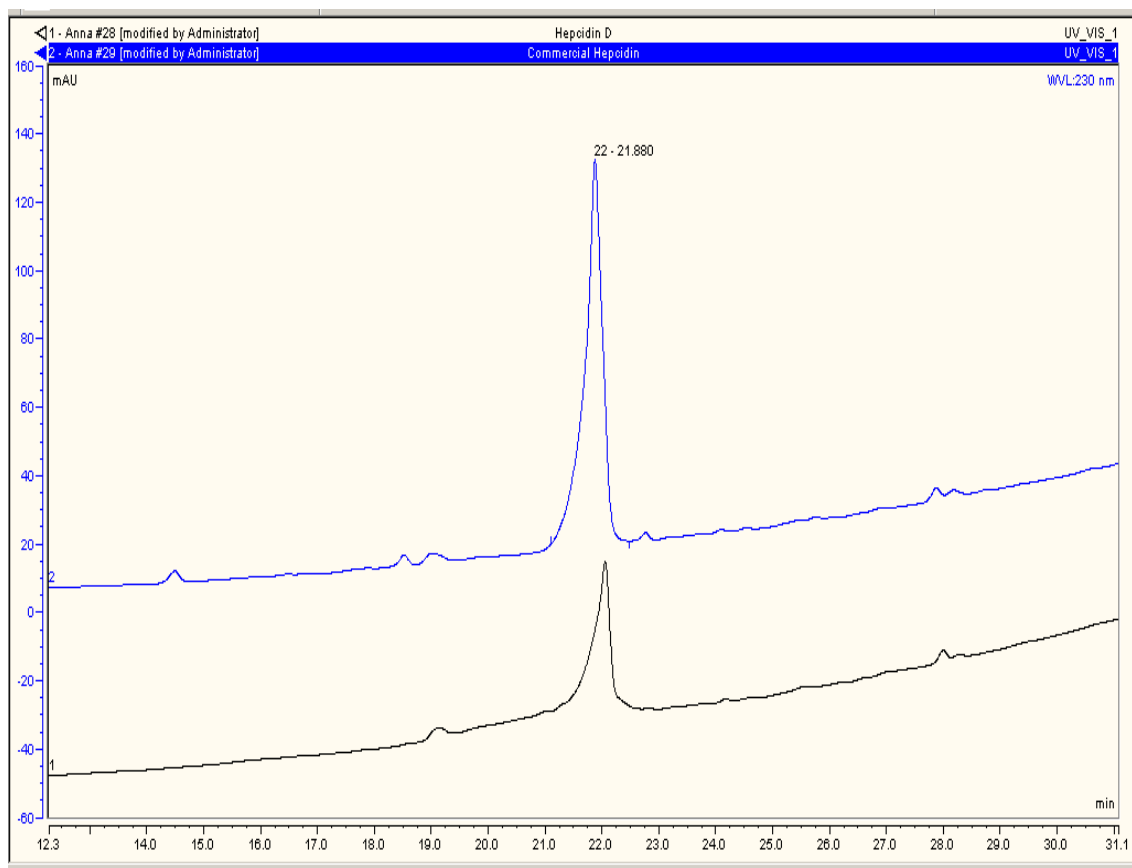
Figure 2.7 HPLC spectra showing commercial and in house hepcidin

The HPLC trace shows hepcidin produced in house in black and the commercial hepcidin in blue. The difference in height between the two peaks is due to the concentration of the commercial sample being higher than that of the synthetic hepcidin.

2.4 Molecular Biology

2.4.1 RNA extraction and verification

Total RNA was isolated from 50-100 mg of mouse placenta or BeWo cells grown in 6-well plates using TRIzol reagent (Invitrogen, Paisley, UK), which is a mono-phasic solution of phenol and guanidine isothiocyanate. The bench top and Gilson pipettes were wiped thoroughly with RNase Zap wipes (Ambion, Foster City, USA) to prevent contamination of RNA. The tissue samples were homogenized in 1 ml of TRIzol reagent with a mortar and pestle (Kontes, Kimble & Chase, Germany), followed by incubation at $25^{o}C$ for 5 min to permit the complete dissociation of nucleoprotein complexes. 0.2 ml of chloroform (BDH Lab supplies, Poole, UK) was added to each tube which was capped and shaken vigorously for 15 seconds by hand. The samples were incubated at $25^{o}C$ for 2 min followed by centrifugation at 10,000 rpm for 15 min at $4^{o}C$ for separation. In this step, the mixture was separated into a colourless upper aqueous phase with RNA and a lower phenol-chloroform phase. The aqueous phase was transferred to a fresh tube and RNA was precipitated from this phase by mixing with 0.5 ml isopropyl alcohol (Sigma-Aldrich, St. Louis, USA). Samples were incubated at $25^{o}C$ for 10 min and centrifuged at 10,000 rpm for 10 min at $4^{o}C$. The supernatant was removed and the gel-like RNA pellet was washed once with 1.5 ml of 75% (v/v) ethanol (VWR, Leicester, UK) by vortexing briefly. The samples were centrifuged at 7500 rpm for 5 min at $4^{o}C$. Ethanol was removed from the tube and the pellet was air-dried at room temperature for 5 min. The pellet was dissolved in 50-75 µl of diethylpyrocarbonate (DEPC) water (Ambion, Foster City, USA) by pipetting several times and incubated at $58^{o}C$ for 10 min. The RNA concentration was

quantified on a Nano Drop instrument using a Nano Drop software, and was stored at -80°C until further use.

To check the purity of RNA, the ratio between the reading at 260 nm and 280 nm (A_{260}/A_{280}) was checked. In DEPC water, a ratio ranging from 1.7 to 2.0 indicates RNA free of protein contamination.

The quality and purity of RNA was also assessed by electrophoresis on an agarose gel. A 1.0% agarose gel was prepared by mixing 2.5 g of agarose powder (Seaken, Rockland, USA) with 250 ml of 1x Tris-acetate-EDTA (TAE) buffer (Sigma, St. Louis, USA). The mixture was heated in a microwave oven until the agarose was completely dissolved in the buffer. 8 µl of ethidium bromide (Invitrogen, Paisley, UK) was added to the mixture to facilitate visualisation of RNA after electrophoresis. The solution was cooled to about 60°C and was poured in to a gel casting tray containing a well comb. The gel was left to solidify at room temperature. The well comb was removed after the gel had solidified and the tray was placed in the horizontal electrophoresis tank which was filled with 1x TAE buffer. 1 to 3 µg of RNA samples were mixed with 1 µl of Blue/Orange 6x loading buffer (Promega, Madison, USA). The DNA ladder (Promega, Madison, USA) and the samples including negative control were loaded into the wells and it was run for 45-60 min at 150V. After electrophoresis RNA bands were visualised under a gel imager.

2.4.2 cDNA synthesis

RNA was reverse transcribed using a Verso cDNA kit (Thermo Fisher Scientific, Surrey, UK) to produce complementary DNA. DNase I treatment was performed to remove genomic and contaminating DNA. For DNase I treatment 1 µg of RNA from each sample was mixed with 1 µl of DNase buffer (Ambion, Foster City, USA), 0.5 µl of DNAse I (Ambion, Foster City, USA), and 9 µl of DEPC water. This mixture was first incubated at $37^{o}C$ for 30 min then incubated at $70^{o}C$ for 10 min. 1 µl of Anchored oligo-dT primers was added to the tubes to provide RNA priming methods for cDNA synthesis and incubated at $70^{o}C$ for 5 min. Meanwhile a master mix was made by mixing 4 µl of 5 x cDNA synthesis buffer, 2 µl of dNTP mix, and 1 µl of enzyme mix for each sample. 8 µl of master mix was added to each tube after incubating with oligo-dT primer and the tubes were first incubated at $47^{o}C$ for 1 hour and then $75^{o}C$ for 10 min in thermal controlled Cycler PCR (PTC-100, MJ Research Inc., USA). cDNA was stored at $-20^{o}C$.

2.4.2.1 Verification of cDNA

To check the quality of complimentary DNA (cDNA) or to check whether there was any genomic DNA contamination, a check PCR was performed using GoTag PCR Core System I kit (Promega, Madison, USA). 1 µl of cDNA was mixed with 2.5 µl of 5% reaction buffer, 1.5 µl of 25 mM MgCl$_2$, 0.25 µl of 5 µg/µl of GoTag DNA polymerase, 0.5 µl of 10 mM PCR nucleotide mix, 17.25 µl of nuclease free water, and 2 µl of β-actin primer. The sequence of the primers is shown in Table 2.1.

Table 2.1 β-actin primer sequences used for check PCR

β-actin forward	5'-ACCTTCAACACCCCAGCCATGTACG-3'
β-actin reverse	5'-CTGATCCACATCTGCTGGAAGGTGG-3'
Tm	65°C
Product length	698 bp

A drop of Mineral Oil (Promega, Madison, USA) was added to avoid evaporation and the mixture was incubated at 95°C (denaturation) for 5 min, 40 cycles of denaturation at 94°C for 30 seconds, annealing at 60°C for 30 seconds, and extension at 72°C for 1 min followed by an incubation at 72°C for 7 min. The PCR product was cooled to 4°C and run on a 1.5% agarose with ethidium bromide and visualised under a UV transilluminator.

2.4.2.2 Agarose gel electrophoresis of cDNA

A 1.5% agarose gel was prepared by mixing 3.75 g of agarose powder (Seaken, Rockland, USA) with 250 ml of 1x Tris-acetate-EDTA (TAE) buffer with pH 8.3 (Sigma, St. Louis, USA). The mixture was heated in a microwave oven until the agarose was completely dissolved in the buffer. 8 µl of ethidium bromide (Invitrogen, Paisley, UK) was added to the mixture to facilitate visualisation of DNA after electrophoresis. The solution was cooled to about $60^{o}C$ and was poured into a gel casting tray containing a well comb. The gel was left to solidify at room temperature. The well comb was removed after the gel had solidified and the tray was placed in the horizontal electrophoresis tank which was filled with 1x TAE buffer. 12 µl of PCR product of a cDNA samples were mixed with 3 µl of Blue/Orange 6x loading buffer (Promega, Madison, USA). The DNA ladder (Promega, Madison, USA) and the samples including the negative control were loaded into the wells and it was run for 45-60 min at 150V. After electrophoresis PCR product was visualised under a UV transilluminator (Figure 2.8).
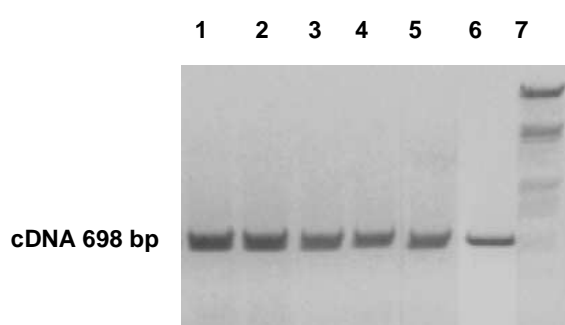
Figure 2.8 Image of agarose gel showing bands of PCR product from cDNA copied from RNA isolated from BeWo cells

Lane 1-3 show the bands of cDNA synthesized from untreated BeWo cells while lane 4-6 show the cDNA of BeWo cells treated with 1 µM hepcidin for 2 hours. Lane 7 shows the DNA ladder.

2.4.3 Real-time PCR

Real-time quantitative gene analysis was performed using a Quantitect SYBR Green PCR kit (Qiagen, Crawley, UK), and a Lightcycler System II (Roche Diagnostics, Mannheim, Germany) with Lightcycler version 3.5 software (Roche Molecular Biochemicals, Mannheim, Germany). 1 µg of cDNA was mixed with 10 µl of SYBR Green dye, 8 µl of nuclease free water, and 0.5 µl of each forward and backward primer. Primers were designed using Primer Express 3 software. The sequence of the primers and additional information is given in Table 2.2 and 2.3. All the experiments were performed in duplicate in parallel with the house keeping gene (β-actin or GAPDH).

2.4.3.1 Cycling parameters of Real-time PCR

The PCR cycling conditions were initiated by a denaturation step at 95°C for 10 min, followed by 40 cycles of denaturation at 95°C for 15 seconds, annealing at 60°C for 20 seconds, and extension at 72°C for 40 seconds. The fluorescence acquisition was set at 65°C for 15 seconds. Melting curve analysis was recorded after every RT-PCR run.

The relative expression ratio of the gene of interest to housekeeping gene was calculated by the Lightcycler Relative Quantification software version 1.0 (Real Quant) (Roche Diagnostics GmbH, Germany).

Table 2.2   Mouse primer sequences used for real-time PCR analysis

Primer	Accession Number*	Forward 5´---------------3´	Tm°	Reverse 5´---------------3´	Tm°	Product length
β-Actin	NM_007393.2	GACGGCCAAGTCATCACTATT	65.0	CCACAGGATTCCATACCCAAGA	66.8	88
DMT1	BC019137.1	GGCTTTCTTATGAGCATTGCCTA	65.1	GGAGCACCCAGAGCAGCTTA	66.7	96
DMT1+IRE	AF029758	TGTTTGATTGCATTGGGTCTG	65.7	CGCTCAGCAGGACTTTCGAG	67.5	106
DMT1-IRE	AK049856.1	CTGCTGAGCGAAGATACCAG	62.7	GTAAACCATAGAAACACACTGG	57.6	102
FPN 1	BC003438.1	CCAGCATCAGAACAAACACG	64.3	ACTGCAAAGTGCCACATCC	63.8	174
Hepcidin 1	AF503444.1	CCTATCTCCATCAACAGATG	57.0	AACAGATACCACACTGGGAA	59.4	170
TfR1	MMTRRMRNA	CAGAAAGTTCCTCAGCTCAACCA	66.6	GTTCAATTCAACGTCATGGGTAAG	65.1	92
TfR2	NM_015799.3	AGCTGGGACGGAGGTGACTT	67.3	TCCAGGCTCACGTACACAACA	66.7	100
ZIP14	BC021530.1	GTAAACCTTGAGCTGCAC	55.8	TGCAGCCGCTTCATGGT	67.1	67

Table 2.3   Human primer sequences used for real-time PCR analysis

Primer	Accession Number*	Forward 5´--------------3´	Tm°	Reverse 5´--------------3´	Tm°	Product length
GAPDH	NM_002046	TGGTATCGTGGAAGGACTC	60.1	AGTAGAGGCAGGGATGATG	59.2	93
DMT1	NM_001174130.1	GTCATTGGCTCAGCCATTGC	67.9	ATGCCCTTGAGTACCTGGCT	64.8	188
H-Ferritin	NM_002032.2	CGCCGCCTCTCCTTAGTC	65.0	GTTCTTCAAAGCCACATCATCG	65.6	138
L-Ferritin	NM_000146.3	CCTCCTACACCTACCTCTG	56.2	GCTGGCTTCTTGATGTCC	56.7	143
FPN 1	NM_014585.5	CGTCATTGCTGCTAGAATCG	63.4	AGACTGAAATCAATACGAGC	55.9	164
Hepcidin	NM_021175.2	CTGCAACCCCAGGACAGAG	66.0	GGAATAAATAAGGAAGGGAGGGG	65.2	151
TfR1	NM_003234.2	TATAGAAGGTTTGGGGGCTGTG	60.3	GAGACCCTATGAACTTTTCCCTA	63.2	157
Zp	NM_001098672.1	CAAGTGGACAGTGCCTGAGA	64.3	CATTGAGGACGCCCTTTTTA	63.7	110
ZIP14	NM_001135153.1	GTCTGGCCTTTGGCATCCT	66.5	AGGGAACATATCAGCCAGAGAAAT	64.8	62

2.4.3.2 Melting curve analysis of Real-time PCR

Melting curve analysis was performed after PCR amplification cycles. Melting temperature of dsDNA was based on its base pair length and G-C content. Analysis of the melting curve was useful to identify unwanted PCR by-products such as primer-dimers and nonspecific products. The analysis involved heating the PCR product at 65°C for 10 seconds followed by a slow increase in temperature to 95°C with a rate of 0.5^{o}C per second, whilst the fluorescence was recorded continuously. SYBR green binding and fluorescence emission was maximal at 65°C because of the presence of dsDNA in the PCR product and with the increase in temperature DNA starts denaturing. This denaturation resulted in dissociation of SYBR green and reduced fluorescence. Melt curves were made by plotting fluorescence against temperature. The presence of primer-dimers and non-specific products were identified by this method as they usually melt at lower temperatures than the desired products. The presence of a single peak in the melting curve confirmed the specificity of the primers used.

2.5 Tissue and serum iron parameters

2.5.1 Measurement of liver, spleen and placental non-haem iron

Liver and placental tissue samples from mice were placed in open 1.5 ml eppendorf tubes and oven-dried at $55^{o}C$ for 72 hours. Dried samples were weighed and placed in fresh tubes. Samples were incubated at $65^{o}C$ for 20 hours with 1 ml of acid solution (30% HCl and 10% trichloroacetic acid). A blank was prepared in the same way excluding the sample. Samples were cooled at $25^{o}C$ before preparing the blanks, standards and samples in plastic cuvettes in triplicate with the amounts as detailed in Table 2.4. The sample mixtures were incubated at $37^{o}C$ for 10 min before measuring the absorbance at 560 nm against a water blank with a spectrophotometer.

Table 2.4 Amounts of working chromogen reagent, iron standard, blank/sample, and distilled water

	Working Chromogen reagent (ml)	Iron standard (µl)	Blank/Sample (µl)	Distilled water (µl)
Blank	1	0	25 blank	225
Standard	1	125	25 blank	100
Samples	1	0	25 sample	225

2.5.2 Serum iron measurements

Serum iron was measured in mouse serum using a kit (Pointe Scientific Inc.) as instructed by the manufacturers. 40 µl of each standard, serum sample and water was added into standard, sample, and blank wells of 96 well plates. 200 µl of iron buffer reagent was added to all wells and the absorbance reading (A1) was taken at 560nm by a plate reader after mixing the reagents in the wells. The 96-well plate was incubated at $37^{o}C$ for 10 min after adding 4 µl of iron colour reagent. The absorbance was measured at 560 nm named A2 and the serum iron was measured with the following equation:

$$\text{Serum iron} = \frac{\text{A2 sample} - \text{A1 sample}}{\text{A2 standard} - \text{A1 standard}} \times 500 \ (\mu g/dl)$$

2.5.3 Measurement of serum unsaturated iron binding capacity (UIBC)

40 µl of each standard and sample was added to standard and sample wells. 80 µl of water was added to the blank well and 40 µl of water was added to a standard well. 40 µl of iron standard was added to the sample wells. Absorbance reading (A1) was measured at 560 nm after adding and mixing 160 µl of UIBC reagent. Then the plate was incubated at $37^{o}C$ for 10 min after the addition of 4 µl of iron colour reagent and the absorbance (A2) was checked at 560 nm. UIBC, total iron binding capacity (TIBC), and transferrin saturation (TFS) were measured by using the following equations:

$$\text{UIBC} (\mu g/dl) = 500 - \frac{\text{A2 sample} - \text{A1 sample}}{\text{A2 standard} - \text{A1 standard}} \times 500$$

TIBC = iron levels + UIBC

TFS = 100 x Serum iron (µg/dl) / TIBC (µg/dl)

2.6 Data analysis

Statistical analysis of the data was performed using the software package GraphPad Prism™ (GraphPad Software, San Diego, CA USA). All the results are presented as the mean$\pm$SEM using Excel and one-way ANOVA followed by the student's unpaired t-test. Means were considered significantly different if p-values were less than 0.05. Variance within treatment groups were expressed as standard error of the mean (SEM). Experiments on all the cell lines were carried out three times with four samples in each set.

2.7 General information of reagents

General reagents were supplied by Sigma, Poole, UK unless otherwise stated.

2.8 Stocks, Solutions, and Buffers

30% acrylamide stock solution

Acrylamide	29.2 g
Bis (N, N'-methylenebisacrylamide)	0.8 g
Per 100 ml of distilled water	

1.5 M Tris-HCl buffer, PH 8.8

Tris hydroxymethyl aminomethane (Tris)	8.2 g
Sodium dodecyl sulphate (SDS)	0.4 g
HCl	2 ml
Per 100 ml of water	

0.5 M Tris-HCl buffer, pH 6.8

Tris	6.1 g
SDS	0.4 g
HCl	4.2 ml

Tank Buffer (Tris-Glycine-SDS buffer) pH 8.6

Tris	25 mM
Glycine	192 mM
SDS	0.1%

Transfer Buffer (Tris-Glycine-SDS-methanol buffer)

Tank buffer	80%
Methanol	20%

Hepes buffer, pH 7.4

NaCl	136 mM
KCl	5 mM
$CaCl_2$	1 mM
$MgCl_2$	1 mM
Hepes	18 mM

Acid Solution (30% HCl and 10% trichloroacetic acid)

HCl (36.5%)	41.1 ml
Trichloroacetic acid	5 g

Volume was made up to 50 ml with distilled water

Stock iron standard solution, 20 mM

Carbonyl iron powder	22.3 mg
HCl (36.5%)	1.096 ml

Solution was left to stand overnight at RT and volume was made up to 20ml with distilled water

Working iron standard solution, 200 µM

Stock iron standard solution	0.5 ml
HCl (36.8%)	0.27 ml

Volume was made up to 50 ml with distilled water

Chromogen reagent (0.1% bathophenanthroline sulphonate and 1% thioglycolic acid)

Dissodium-4,7-diphenyl-1,10-phenanthroline sulphonic acid	50 mg
Distilled water	25 ml
Thioglycolic acid (100%)	0.5 ml

Volume was made up to 50 ml with distilled water

Chromogen working solution

Distilled water	20 ml
Saturated sodium acetate	20 ml
Chromogen reagent	4 ml

Iron standard solution

Distilled water	0.423 ml
HCl	0.027 ml
Stock iron solution	0.050 ml

50x Tris-acetate-EDTA (TAE) buffer

Tris base	242g
EDTA pH 8.0	0.5 M (100ml)
Glacial acetic acid	57.1 ml

Volume was made up to 1000 ml with distilled water, diluted 1x for working solution

RIPA buffer

NaCl	8.6 g
Tris HCl	1.6 g
EDTA.2H$_2$O	0.4 g
NP40	10 ml
20% SDS	5 ml

Volume was made up to 1000 ml with distilled water

Chapter 3

Hfe-dependent regulation of iron transfer

across the placenta

3.1 Introduction

Iron requirement during pregnancy in humans increases as the gestation progresses. The reasons for high iron requirements are mainly due to the expansion of blood volume in the mother and the transfer of iron to the growing foetus, which reaches a maximum limit during the third trimester (Hallberg 1988). Iron deficiency anaemia in pregnant mothers is common even in developed countries (Bothwell et al. 1979). This can result in premature birth, developmental problems in the foetus and risk of high blood pressure in adulthood (Crowe et al. 1995; Gambling et al. 2003 a).

A few studies suggest that more than 30% of women in their child bearing age in developed countries do not have adequate iron stores (Hallberg 1995; WHO 2001). WHO reported iron deficiency anaemia in 18% of pregnant women in industrialised countries (WHO 1993; 2001). Therefore, WHO has recently recommended iron-folic supplementation or fortification of staple food in areas where the prevalence of anaemia is more than 20% in women of child bearing age (WHO 2009). This shows the importance of iron in the diet of fertile women to start gestation with adequate iron stores in order to avoid prenatal iron supplementation, which is considered as controversial. Previous studies have shown the risk of increased oxidative stress and haem concentration affecting the health of pregnant women and foetal development, when given iron supplementation (Casanueva & Viteri 2003; Milman 2006).

Many proteins involved in iron influx and efflux across the apical (maternal side) and basolateral (foetal side) membranes of syncytiotrophoblasts have

been identified but there are still unanswered questions about the mechanism of regulation and transport of iron across the placenta. However, it has been postulated that in the syncytiotrophoblasts, iron is taken up by TfR1 (a protein important for cellular iron uptake) on the microvillar membrane, followed by internalization into the endosome. The release of iron into the cytosol probably occurs through DMT1 (an iron channel protein) after the acidification of the vesicle, and is transferred across the basolateral membrane via FPN1 (reviewed in Gambling et al. 2003 b).

HFE, a 343 amino acid membrane protein, mutated in hereditary haemochromatosis, predominantly expressed in liver hepatocytes (Zhang et al. 2004) is also found in placental syncytiotrophoblasts (Parkilla et al. 1997). It is believed that HFE competes with Tf to bind TfR1 on the apical side of the syncytiotrophoblasts (Feder et al. 1998). In a recent study, introduction of mutations into mice to strengthen the TfR1-HFE interaction showed that this interaction was responsible for hepcidin deficiency and iron-overload in mice (Schmidt et al. 2008). On the other hand, mice with mutations that interfere with the TfR1-HFE interaction or mice with higher HFE levels than normal had iron deficiency and high hepcidin levels. This provides strong evidence that HFE induces hepcidin expression that in turn regulates intestinal iron absorption. However, very little data is available on the role of HFE in regulating iron transport across the placenta.

The aim of this research is to identify the mechanism of iron transport across the placenta regulated by maternal or foetal *Hfe* and the effect of different levels of iron in the maternal diet.

3.2 Experimental design

All experimental procedures were approved and conducted in accordance with the UK Animals (Scientific Procedures) Act, 1986. *Hfe* knockout (KO) mice were used, which were mixed 129/Ola-C57BL/6 background strain, with a 2kb pgk-neor gene flanked by loxP sites replacing a 2.5kb BglII fragment (Bahram *et al,* 1999). *Hfe* KO mice were mated with wild type (WT) mice to produce progeny of heterozygous (HET). HET females were mated with HET males to produce progeny of all genotypes.

After weaning, 21 day old mice were fed a high iron diet (150ppm) for a week and the dams were divided into three groups. The three groups were fed on iron deficient (12.5ppm), normal/adequate (50ppm) or high iron (150ppm) diets. Three weeks later, dams of all genotypes were mated with HET males and were kept on their respective diet throughout pregnancy (Figure 3.1). The confirmation of pregnancy was detected by a vaginal plug and this day was denoted day 0.

Term in mice is 18 to 21 days, so we chose day 18 (D18) of gestation to sacrifice dams. On D18, dams from each group were anaesthetised with pentobarbitone. The foetuses were delivered by caesarean section and killed by decapitation. Dam's blood, liver, spleen, placenta and the foetal liver were

collected by Dr. Sara Balesaria, UCL Royal Free Campus, UK. After collection, tissues were snap frozen in liquid nitrogen and stored at -80°C until used. All animals were reared in a 12 hour light/12 hour dark cycle and given food and water *ad libitum.*

Mating

WT   *Hfe* KO

Progeny F1

HET   HET

Progeny F2

WT   HET   *Hfe* KO

After weaning, mice of each genotype, were fed on a high iron diet (150ppm) for a week

Female mice

WT   HET   *Hfe* KO   WT   HET   *Hfe* KO   WT   HET   *Hfe* KO
Iron deficient diet (12.5ppm)   Iron sufficient diet (50ppm)   High iron diet (150ppm)

Mice were given their respective diet for 3 weeks before mating with HET males and the diets were maintained throughout pregnancy until day 18 of gestation (D18). At D18 pregnant dams were sacrificed and their blood and tissues were collected including tissues from foetus

Figure 3.1 Schematic diagram showing the experimental design 1

WT dams were mated with Hfe KO males which produced progeny of HET mice. HET females were then mated with HET males to produce progeny of all genotypes. They were fed 150ppm dietary iron for one week after weaning. The dams were divided into 3 groups on the basis of iron content in diets. They were fed their respective diets for 3 weeks.

3.2.1 Experimental design to determine the effect of maternal genotype and dietary iron levels on maternal and foetal iron homeostasis

Female mice were divided into three groups and fed on diets with different iron content for three weeks. To study the effect of maternal *Hfe* on iron transport across the placenta, WT and *Hfe* KO dams were mated with HET males. From the progeny HET pups were selected. At D18, dams were sacrificed and the placenta and liver of HET pups were collected in order to keep the genotype of the foetus or pups same, Figure 3.2 (a). Blood, liver and spleen of pregnant dams were also collected.
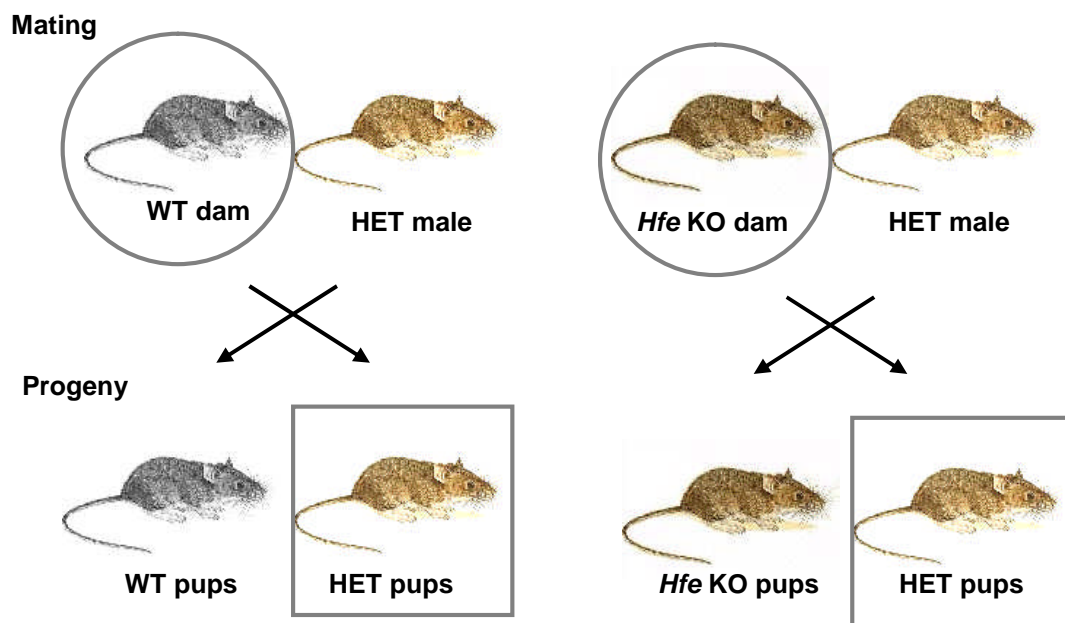
Figure 3.2 (a) Schematic diagram showing the experimental design 2 (a)
WT and Hfe KO dams were mated with HET males and HET pups were selected from the progeny. On D18, dams were sacrificed and their blood and tissues were collected. Placental and hepatic tissues of HET pups were also collected.

3.2.2 Experimental design to determine the effect of foetal genotype and dietary iron levels on maternal and foetal iron homeostasis

To determine the effect of foetal *Hfe*, HET dams were mated with HET males. From the progeny, WT and *Hfe* KO pups were selected and their placental and hepatic tissues were collected after the pregnant dams were sacrificed on D18 of gestation, Figure 3.2 (b).
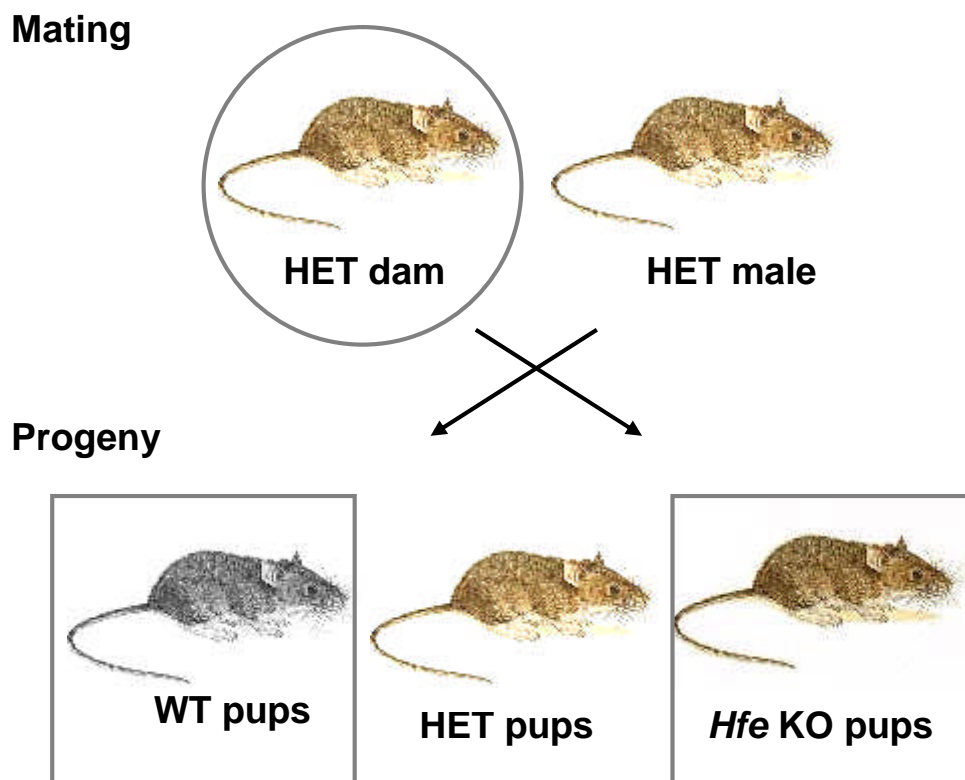
Figure 3.2 (b) Schematic diagram showing the experimental design 2 (b)
HET dams were mated with HET males to produce progeny of all genotypes. On D18 of gestation, dams were sacrificed and their blood and tissues were collected. Placental and hepatic tissues of WT and Hfe KO pups were also collected.

3.3 Results

3.3.1 Effect of maternal genotype and different dietary iron levels on maternal and foetal iron homeostasis

3.3.1.1 Serum iron levels and transferrin saturation of WT and *Hfe* KO pregnant dams

At term (D18), serum iron levels in WT pregnant dams fed on an iron deficient diet (12.5ppm) was the lowest. In the second group of WT dams fed on normal dietary iron, there was a trend towards increased iron levels in serum but the difference did not reach significance between WT pregnant dams fed on low and normal iron diets. However, in WT dams, the level of serum iron increased significantly from 39.87 µg/dL to 104.42 µg/dL (p=0.01) when fed 12.5ppm and 150ppm iron in diets, respectively. It appeared that serum iron levels in *Hfe* KO dams, fed 12.5ppm and 150ppm iron diets, differed largely ranging from 38.79 µg/dL to 181.53 µg/dL (p=0.0002), respectively. Overall, *Hfe* KO dams had higher iron levels in their serum as compared with WT except when fed an iron deficient diet, Figure 3.3 (a).

Transferrin saturation (TFS) in the serum of WT pregnant dams seemed to increase with the increase in dietary iron intake but the difference was not significant between WT dams fed on 12.5 and 50ppm dietary iron. The difference was found to be significant (p=0.01) between WT pregnant dams fed on 12.5ppm and 150ppm iron content in diets. Surprisingly, it did not alter

in *Hfe* KO dams ingesting varying levels of iron in diet and was not correlated with the serum iron levels. Moreover, TFS was also affected by *Hfe* status of the dams as were serum iron levels with an increased concentration found in *Hfe* KO as compared with WT dams, Figure 3.3 (b). Together these findings suggest that HFE status and increased dietary iron can result in increased circulation of iron in the body during pregnancy.
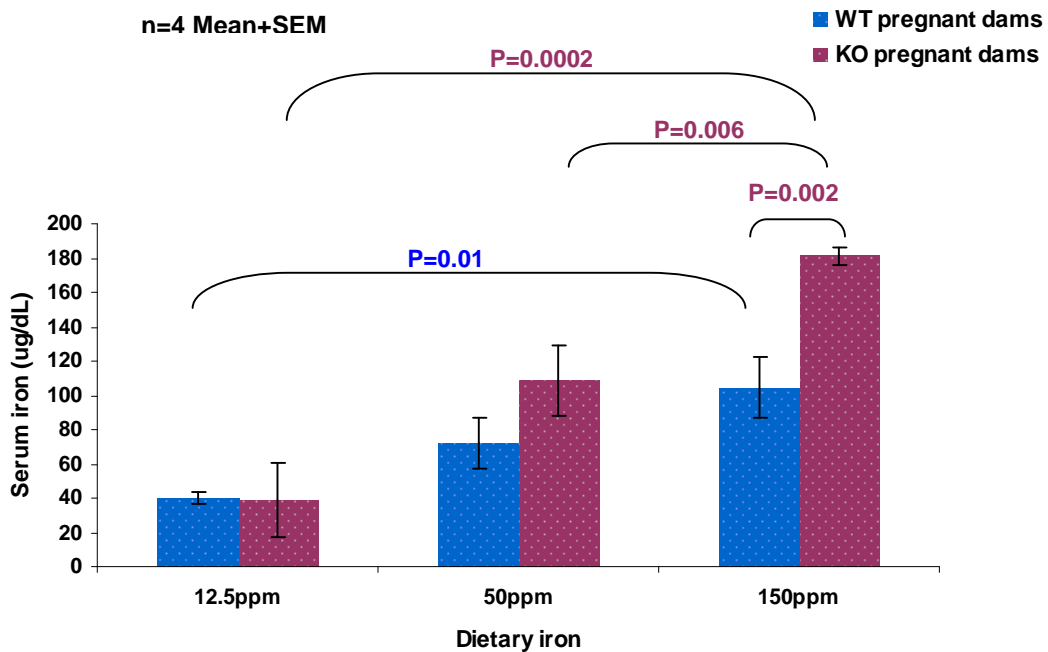
Figure 3.3 (a) Serum iron levels in WT and *Hfe* KO pregnant dams fed different levels of dietary iron.

Serum was separated from the blood taken from WT and Hfe KO pregnant dams on D18 of gestation. Iron level in serum seems to be increased with the increase in dietary iron content irrespective of maternal genotype. Bars denote mean ± SEM of four samples from each group. p value in magenta colour shows the significance difference between the Hfe KO dams while p value in blue colour represents the difference between WT dams fed diets containing different iron content.
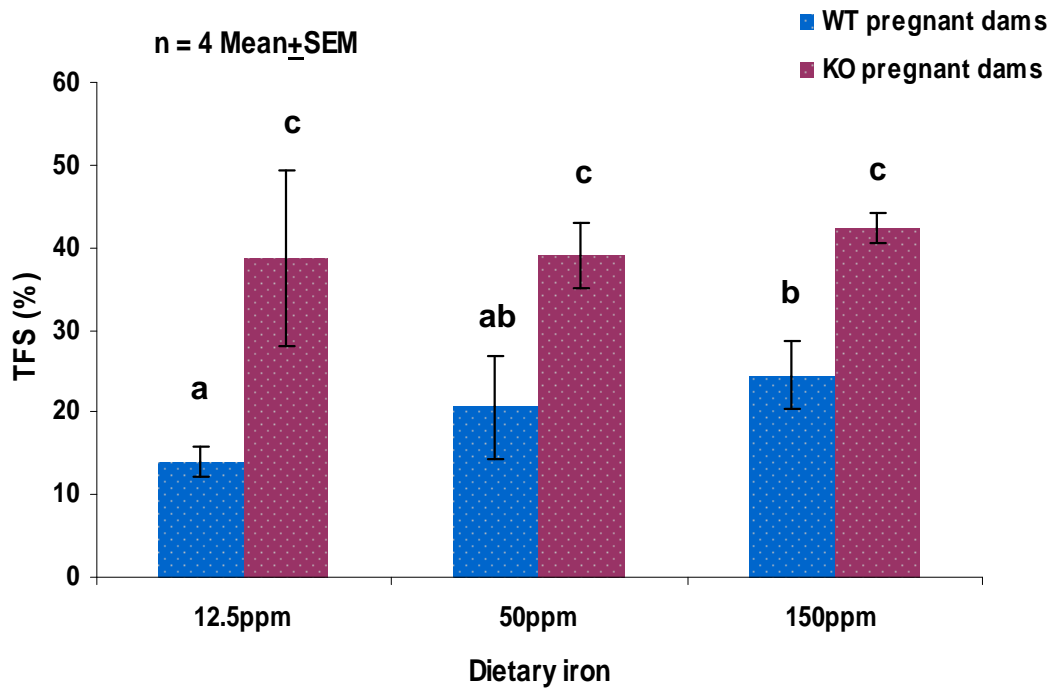
Figure 3.3 (b) Transferrin saturation in the serum of WT and *Hfe* KO pregnant dams

Serum was separated from the blood taken from WT and Hfe KO pregnant dams on D18 of gestation .Pregnant dams lacking Hfe have significantly higher TFS in their serum as compared with WT dams but this does not seem to be affected by the dietary iron content. Bars show mean $\pm$ SEM and statistically significant values between each iron diet and each genotype are indicated by different letters above the bars ($p<0.05$; n = 4). However, letters ab indicate that there is no significant difference between a and ab; ab and b.

3.3.1.2 Liver and spleen iron levels of WT and *Hfe* KO pregnant dams

Iron in liver was measured in order to determine the effect of dietary iron content and the role of maternal genotype. On a low iron diet, dams from both genotypes stored almost the same amount of iron in their livers. However, as the iron content increased in the diet, *Hfe* KO dams started storing more iron in their liver as compared with WT dams, Figure 3.4 (a). The iron content increased almost 2 fold in *Hfe* KO pregnant dams fed a high iron diet and correlated with high serum iron and TFS levels (unpublished data taken from Dr. Balesaria)

Spleen iron levels seemed not to be affected by the genotype of the dams. However, spleen from the dams of both genotypes fed a diet with 150ppm iron had higher iron content, Figure 3.4 (b).
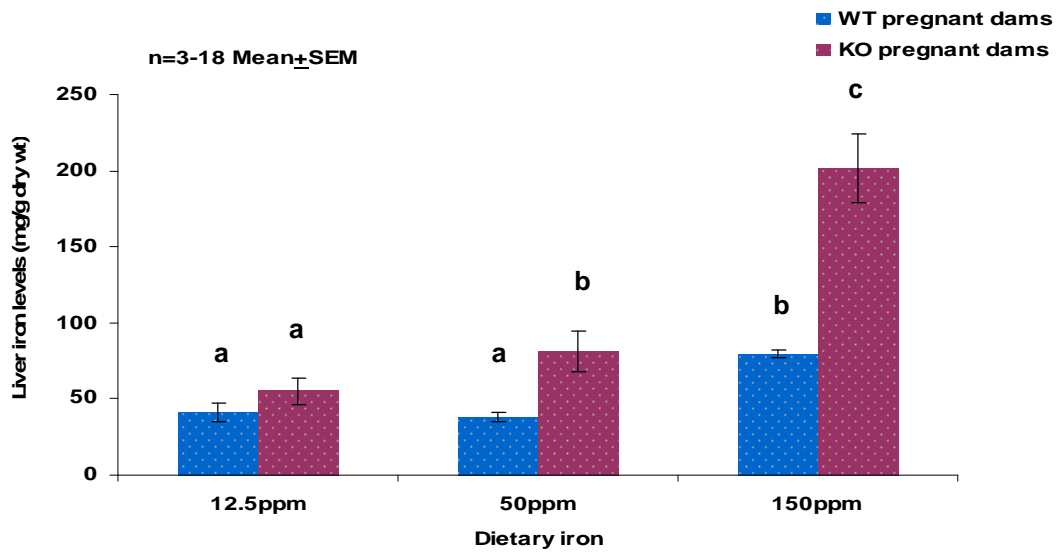
Figure 3.4 (a) Liver iron levels of WT and *Hfe* KO pregnant dams fed on diet containing 12.5ppm, 50ppm or 150ppm iron

WT dams fed a diet with 50ppm or 150ppm iron content have significantly lower hepatic iron storage as compared with Hfe KO dams. Statistically significant values (p<0.05) between dams of each genotype fed different dietary iron content are indicated by different letters (a, b or c) above the bars representing mean±SEM.
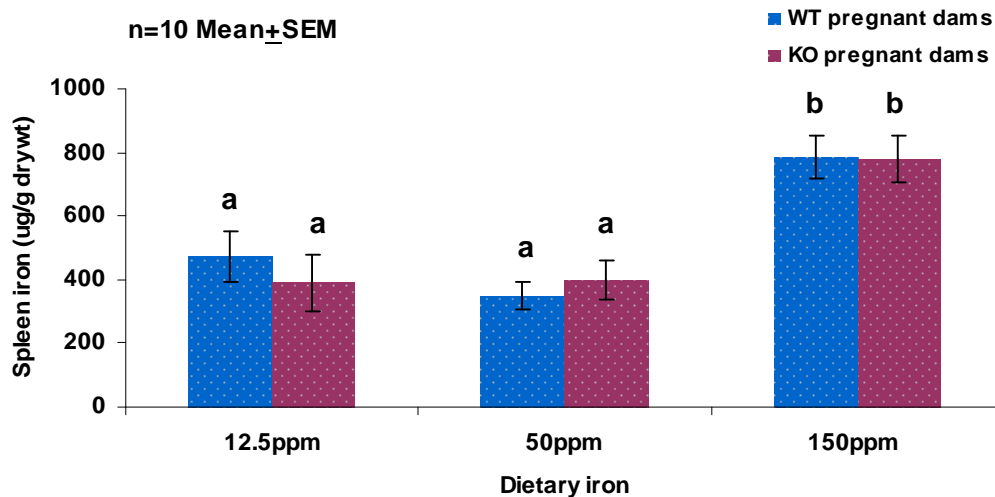
Figure 3.4 (b) Spleen iron levels of WT and *Hfe* KO pregnant dams fed on diet containing 12.5ppm, 50ppm or 150ppm iron

Genotype does not seem to affect the spleen iron storage. However, dams fed on a diet with 150ppm iron content have higher iron storage in their spleen than dams fed 12.5 and 50ppm dietary iron. Bar represents mean ± SEM of 10 samples and different letters (a,b,or c) above the bars shows significant difference between dams of both genotypes fed different iron content in diets.

3.3.1.3 Placental iron levels of HET pups from WT and *Hfe* KO dams

To further investigate whether the placenta is storing more iron, placental iron levels were measured when the *Hfe* KO dams have higher liver and serum iron levels. When fed a normal iron diet (50 ppm), the placenta of HET pups from *Hfe* KO mice have higher iron levels as compared with the placenta from WT dams. In contrast, HET foetuses from dams of both genotypes fed 150ppm dietary iron content have the same amount of iron in their placenta as shown in Figure 3.5.
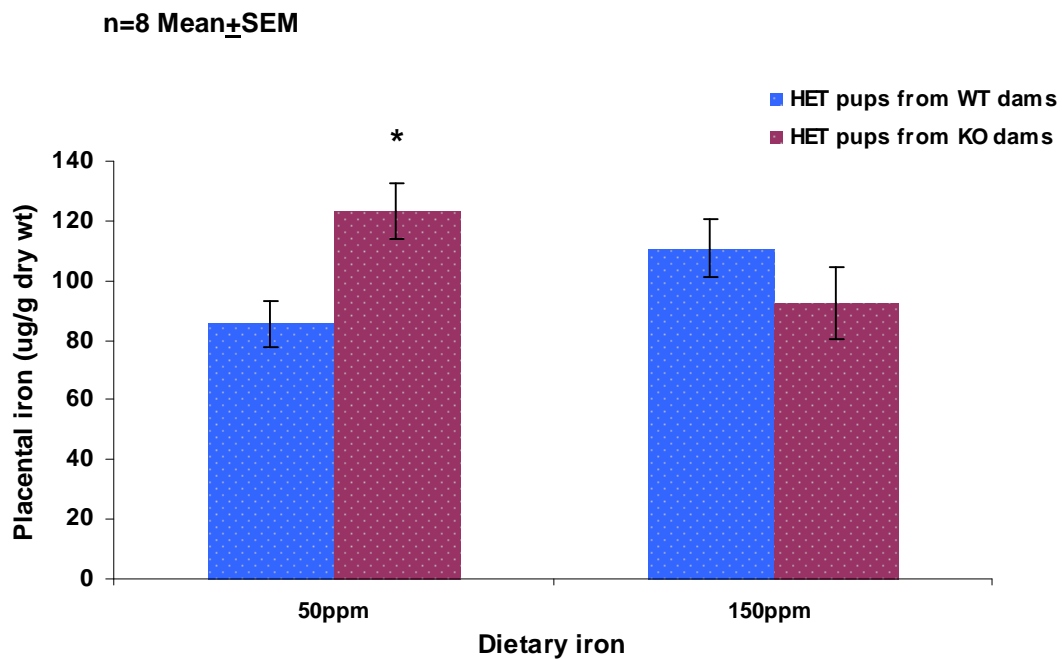
Figure 3.5 Placental iron levels in HET pups from WT and *Hfe* KO dams

*Placenta was collected at D18 of gestation and iron was quantified. When fed a normal iron diet, the placenta of HET pups from Hfe KO mice have more iron as compared to WT dams. Placenta has almost same amount of iron regardless of genotypes of the dams when fed a high iron diet. Bars represent mean ± SEM of 8 samples from each category and * shows significant difference at p-value 0.01.*

3.3.1.4 Placental gene expression of HET pups from WT and *Hfe* KO dams fed a diet containing 12.5ppm, 50ppm or 150ppm iron

Transcript levels of *TfR1,* an iron uptake membrane protein, *DMT1+IRE,* an intracellular metal transporter, and *FPN1,* an iron efflux protein, were measured by RT-PCR. *DMT1+IRE* expression was increased about two-fold in HET pups from *Hfe* KO dams compared to HET pups from WT dams fed an iron deficient diet (P=0.04). However, neither *FPN1* nor *TfR1* mRNA expression altered significantly in HET pups from the two different genotypes of dams fed iron deficient diet, Figure 3.6 (a). When the dams were fed a normal iron diet, the mRNA expression of the above mentioned iron transporter genes was up-regulated in the placenta of HET pups from *Hfe* KO dams compared to HET pups from WT dams indicating that maternal *Hfe* regulates important iron transporter genes. There was a significant increase of almost two-fold in mRNA expression of all the genes tested, Figure 3.6 (b).

HET pups from *Hfe* KO dams fed a high iron diet have significantly higher placental *FPN1* mRNA expression (p=0.01) than HET pups from WT dams and no significant difference was found in *TfR1* and *DMT1+IRE* expression between the pups from WT and *Hfe* KO mothers (P≥0.05), Figure 3.6 (c).

(a)

12.5ppm dietary iron
n=6 Mean±SEM

(b)

50ppm dietary iron
n=9 Mean±SEM

(c)

150 ppm dietary iron
n=9 Mean±SEM

- HET pups from WT dams
- HET pups from KO dams

Relative gene expression/B-actin
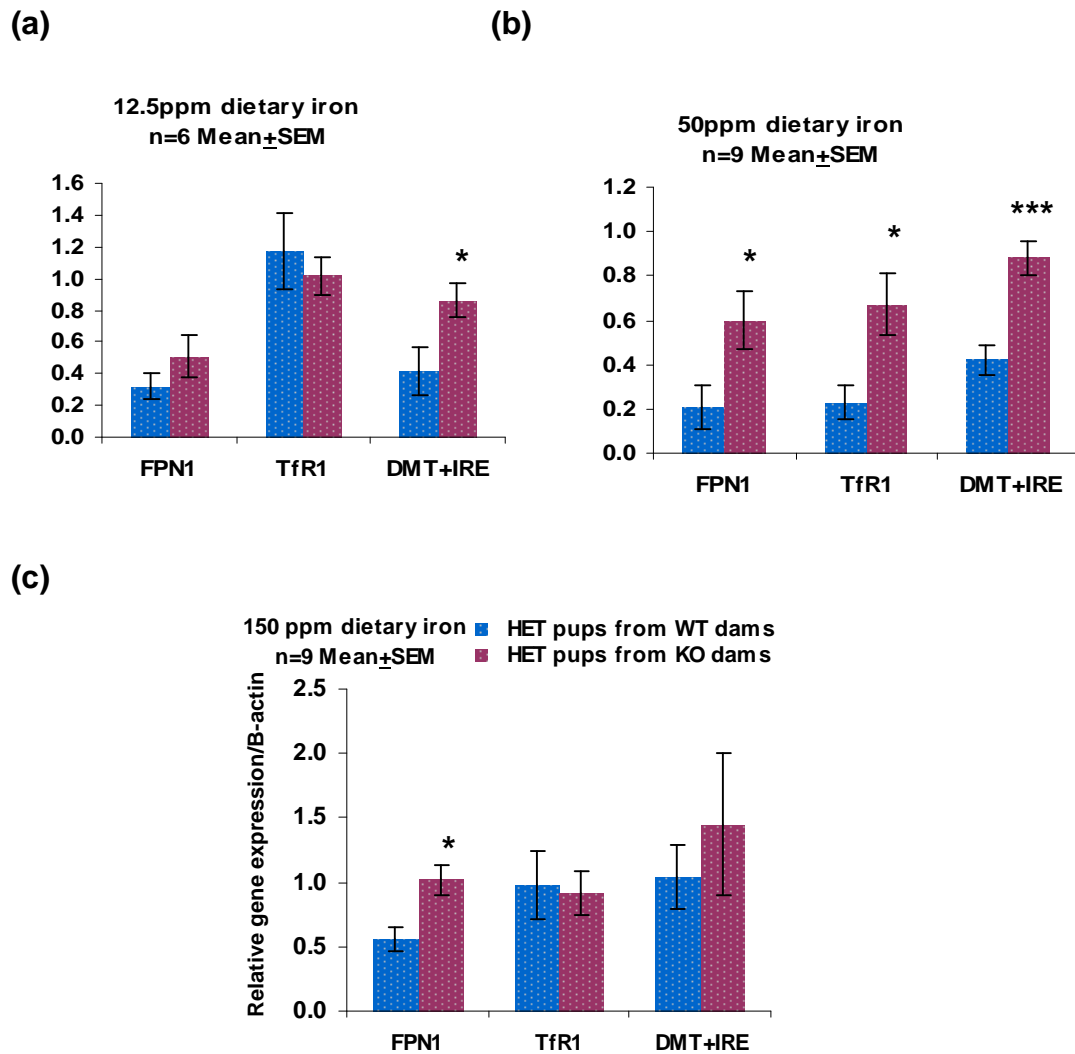
Figure 3.6 Relative placental gene expression in HET pups from *Hfe* KO and WT dams fed diets with different iron contents

*mRNA expression of FPN1, TfR1 and DMT1+IRE in placenta was analysed by RT-PCR (a) Placental expression of DMT1+IRE was significantly decreased in HET pups from WT dams fed an iron deficient diet, whereas no change was observed in FPN1 and TfR1 expression levels. (b) Expression of FPN1, TfR1 and DMT1+IRE was significantly higher in the placenta of HET pups from Hfe KO dams as compared to pups from WT dams fed an iron sufficient diet. (c) When the dams were fed a high iron diet, placental FPN1 expression was higher in HET pups from Hfe KO dams. Bars indicate mean±SEM. * denotes significant difference between the groups at p<0.05 while *** denotes p<0.0001.*

3.3.1.5 Comparison of placental gene expression in HET pups from WT and *Hfe* KO dams fed different amounts of iron in the diet

The placental *FPN1* mRNA expression was compared in the HET pups from dams of different genotypes fed 12.5ppm, 50ppm and 150ppm dietary iron. Overall there was higher placental *FPN1* expression in HET pups from *Hfe* KO dams as compared with HET pups from WT dams fed normal or high iron diets. When fed an iron deficient diet, the difference in the expression of FPN1 mRNA did not reach significance, Figure 3.7.
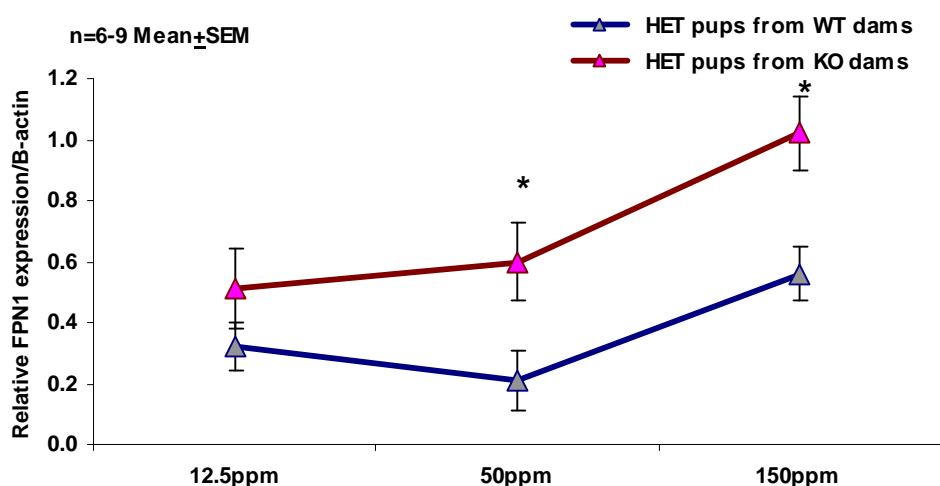
Figure 3.7 Comparison of placental *FPN1* mRNA expression in HET pups from WT and *Hfe* KO dams

*Line graph represents Mean+SEM and shows higher placental FPN1 mRNA expression in HET pups from Hfe KO dams as compared with HET pups from WT dams fed normal or high iron diets. * denotes significant difference between the groups at p<0.05.*

TfR1 mRNA expression was down-regulated in the placenta of HET pups from WT dams fed a normal iron diet as compared with pups from WT dams on iron deficient and supplemented diets. There was not any significant difference in the *TfR1* mRNA expression in HET pups from KO dams raised on varying iron diets, Figure 3.8.
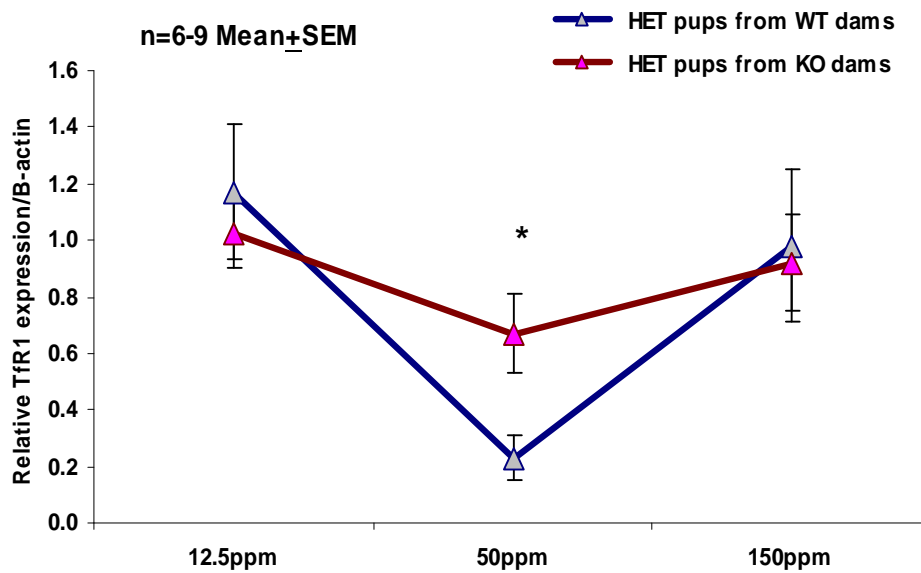
Figure 3.8 Comparison of *TfR1* mRNA expression in HET pups from WT and *Hfe* KO dams on varying iron diets

Line graph represents Mean+SEM and shows lower TfR1 *mRNA expression in HET pups from WT dams fed 50ppm dietary content. * denotes significant difference between the groups at p<0.05.*

When fed iron deficient and normal diet, placental *DMT1+IRE* expression was significantly higher in HET pups from *Hfe* KO dams as compared with the placenta from WT dams. On iron sufficient diet (150ppm), due to higher variation in the results, the difference in the *DMT1+IRE* expression between the placenta of HET pups from WT and *Hfe* KO did not reach significance. However, placental *DMT1+IRE* mRNA expression was increased in HET pups from both genotypes of dams (WT and *Hfe* KO) fed on 150ppm iron diet as compared with pups from dams fed 12.5 and 50ppm iron content in diet, Figure 3.9.
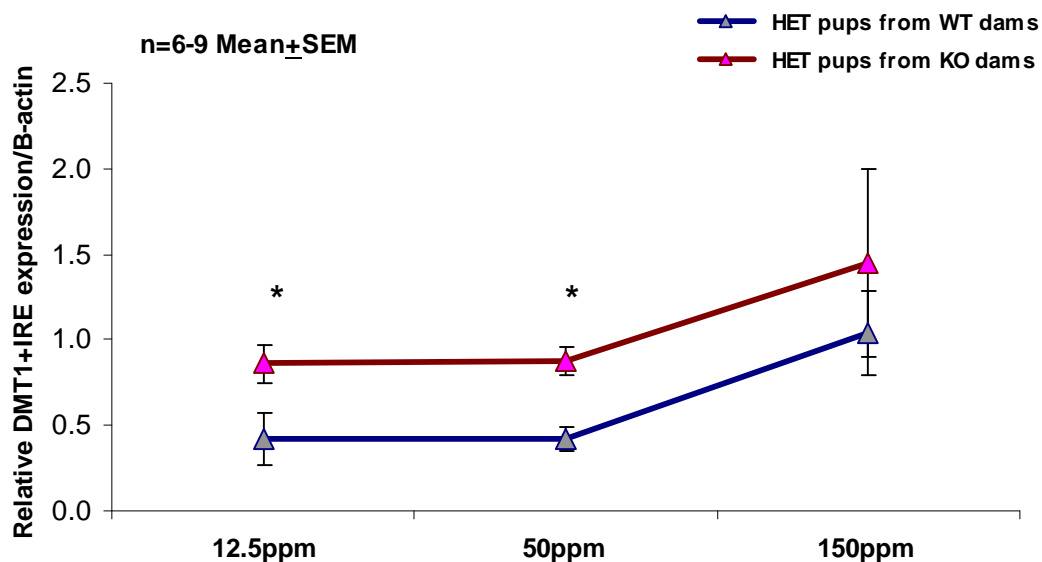
Figure 3.9 Comparison of *DMT1+IRE* mRNA expression in HET pups from WT and KO dams on varying iron diets

Line graph represents Mean+SEM and shows increased DMT1+IRE *mRNA expression in HET pups from WT dams fed 12.5, 50 and 150ppm iron content in diet. * denotes significant difference between the groups at p<0.05.*

3.3.1.6 Placental FPN1 protein expression in HET pups from WT and *Hfe* KO dams fed different amounts of iron in the diet

FPN1 protein was expressed in all samples. The amount of FPN1 protein was higher in the placenta of HET pups from *Hfe* KO dams as compared with the HET pups from WT dams fed the three different iron diets, Fig 3.10 (a) and (b).
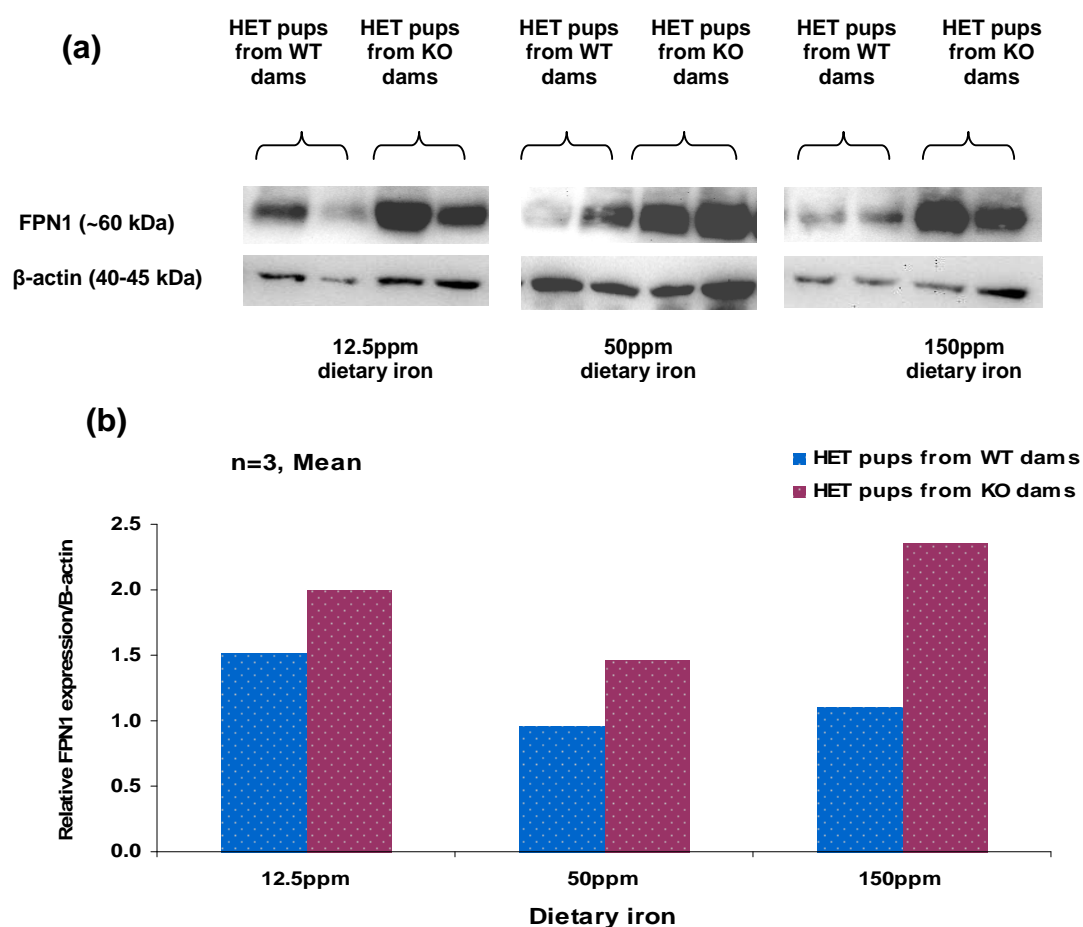
Figure 3.10 Placental FPN1 protein expression of HET pups from WT and HFE KO dams fed different dietary iron

(a) Western blot revealing protein expression of FPN1 (~60kDA) and β-actin (40-45kDa) in placental tissues of HET pups from WT and HFE KO dams. Lanes 1and 2 correspond to FPN1 protein expression in placenta of HET pups from WT dams and lanes 3 and 4 correspond to HET pups from HFE KO dams fed different dietary iron probed with antibody against FPN1. (b) Histogram of relative FPN1 protein expression showing lower protein expression in HET pups from WT dams fed different dietary iron. Histogram represent mean of 3 samples from each group.

3.3.1.7 Liver iron levels of HET pups from WT and *Hfe* KO dams

To analyse the effect of maternal genotype on foetal liver iron stores, liver iron levels of HET pups from WT and *Hfe* KO dams were determined. Foetal liver iron levels indicated that maternal genotype had an effect on iron accumulation in foetal liver because HET pups from *HFE* KO dams had significantly higher liver iron content than HET pups from WT dams fed either 50 or 150ppm iron diet. No significant difference was found in the foetal liver iron level when the dams were fed an iron deficient diet (12.5ppm iron diet), Figure 3.11. This might be because dams of both genotypes struggled to transfer iron to their foetuses. Foetal liver iron level in HET pups from dams of both genotypes, fed an iron deficient diet, had significantly lower iron storage in liver than pups from dams fed an iron adequate or replete diet.
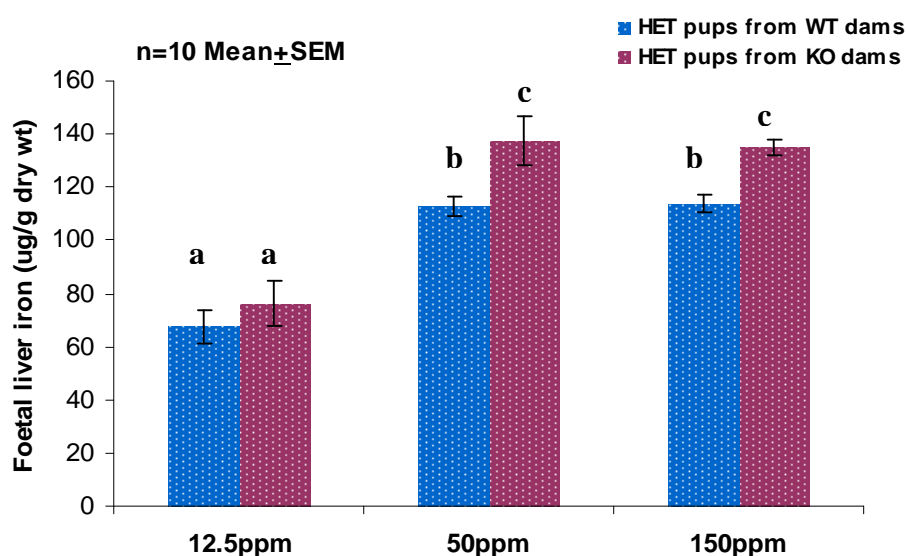
Figure 3.11 Liver iron levels of HET pups from WT and *Hfe KO* dams fed 12.5, 50 or 150ppm iron diets

When the pregnant dams from both genotypes were fed 50ppm and 150ppm dietary iron, HET pups from KO dams had significantly higher liver storage. Bars indicate mean±SEM. Different letters (a,b,c) above the bars shows significant difference at p<0.05.

3.3.2 Effect of foetal/pup's genotype and dietary iron levels on iron homeostasis in the mother and foetus

3.3.2.1 Serum iron concentration and transferrin saturation of pregnant HET dams fed different dietary iron

At term, HET dams fed a high iron diet had more serum iron and higher transferrin saturation in their circulation than HET dams fed deficient or normal iron diets, Figure 3.12 (a) and (b).

(a)   **(b)**
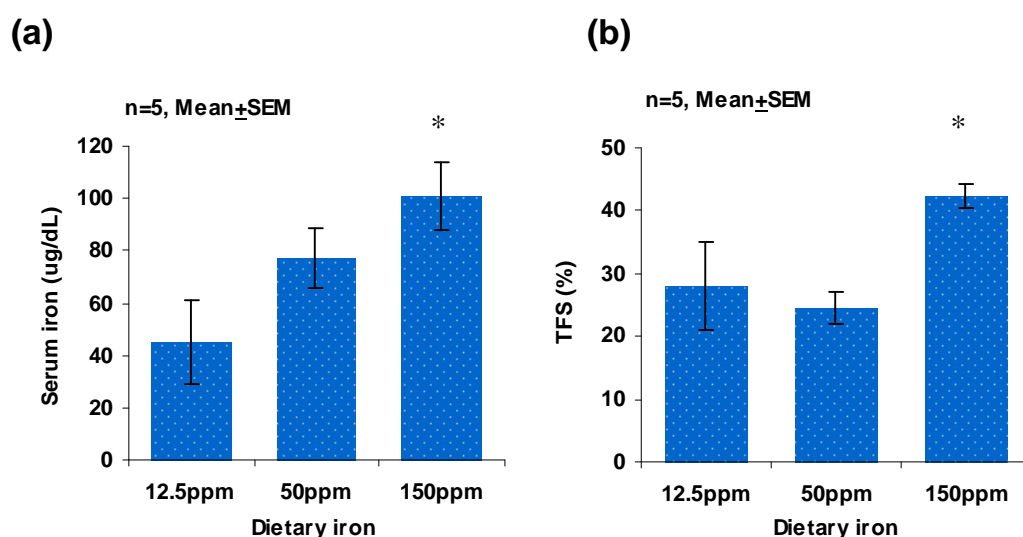
Figure 3.12 Serum iron concentration and percent TFS in pregnant HET dams
*(a) Serum iron levels in pregnant HET dams fed different dietary iron. Serum was separated from the blood to measure the iron levels. An increase in dietary iron increased the iron circulation in the body (as measured by iron presence in the serum). * represents difference between serum iron levels of HET dams fed an iron replete and deficient diet at p-value 0.03 (b) Transferrin saturation of iron in the serum of pregnant HET dams. When fed an iron replete diet, HET pregnant dams showed an increase in TFS level. Bars represents mean+SEM of 5 samples and * show the significance difference between serum iron levels of HET dams fed an iron replete and deficient diet.*

3.3.2.2 Liver and spleen iron levels of pregnant HET dams

High iron concentration in the circulation of pregnant HET dams, fed a high iron diet resulted in high iron storage in the maternal liver and spleen as compared with HET dams fed a deficient or normal iron diets, Figure 3.13 (a) and (b).

(a)   **(b)**
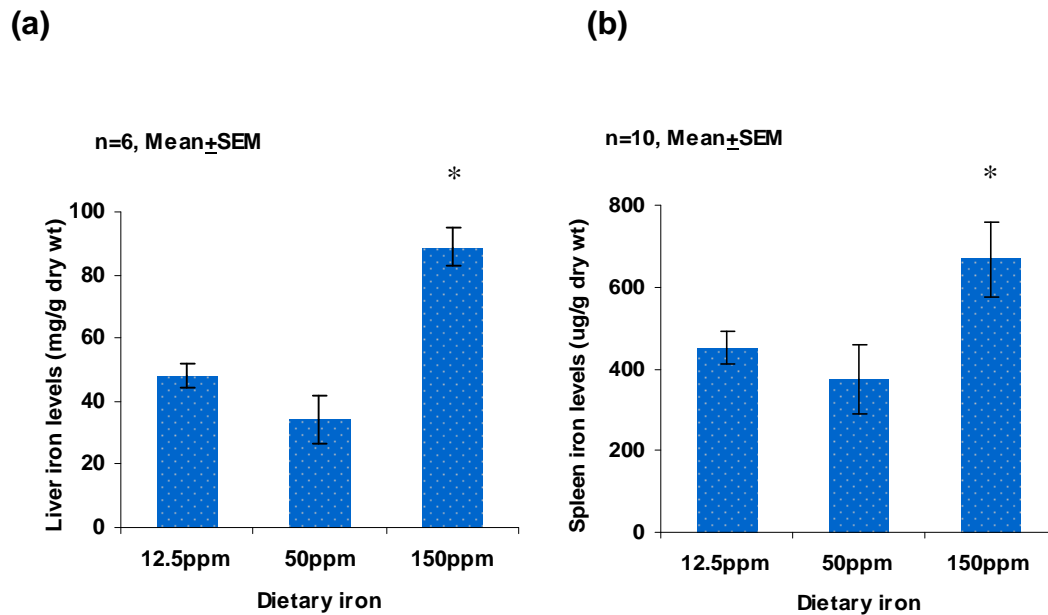
Figure 3.13 Liver and spleen iron levels in pregnant HET dams fed varying levels of dietary iron

*(a) Livers from pregnant HET dams were collected on D18 of gestation and iron level was measured by spectrophotometric analysis. Dams on a high iron diet had significantly higher liver iron storage. (b) Similarly, spleen iron levels were higher in dams fed a diet with 150ppm iron content. Bars represents mean+SEM and * show the significance difference between liver and spleen iron levels of HET dams on replete iron diet as compared with dams on iron deficient or sufficient diets.*

3.3.2.3 Placental iron levels of WT and *Hfe* KO pups from HET dams

Placental iron levels did not appear to be affected by the dietary iron and

genotype of the pups from HET dams, Figure 3.14.
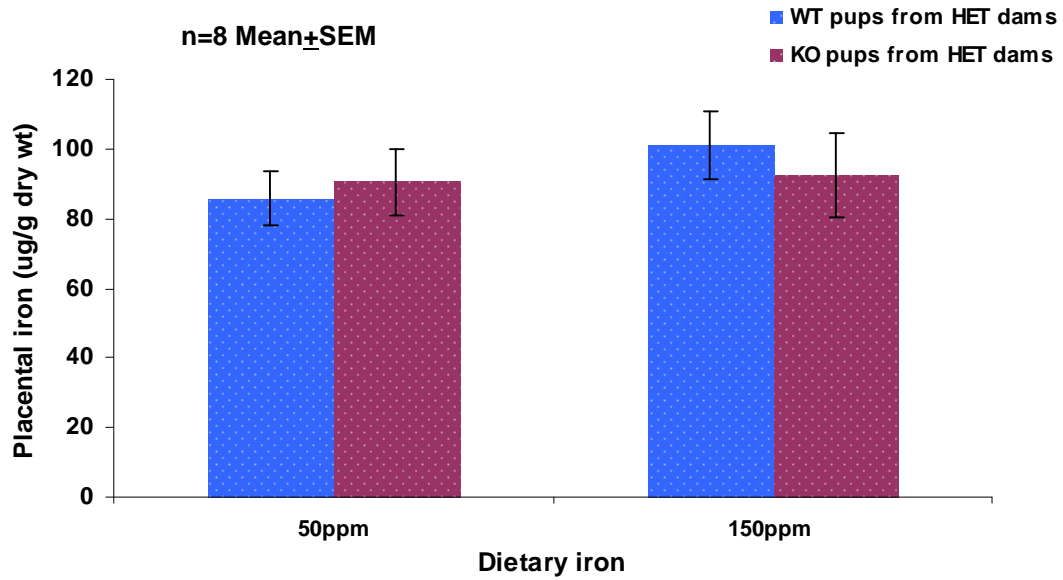
Figure 3.14 Placental iron levels of WT and *HFE* KO pups from HET dams

Placenta was collected at D18 of gestation and iron was quantified. The placenta stored almost the same amount of iron regardless of genotype of the pups or the diet of the dams. Bars represent mean ± SEM of 8 samples from each category.

3.3.2.4 Placental gene expression in WT and *Hfe* KO pups from HET dams

Placental *FPN1*, *TfR1* and *DMT1+IRE* mRNA expression did not appear to alter significantly in WT and *Hfe* KO pups from HET dams that were fed an iron deficient or a normal diet, Figure 3.15 (a) and (b). There was a significantly higher expression of *DMT1+IRE* mRNA in *Hfe* KO pups from HET dams raised on a 150ppm iron diet (p=0.001) as compared with the WT pups from HET dams, Figure 3.15 (c).

(a)

12.5ppm dietary iron
n=6 Mean±SEM

Relative gene expression/B-actin

FPN1   TfR1   DMT+IRE

(b)

50ppm dietary iron
n=7 Mean±SEM

Relative gene expression/B-active

FPN1   TfR1   DMT+IRE

(c)

150ppm dietary iron
n=8 Mean±SEM

■ WT pups from HET dams
■ KO pups from HET dams

**

Relative gene expression/B-actin

FPN1   TfR1   DMT+IRE
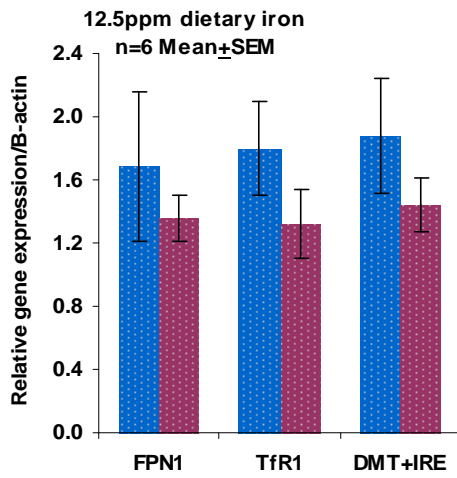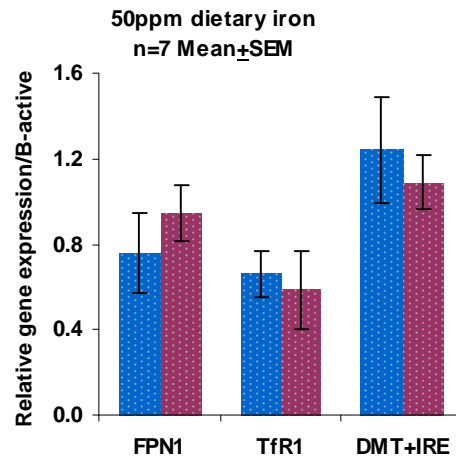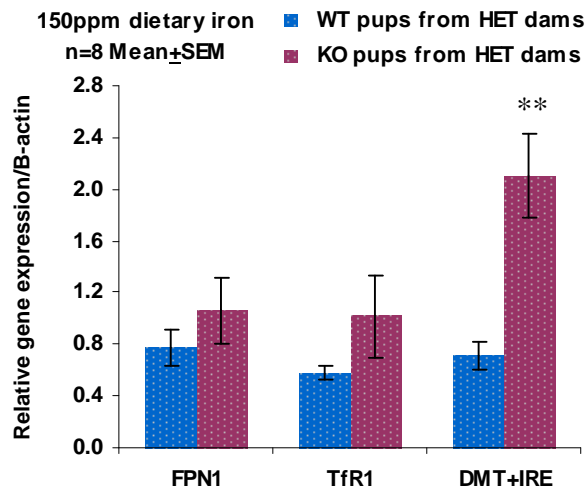
Figure 3.15 Relative placental gene expression in WT and *Hfe* KO pups from HET dams fed diets with 12.5ppm, 50ppm or 150ppm iron content

*** denotes significant difference between the two group with P < 0.001 and bar indicated mean of 6 with SEM.*

3.3.2.5 Placental FPN1 protein expression in WT and *Hfe* KO pups from HET dams fed different dietary iron

FPN1 protein expression seemed to be higher in the placenta of WT pups from HET dams fed low or normal dietary iron. However, when the dams were fed high iron diet FPN1 protein was increased in the *Hfe* KO pups of Het dams. The western blot image showing FPN1 and β-actin bands is shown in Figure 3.16 (a) and the histogram is shown in Figure 3.16 (b).
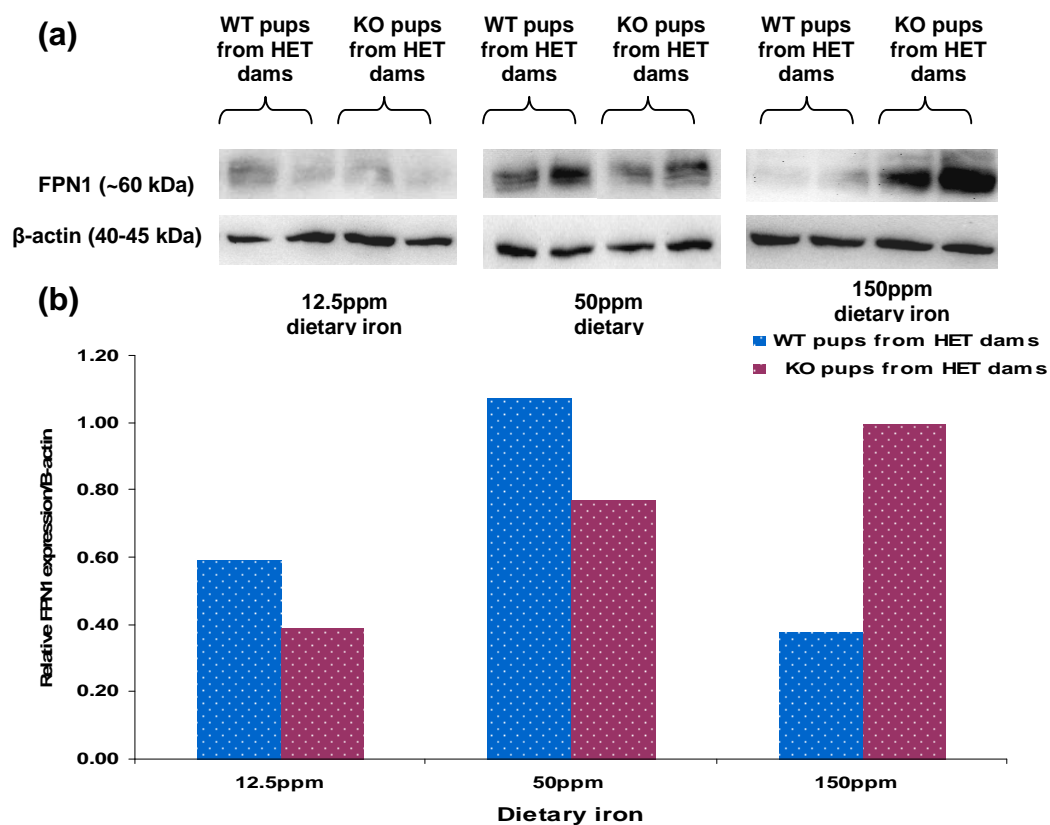
Figure 3.16 Placental FPN1 protein expression of WT and *Hfe* KO pups from HET dams

(a) Western blot revealing protein expression of FPN1 (~60kDA) and β-actin (40-45kDa) in placental tissues of WT and Hfe KO pups from HET dams. Lanes 1and 2 correspond to FPN1 protein expression in placenta of WT pups from HET dams and lanes 3 and 4 correspond to Hfe KO pups from HET dams fed different dietary iron. (b) Histogram of relative FPN1 protein expression and Bars represent mean of 3 samples from each group.

3.3.2.6 Liver iron levels of WT and *Hfe* KO pups from HET dams

To study the effect of foetal *Hfe*, HET dams were mated with HET males and foetuses with *Hfe* KO and WT genotypes were selected and their liver iron levels were quantified. Results showed that liver iron accumulation was highest in *Hfe* KO pups from HET dams fed a diet with a high iron content (150 ppm), Figure 3.17.
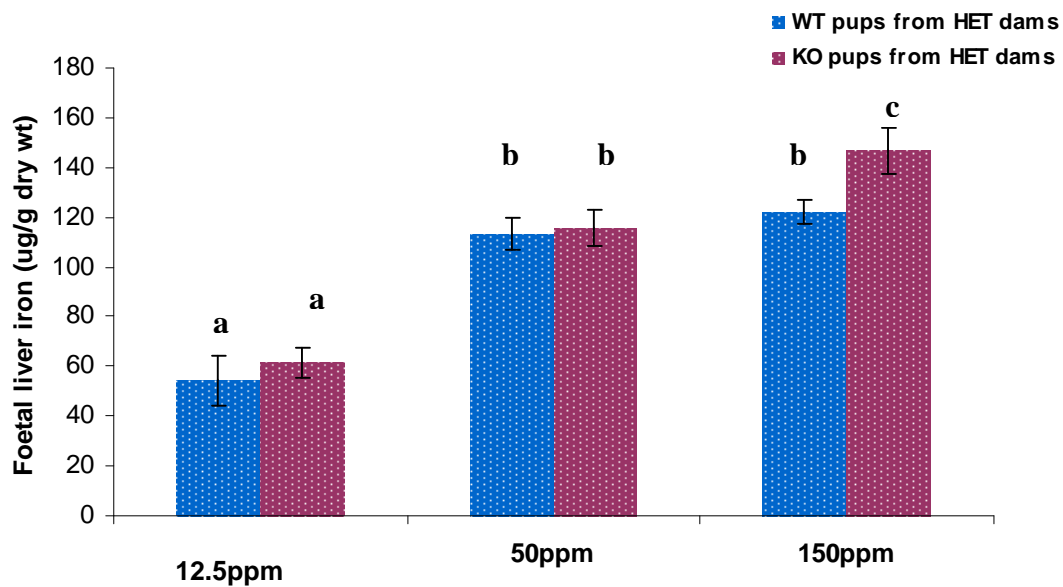
Figure 3.17 Liver iron levels of KO and WT pups from HET dams fed 12.5, 50 or 150ppm iron in their diet

KO pups from HET dams had high liver iron than Wt pups from HET dams. Bars indicate mean iron levels in ug/g dry weight and different letters (a,b,c) show significance difference at p<0.05. The same letters show the difference is not significance.

3.4 Discussion

During the third trimester of pregnancy, iron is transported from mother to foetus against a concentration gradient. It is clear from previous studies that iron transport across the placenta is regulated to avoid iron deficiency or overload which can affect the development and function of red blood cells, brain, heart and liver of the foetus (Grantham-McGregor and Ani 2001; Choi et al. 2000). The mechanism by which *Hfe,* a negative iron regulator and modulator of hepcidin production, regulates iron homeostasis in mothers and foetuses is not clearly understood. In a previous study, Prof. Srai and colleagues were able to infer by correlation data that foetal liver starts regulating placental iron uptake when the mothers are given iron deficient and supplemented diets (Gambling et al. 2001, 2009). Based on these studies they proposed that foetal liver iron levels, by regulating hepcidin, were involved in regulating iron transfer across placenta. In the current study, the mating strategy between WT, HET and *Hfe* KO mice fed different dietary iron levels has allowed us to confirm the involvement of foetal liver in iron supply to the foetus. Our results have also shown that maternal *Hfe* status and dietary iron levels play an active role in placental iron transport and maintaining foetal iron homeostasis.

Previously it had been shown that iron absorption increases in the maternal gut during pregnancy (O' Brien et al. 2003; Gambling et al. 2009) with an up-regulation of *DMT1*, *Dcytb* and *FPN1* expression in the duodenum of pregnant WT dams (S. Balesaria, unpublished data). Here, we have found that during pregnancy maternal serum iron levels, transferrin saturation and body iron

stores depend on adequate dietary iron intake. WT pregnant dams' serum iron levels, transferrin saturation and liver iron stores increased significantly when fed a high iron diet as compared with dams fed an iron deficient diet. A number of studies in pregnant women have shown the beneficial effects of iron supplements including increased iron in the maternal circulation and reduced prevalence of anaemia (Bothwell et al. 1979; Sloan et al. 1992; Yip 1996; Cogswell et al. 2003). Previous studies have shown *Hfe* KO non-pregnant mice accumulating more iron in their liver and increased serum iron levels (Vujic Spasic et al. 2007). We have confirmed this in *Hfe* KO pregnant dams with high serum iron and increased liver iron storage compared with WT pregnant dams and these two parameters increased with the increase in dietary iron content. These results are in agreement with previous findings where low hepatic hepcidin expression during pregnancy (Rehu et al. 2010) and mutation in *Hfe* increased duodenal iron absorption which leads to high maternal serum iron levels (Vujic Spasic et al. 2007). This was further confirmed in a parallel study by Dr. S. Balesaria (unpublished data), who has found up-regulation *in DMT1, Dcytb* and *FPN1* expression in the duodenum of pregnant *Hfe* KO pregnant dams as compared with non-pregnant dams. When pregnant dams are fed a low iron diet, iron transport to the foetus seems to be provided by the maternal body iron stores (liver) resulting in low maternal hepatic iron levels in both WT and *Hfe* KO dams.

Iron transport across the placenta is mainly a function of three major transporter proteins: TfR1 (iron uptake membrane protein), DMT1 (intracellular metal transporter) and FPN1 (iron efflux protein) (Bergamaschi et

al. 1990; Georgieff 2000; Petry et al. 1994; Verrijt et al. 1999). In order to protect the foetus from iron deficiency or overload, these proteins are regulated in the placenta (Georgieff et al. 2000; Donovan et al. 2000, Gambling et al 2003). To further understand the role of maternal *Hfe* status and dietary iron on the expression of these transporters in the placenta, their mRNA levels were determined. Our results show that *TfR1*, *DMT1* and *FPN1* gene expression was higher in HET foetuses from *Hfe* KO dams fed a normal dietary iron, with higher placental iron levels, in comparison with those derived from WT dams. When fed a high iron diet, the expression of placental FPN1 was up-regulated in the *Hfe* KO dams but placental iron levels remained the same. This correlates very well with the FPN1 protein expression in the placenta of foetuses from *Hfe* KO dams. These data suggest that increased iron transport across the placenta may be due to increased FPN1 expression under iron-replete conditions; this was in contrast with dams fed a low iron diet as also shown in a previous study (O' Brien et al. 2003). HET foetuses from *Hfe* KO dams fed normal and high iron diets had high hepatic iron stores and higher body weights than those derived from WT dams fed all three different iron diets (S. Balesaria unpublished data). A study in humans has demonstrated that babies born from mothers with mutant forms of *HFE* had higher body weights at the time of birth (Dorak et al. 2009). In conclusion, maternal genotype and dietary iron intake play an important role in regulating placental iron transport and foetal iron accumulation.

To determine the effect of foetal *Hfe* status in regulating placental iron transport, iron transporter expression in placenta of WT and *Hfe* KO foetuses

derived from HET dams were determined in addition to the measurement of maternal iron levels and foetal iron stores. Previous studies have shown a clear contribution of foetal liver hepcidin in regulation of iron transport across the placenta in WT animals (Gambling et al. 2009). Our data suggested that *Hfe* KO pups from HET dams with high iron stores when fed a high iron diet were unable to control normal regulation of iron uptake which resulted in increased placental FPN1 expression, more iron transport and high foetal liver iron levels as compared with WT pups. *Hfe* KO pups born from HET dams on a high iron diet also had more body iron (Unpublished data by Dr. S. Balesaria). This increased iron uptake in *Hfe* KO pups as compared to WT pups may be due to the production of hepatic hepcidin in the latter. Our data suggests that up-regulated placental FPN1 expression by the foetal liver may have controlled foetal iron uptake. Foetal genotype seemed to affect liver iron accumulation and *FPN1* gene expression only with high iron intake by the mother.

In conclusion, iron metabolism and production of normal and healthy offspring during pregnancy is dependent on the iron status and genotype of the mother. Deletion of *Hfe* in both dams and pups caused increased iron levels in the maternal circulation, and storage in the liver; however this effect was clearly diet-dependent. When mothers are fed a low or normal iron diets, foetal liver was able to control iron transport across the placenta or its availability to the foetus.

Chapter 4

Iron transport across placenta: role of hepcidin

4.1 Introduction

The coordinated interaction between hepcidin and the iron exporter (FPN1) regulates duodenal iron absorption, its storage in the liver and circulation in the body. Hepcidin is an amphipathic 25 amino acid peptide belonging to the defensin family of antimicrobial peptides. The role of hepcidin as an iron regulatory peptide was identified after the deletion of the *HAMP1* gene, responsible for encoding hepcidin. This targeted deletion of the *HAMP1* gene resulted in high iron accumulation in the parenchymal tissues of mice (Nicholas et al. 2001). Whereas, over-expression of hepcidin resulted in severe iron deficiency anaemia in mice (Nicholas et al. 2002). These findings led to the supposition that hepcidin functions as a negative regulator of iron metabolism.

Previous studies have demonstrated the mode of action of hepcidin by binding to FPN1 followed by its internalisation and finally degradation (Nemeth et al. 2004). Hepcidin seems to have a cell-specific response and previous studies have shown the reduction of FPN1 expression in macrophages (THP1 cells), erythroblast cell lines and primary erythroblasts (K569) (Chung et al. 2009; Zhang et al. 2011). However, FPN1 expression was not altered in duodenal enterocytes (Caco-2 cells) after hepcidin treatment (Chung et al. 2009). How hepcidin regulates placental iron transport is not clearly known.

Hfe KO mice absorb and accumulate more iron in their body and can take up more NTBI than WT mice (Chua et al. 2004; Zhou et al. 1998). A number of

studies have shown that mutations in the *Hfe* gene result in an inappropriately low level of hepcidin expression (Ahmad et al. 2002, Schmidt et al. 2008; Vujic et al. 2008). The decrease of circulating hepcidin leads to an increased FPN1-mediated iron efflux from reticuloendothelial cells and duodenal enterocytes resulting in increased circulating iron and eventually the saturation of transferrin. Moreover, when *Hfe* KO mice were crossed with mice over-expressing hepcidin, their overload status was normalized (Nicholas et al., 2003). Also, HFE participates in the regulation of intestinal iron absorption by modulating hepcidin expression (Mura et al., 2004). The results presented in Chapter 3 have demonstrated that the absence of *Hfe* in pregnant dams has increased iron transport across placenta and resulted in high iron accumulation in the foetal liver. However, there are difficulties in distinguishing the primary effects of HFE on cellular iron status and its secondary effects resulting from changes in hepcidin expression. HFE is also expressed in coated pits on the apical side of syncytiotrophoblasts where it is believed that it forms a complex with the TfR1 and β-2-microglobulin (Parkkila et al. 1997). In contrast, Bastin et al. (2006) found HFE on some parts of the basal syncytiotrophoblasts in large amounts where FPN1 are strongly expressed. Furthermore, there is very little data on the role of HFE and hepcidin in the regulation of iron transport across placenta.

The aim of this study is to investigate the regulation of iron transport across the placenta by studying the coordinated interaction between hepcidin and FPN1.

4.2 Experimental design

4.2.1 *In vivo* studies

All experimental procedures were approved and conducted in accordance with the UK Animals (Scientific Procedures) Act, 1986. *Hfe* knockout (KO) mice were used, which were mixed 129/Ola-C57BL/6 background strain, with a 2kb pgk-neor gene flanked by loxP sites replacing a 2.5kb BglII fragment (Bahram *et al,* 1999). 129/Ola-C57BL/6 mixed background mice strains were used as WT.

After weaning, mice were fed 150ppm iron diet (150mg Fe/kg diet) for two weeks followed by mating with males of the corresponding genotype (WT or *Hfe* KO). Pregnancy was confirmed by detection of a vaginal plug and the day this was observed was denoted as day 0. From day 14 of gestation, females were injected every 24 hours with either 0.15M NaCl or 10µg hepcidin dissolved in 0.15M NaCl via the intraperitoneal route, Figure 4.1.

On day 18 of gestation, dams from each group were anaesthetised with pentobarbitone. The foetuses were delivered by caesarean section and killed by decapitation. Maternal blood and placenta were collected and rapidly frozen in liquid nitrogen before being stored at -80°C for RNA extraction, protein purification and tissue non-haem iron measurements.
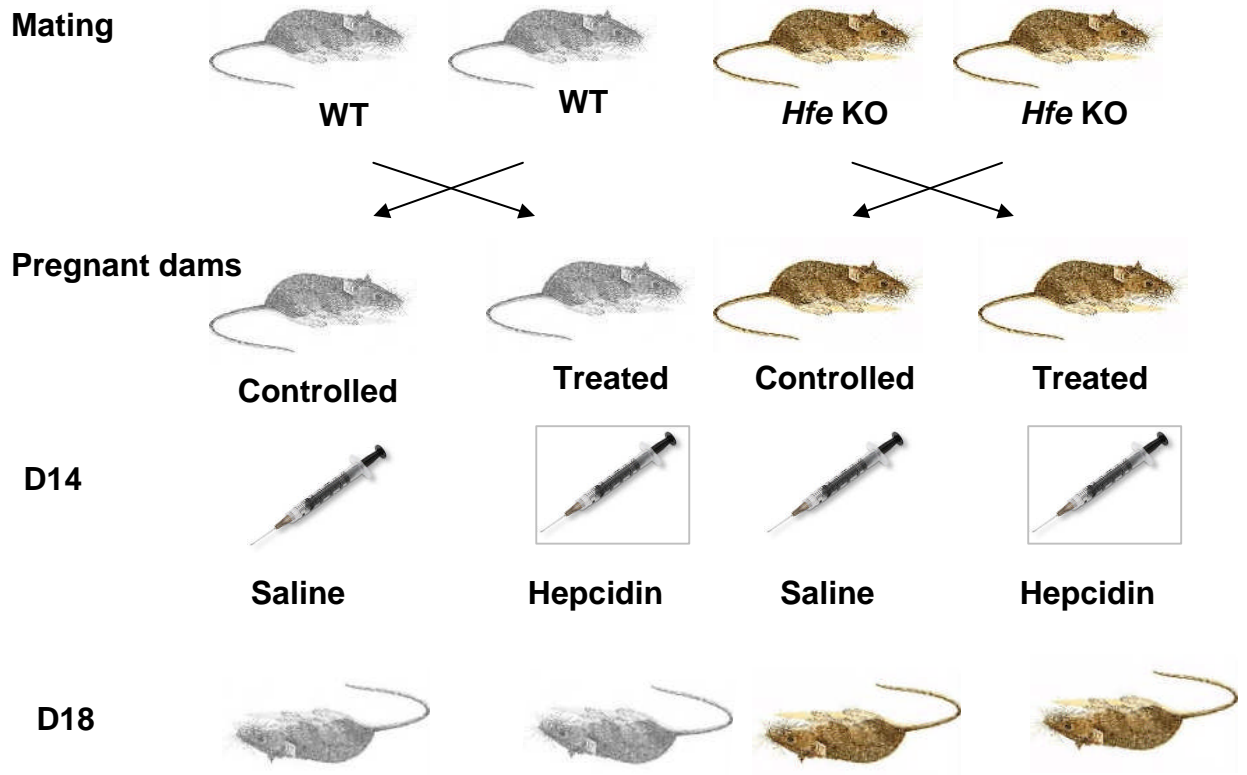
Figure 4.1 Experimental design of *in vivo* studies

WT and Hfe KO pregnant dams were injected with either saline or hepcidin from D14 of gestation and every 24 hours till D18 of gestation. On D18 of gestation, dams were sacrificed and their blood and placental tissues were collected.

4.2.2 *In vitro* studies

BeWo cells were seeded on inserts and treated with hepcidin on either the apical or the basolateral side when the confluency reached 100%. The confluent layer of BeWo was observed by measuring the transepithelial electrical resistance by a TEER voltohmmeter, Figure 4.2. Total RNA or protein was extracted from BeWo cells after a time course treatment with 1µM hepcidin.
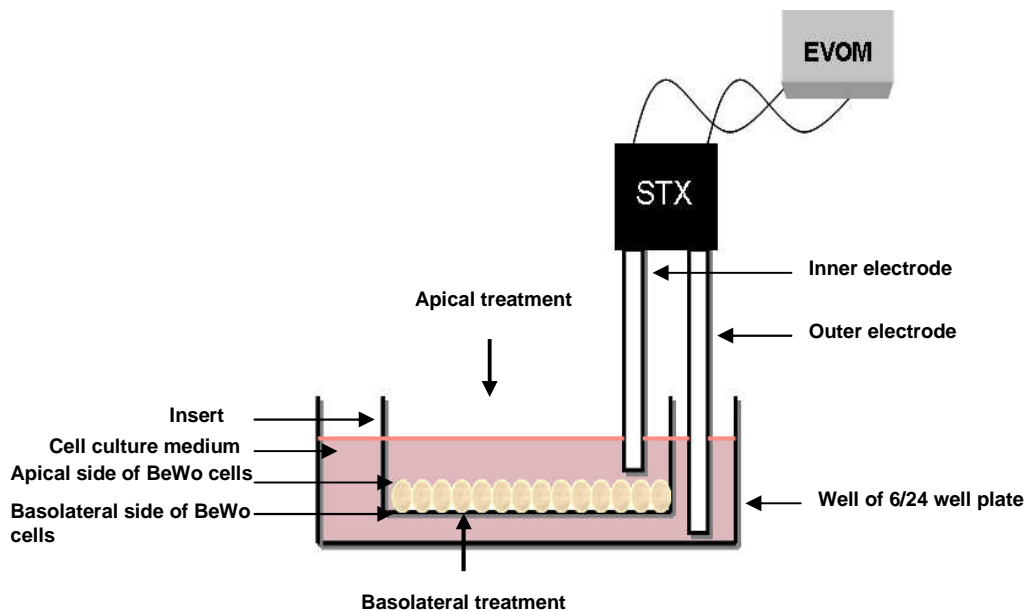
Figure 4.2 Experimental design of *in vitro* studies

BeWo cells were polarised by seeding them on inserts and the confluent monolayer was measured by a TEER voltohmmeter followed by hepcidin treatment on either the apical or basolateral side.

4.3 Results

4.3.1 *In vivo* studies of hepcidin-dependent placental iron transport

4.3.1.1 Effect of hepcidin injection on serum iron levels and transferrin saturation of WT pregnant dams

Hepcidin was injected in pregnant dams in order to understand its role in regulating iron transport during the last trimester of pregnancy. Serum iron levels and transferrin saturation were measured after collection of blood at D18 of gestation. For control experiments, the dams were injected with the same amount of saline. Treatment with hepcidin caused a significant decrease in serum iron levels ($p = 0.01$). Transferrin saturation was also reduced after the injection of hepcidin but it did not reach statistical significance ($p < 0.05$), Figure 4.3 (a) and (b).

(a)   **(b)**
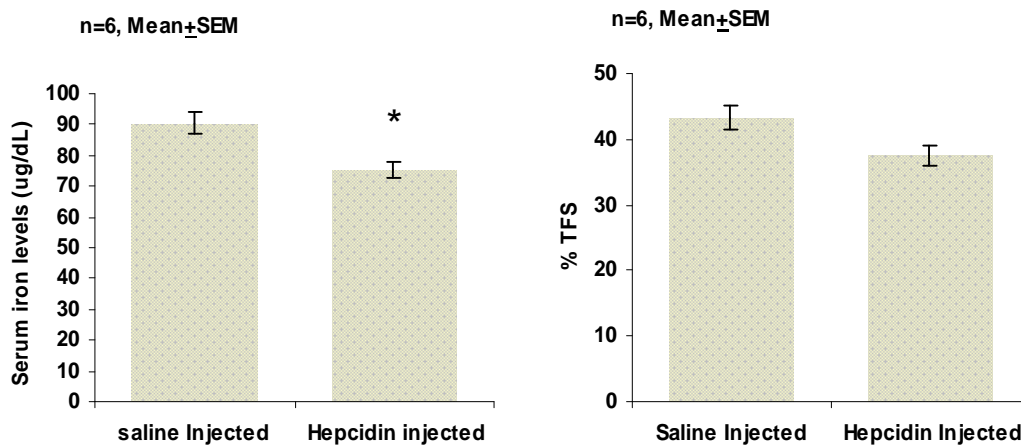
Figure 4.3 Serum iron levels and transferrin saturation after hepcidin injection

*Blood was collected from the pregnant dams at D18 of gestation and serum was separated from it. (a) Serum iron levels were lowered significantly after injection of hepcidin. (b) Transferrin saturation is also decreased in hepcidin injected dams but the difference was not significant. Bar graphs represent Mean ± SEM of 6 samples and * denotes significance at p < 0.05.*

4.3.1.2 Effect of hepcidin injection on placental FPN1 protein and iron transporter gene expression in WT dams

To further investigate the regulation of iron across the placenta by hepcidin, FPN1 protein expression was measured by western blot analysis. Placental tissues were collected 24 hours after the last dose of hepcidin injection. Increased FPN1 protein expression was observed in hepcidin-treated mice when compared with controlled WT pregnant mice injected with saline, Figure 4.4 (a) and (b). The expression of *DMT1+IRE* and *ZIP14* was up-regulated in the placenta of WT pregnant mice injected with hepcidin, while mRNA expression levels of *TfR1*, *TfR2*, *DMT1-IRE* and *FPN1* remained unchanged, Figure 4.5.

(a)   **(b)**
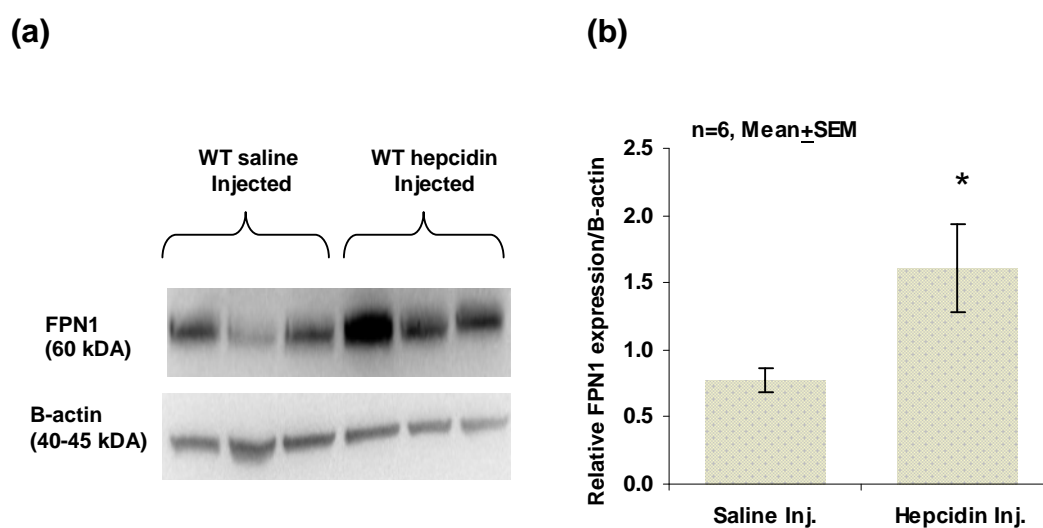
Figure 4.4 Effect of hepcidin injection on placental FPN1 expression

(a) Western blot analysis of placental tissue lysates from saline and hepcidin injected pregnant WT dams using an antibody to FPN1; Anti-β-actin was used as a loading control. (b) Histograms show the mean ± SEM of relative band intensity with an increase in placental FPN1 expression after hepcidin treatment.
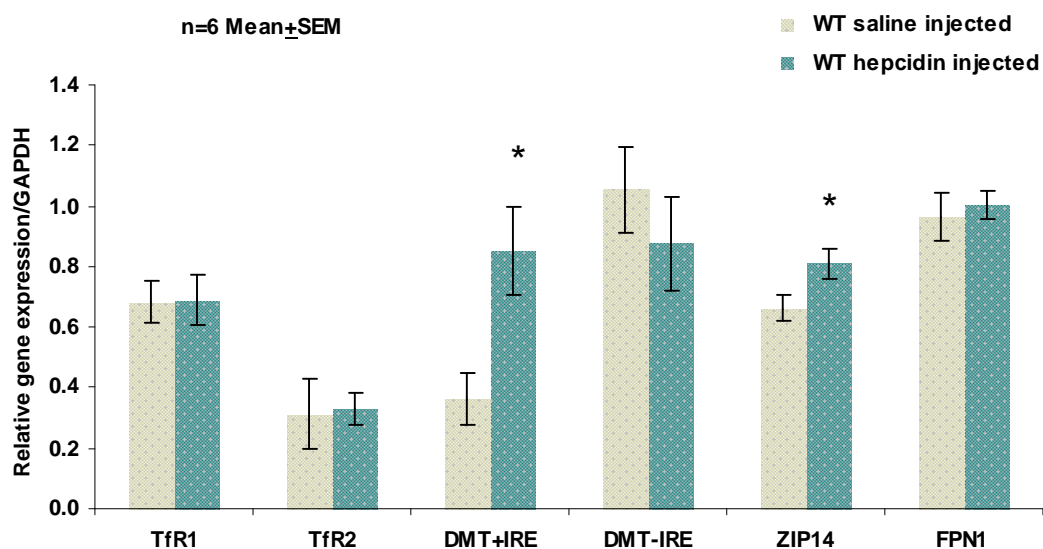
Figure 4.5 Relative placental gene expression after hepcidin treatment of WT pregnant dams

Quantitative RT-PCR analysis of placental gene expression showed a significant increase in mRNA levels of DMT1+IRE and ZIP14 in the placenta of WT pregnant dams injected with hepcidin as compared to control with p<0.05 represented by *, while the expression of TfR1, TfR2, DMT1-IRE and FPN1 remained unchanged. Bar graph represents mean ± SEM of 6 samples.

4.3.1.3 Effect of hepcidin injection on serum iron and transferrin saturation levels of *Hfe* KO pregnant dams

To further understand the possible link between HFE and hepcidin in regulating iron transport across the placenta, *Hfe* KO pregnant dams were treated with hepcidin. Serum iron levels and transferrin saturation remained unchanged in the *Hfe* KO pregnant dams after the treatment with hepcidin compared with the dams injected with an equivalent volume of saline, Figure 4.6 (a) and (b).

(a)   **(b)**
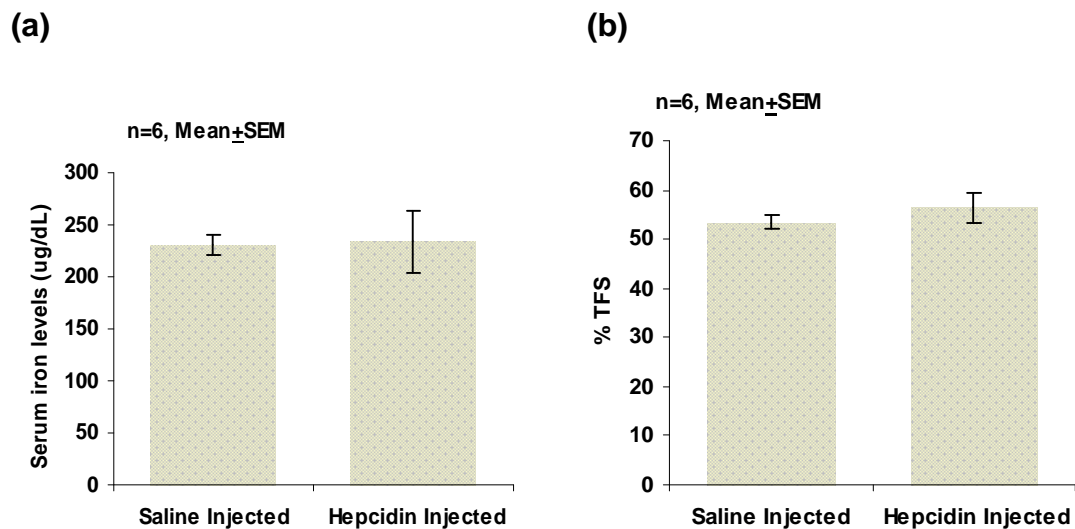
Figure 4.6 Effect of hepcidin treatment on serum iron levels and transferrin saturation of *Hfe* KO dams

(a) Serum iron levels in Hfe KO pregnant dams did not alter after hepcidin injected. (b) Transferrin saturation was also the same in saline and hepcidin injected Hfe KO dam. Data are mean $\pm$ SEM of 6 samples.

4.3.1.4 Effect of hepcidin injection on placental FPN1 protein and iron transporter gene expression of *Hfe* KO mice

FPN1 protein expression increased in placental tissue collected from hepcidin-treated *Hfe* KO pregnant dams as compared with saline injected dams but the change did not reach significance ($p > 0.05$). Western blot images and histograms of mRNA expression are shown in Figure 4.7 (a) and (b). Hepcidin treatment significantly increased the mRNA expression of *TfR1*, *DMT1+IRE* and *ZIP14*. On the other hand the treatment had no effect on *TfR2*, *DMT1-IRE* and *FPN1* gene expression, Figure 4.8.

(a)   **(b)**
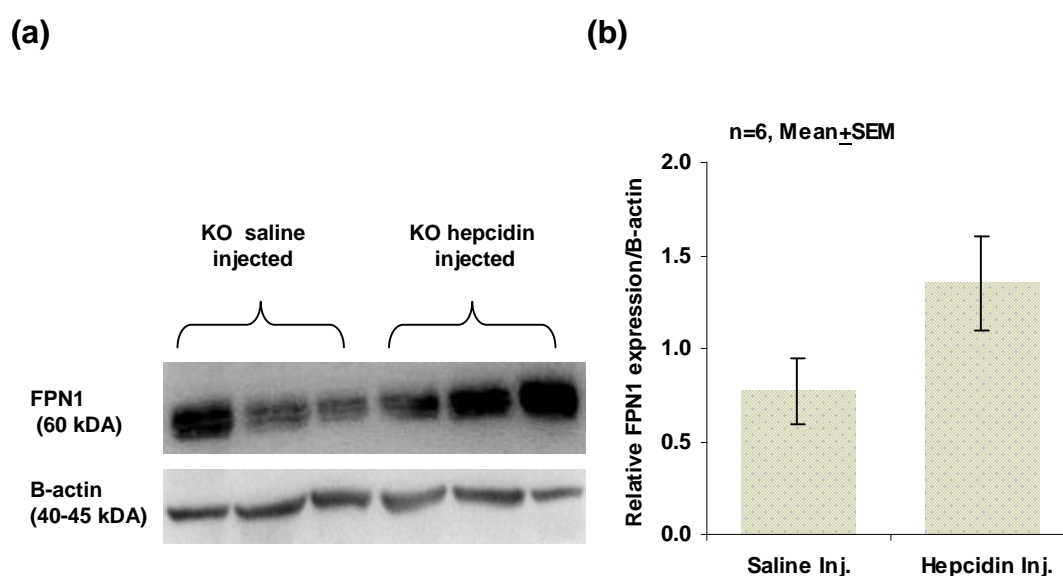
Figure 4.7 Effect of hepcidin injected on placental FPN1 protein expression in *Hfe* KO dams

Western blot analysis revealed an increase trend in the placental FPN1 protein expression in hepcidin injected Hfe KO pregnant dams but the change was not statistically significance. Bars show the mean of relative band intensity from both treatments of 6 samples.
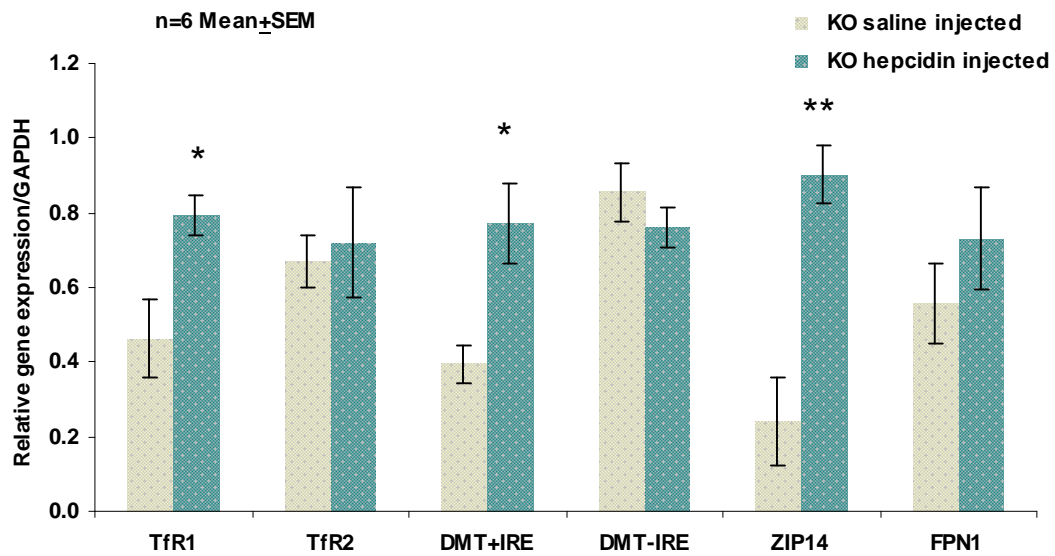
Figure 4.8 Effect of hepcidin treatment on placental iron transporter gene expression in *Hfe* KO pregnant dams.

*TfR1, TfR2, DMT1+IRE, DMT1-IRE, ZIP14 and FPN1 mRNA expression were analysed by RT-PCR. Hepcidin treatment increased the mRNA expression of TfR1, DMt1+IRE and ZIP14 with no change in mRNA expression of FPN1. Bars denotes mean ± SEM of 6 samples per group. * represents p < 0.05 and ** stands for p < 0.001 in hepcidin injected KO mice compared to saline injected controls.*

4.3.2 *In vitro* studies of hepcidin-dependent placental iron transport

BeWo cells were used to study the molecular mechanism of iron transport across syncytiotrophoblasts regulated by hepcidin.

4.3.2.1 Transepithelial electrical resistance of BeWo cells

BeWo cells were grown on the anopore inserts and the transepithelial electrical resistance (TEER) was measured daily from the 3rd day of seeding until confluence was obtained on day 8 or 9 post seeding. The TEER readings increased as the number of cells increased.

Days post seeding	3	4	5	6	7	8	9
TEER (Ωcm^2)	107	150	182	204.5	244.9	309.3	321.6
SD $\pm$	5.6	5.8	8.4	6.7	6.9	5.01	9.17

Table 4.1 Transepithelial electrical resistance of BeWo cells grown on inserts
The resistance (Ωcm^2) was measured on the 3rd day of seeding of BeWo cell until the confluency was reached and the resistance became constant. Mean resistance was measured from 4-6 samples from 3 separate experiments to measure 100% confluent cell layer which was later used in the experiments. SD represents standard deviation of 4-6 samples.

4.3.2.2 Effect of hepcidin treatment on iron transporter proteins and gene expression in BeWo cells

BeWo cells were grown on inserts and after the formation of a confluent layer they were treated with 1 μM hepcidin on either the apical or the basolateral side for 2, 4, 6, 12, 24 and 48 hours. The time course treatment did not alter the FPN1 protein expression as shown in Figure 4.9 (a) and (b). Similarly, hepcidin did not change the protein expression of DMT1 in cells treated for 2 or 4 hours, Figure 4.10.

Similarly, hepcidin treatment for 2 to 48 hours did not have any effect on the mRNA expression of TfR1, DMT1 and FPN1, Figure 4.11 (a), (b) and (c).

(a)
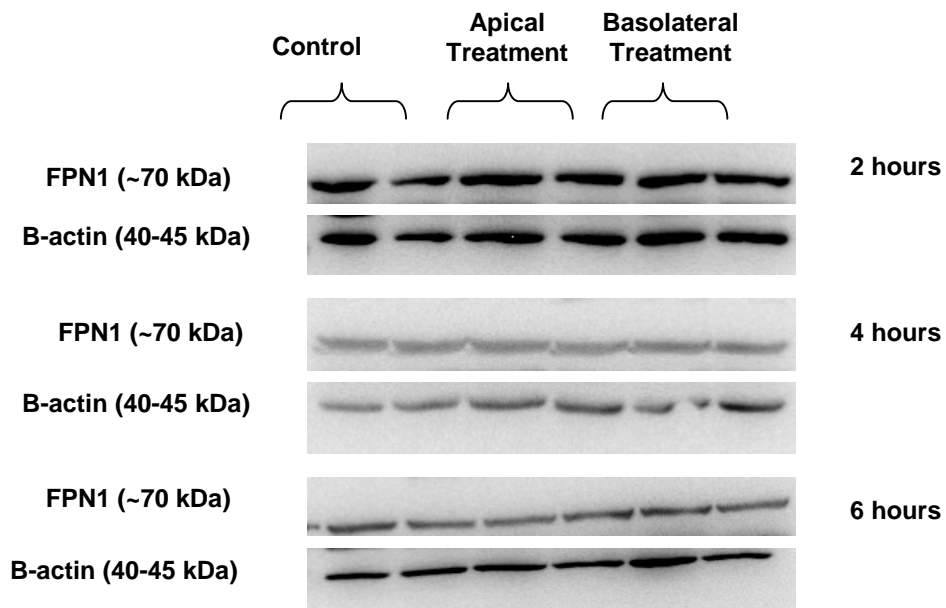
(b)
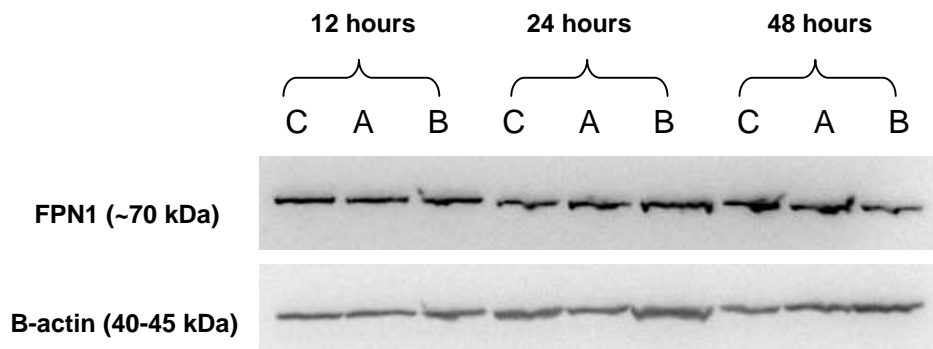
Figure 4.9 Effect of hepcidin on FPN1 protein expression in BeWo cells

BeWo cells were grown on inserts and treated for 2, 4, 6, 12, 24 or 48 hours with 1µM hepcidin on the apical or the basolateral side. Western blot analysis of BeWo cell lysates shows no difference in the treated and control cells. In (b) C represents controlled cells treated with saline; A denotes apical treatment and B stands for basolateral treatment. B-actin was used as a loading control.
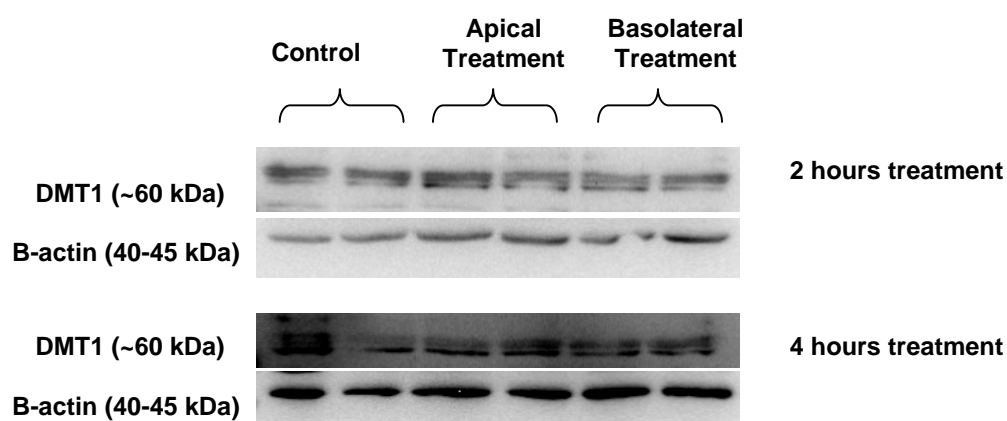
Figure 4.10 Effect of hepcidin on DMT1 expression in BeWo cells

BeWo cells were treated with hepcidin for 2 and 4 hours and DMT1 protein expression was analysed using western blotting. The first 2 lanes show the control cells treated with saline, lane 3 and 4 show DMT1 expression in cells treated on the apical side and the last 2 lanes show protein expression when the cells were treated on the basolateral side.

(a)

(b)

(c)
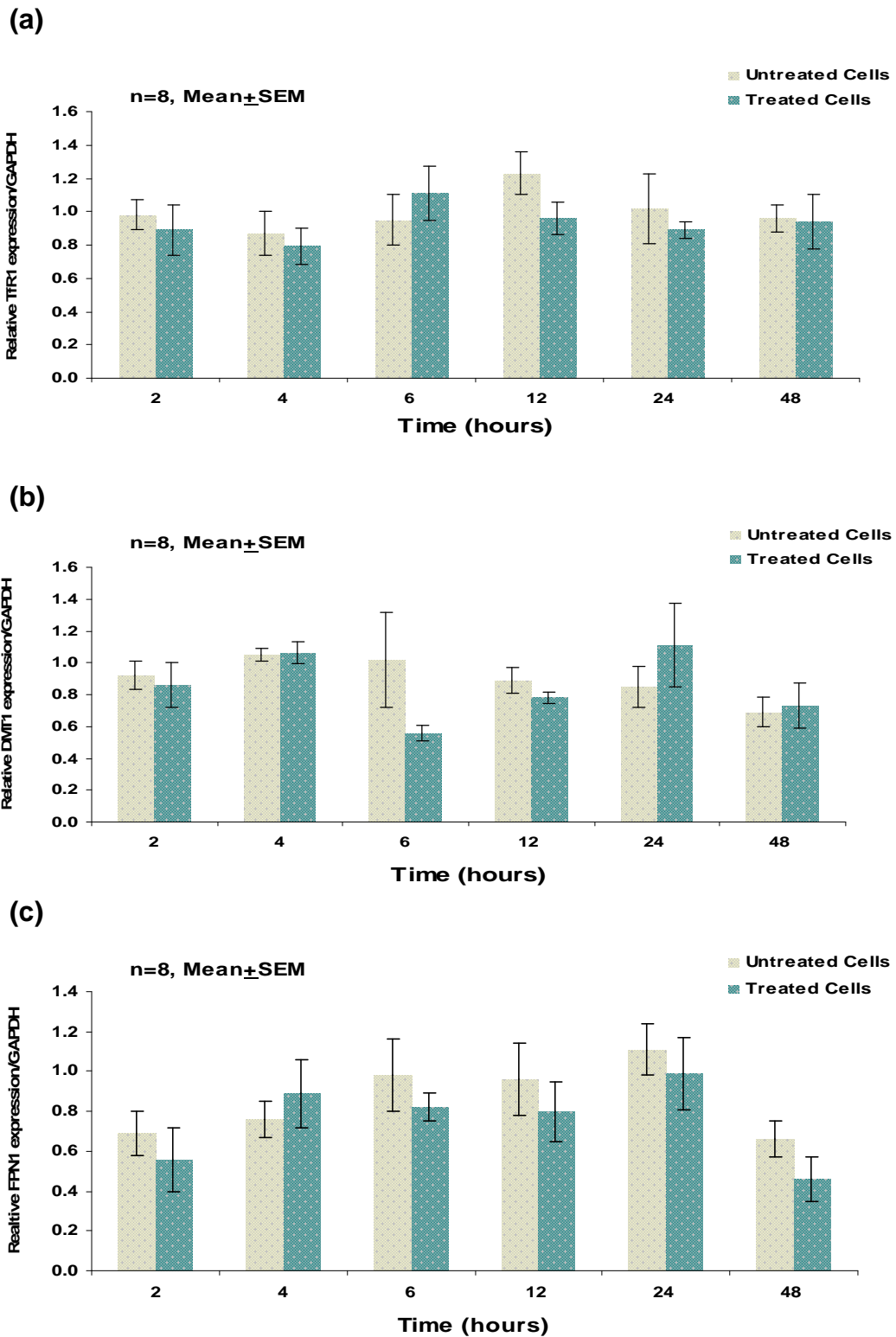
Figure 4.11 Effect of hepcidin on relative mRNA expression of TFR1, DMT1 and FPN1 in BeWo cells

BeWo cells were treated with 1µM hepcidin on the apical side for 2, 4, 6, 12,24 and 48 hours. mRNA expression of TfR1 (a) and DMT1 (b) was measured with RT-PCR shows no difference in treated and untreated cells. (c) Hepcidin did not alter the FPN1 mRNA expression when the cells were treated on the basolateral sides. Bars represent mean ±SEM with n=8.

4.3.2.3 Effect of hepcidin on FPN1 expression in HEK 293 cells

To check the bioactivity of commercial and in-house hepcidin, HEK 293 (Tet-On hFPN-GFP) and HEK 293 (Tet-Off hFPN-GFP) were treated with both forms of hepcidin at 1µM concentration for 2 hours after turning on the GFP expression which was measured using FACs. GFP-tagged FPN1 expression was repressed significantly after treatment of HEK 293 Tet-On and Tet-off cells with both commercial and in-house hepcidin, Figure 4.12 (a) and (b).

(a)   **(b)**
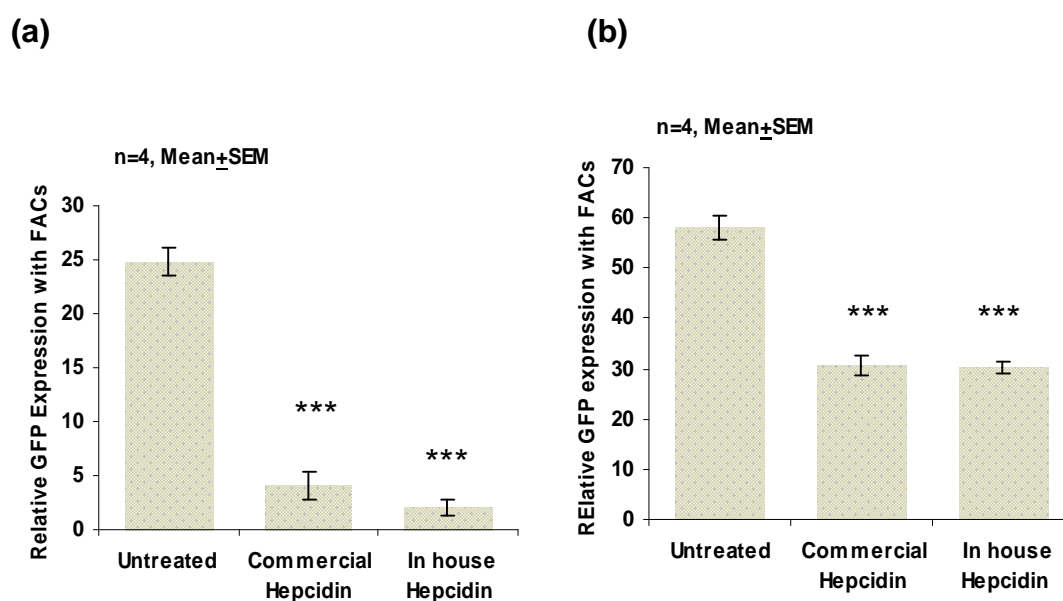
Figure 4.12 Effect of hepcidin treatment on GFP-tagged FPN1 expression in HEK 293 cells

HEK 293 Tet-On and Tet-Off were collected in PBS after treatment with commercial and in-house hepcidin for 2 hours and GFP tagged FPN1 expression was measured using FACs. Both forms of hepcidin have repressed the expression of GFP-tagged FPN1 significantly in HEK 293 Tet-On cells (a) and HEK 293 Tet-off cells (b). Bar graphs represents mean of 4 samples ±SEM and *** shows significance at p<0.001.

4.4 Discussion

In chapter 3 we concluded that foetal hepcidin levels were responsible for down-regulation of placental FPN1 and possible regulation of iron transfer across placenta by foetal liver hepcidin levels. Although regulation of foetal liver hepcidin has not been studied but based on the evidence from studies on adults, hepcidin is regulated by serum iron levels, hypoxia, erythropoiesis and inflammation. Therefore, it is reasonable to assume that these same stimuli are responsible for regulating levels of foetal hepcidin in utero. We have also demonstrated that maternal *Hfe* status has a bearing on iron transport across the placenta but this is independent of hepcidin. In order to understand the regulation of placental iron transport by maternal hepcidin WT and *Hfe* KO pregnant dams were injected with hepcidin on D14 of gestation for every 24 hours till D18 of gestation.

We have found that in WT pregnant dams, hepcidin administration has decreased serum iron levels. This decrease has also been demonstrated in previous studies when non-pregnant mice were injected with hepcidin (Rivera et al. 2005; Chaston et al. 2008) and was linked with the reduction in FPN1 protein expression in the macrophages of spleen (Chaston et al. 2008). Previous studies in non-pregnant animals have shown unaltered liver iron stores after hepcidin injection as compared with saline injected WT mice (Laftah et al. 2004). In parallel studies, Dr. S. Balesaria's results were consistent with previous findings, no change in liver iron levels observed in WT pregnant dams after hepcidin administration. However, KO pregnant

dams showed decreased liver iron stores after hepcidin injection but there was no change in serum iron concentration and transferrin saturation.

In this study we have found that placental FPN1 expression in WT and *Hfe* KO dams is significantly increased on hepcidin administration. These results are in contrast to the previous studies conducted in iron transporter tissues such as macrophages, hepatocytes and duodenal enterocytes of non-pregnant animal models. In these rodent tissues, hepcidin was found to either down-regulated DMT1 with no change in FPN1, FPN1 (and DMT1 expression was not measured) (Viatte et al. 2006) or both transporters' expression (Harrison-Findik et al. 2006). Non-pregnant mice produced profound hypoferremia after administration of synthetic hepcidin (Rivera et al. 2005), demonstrating the in vivo iron-regulatory activity of the 25 amino acid hepcidin peptide. We can speculate that in WT pregnant mice reduction in serum iron levels due to hepcidin injection might have increased placental FPN1 expression with *DMT1+IRE* and *ZIP14* mRNA expression in order to ensure iron transport needed by the foetus. We can also suggest that the tissues were not collected from the dams for analysis until 24 hours after the last treatment of hepcidin, which could allow FPN1 transcript levels to recover and plateau subsequent to hepcidin injection.

Placental *TfR2, DMT1-IRE, FPN1* mRNA expression remained unaltered in dams from both genotypes after hepcidin injection. Whereas, the up-regulation of mRNA levels of *DMT1+IRE* and *ZIP14* in the placenta of both genotypes may indicate iron transport across placenta through alternative

pathways as DMT1 and ZIP14 are NTBI transporters shown previously (Gunshin et al. 1997; Gruenheid et al. 1995; Liuzzi et al. 2006). Our results, discussed in Chapter 6, have shown increased *ZIP14* expression after provision of non-transferrin bound iron (NTBI) to BeWo cells. We have also found that in BeWo cells *DMT1+IRE* expression did not alter after NTBI supplementation so we decided to find out the localisation of DMT1 in these cells (results shown in Chapter 5). In parallel studies S. Balesaria has shown the same amount of liver iron concentration in the pups derived from WT and *Hfe* KO dams after hepcidin administration compared with pups from saline injected dams. These results suggest that maternal hepcidin is not disrupting iron supply to the foetus during pregnancy.

Previous studies have demonstrated the mode of action of hepcidin by binding to FPN1 followed by its internalisation and finally degradation (Nemeth et al. 2004). Hepcidin seems to have a cell-specific response as shown in previous studies where hepcidin treatment reduced FPN1 expression in macrophages (THP1 cells), erythroblast cell lines and primary erythroblasts (K569) (Chung et al. 2009; Zhang et al. 2011). However, our results have shown that FPN1 protein and mRNA expression did not change in BeWo cells after hepcidin treatment for 2 to 48 hours. These results are consistent with previous finding with no change in FPN1 expression in duodenal enterocytes (Caco-2 cells) after hepcidin treatment as compared with non-treated cells (Chung et al. 2009). We could speculate that hepcidin has cell/tissue-specific effects. However, FPN1 expression was decreased significantly when the HEK 293 cells transfected with GFP-tagged FPN1 were

treated with both commercial and in-house hepcidin. The FPN1-GFP fusion construct in these cells lines are localised to the cell membrane (Nemeth et al. 2004). We could speculate that FPN1 in BeWo cells was not present on the cell membrane to act as a hepcidin receptor. Therefore, we localised FPN1 in BeWo by immunostaining and the results are shown in Chapter 5.

In conclusion, maternal hepcidin does not affect the iron demand of the foetus and we can suggest that the placenta develops a mechanism to continue placental iron supply as shown by up-regulation of iron transporter mRNA expression. When BeWo cells were treated with hepcidin, we did not see equivalent change that was observed in placental tissue. The response of placental tissue to dietary iron, *Hfe* genotype and hepcidin treatment may be due to the presence of syncytiotrophoblasts, cytotrophoblasts, connective tissue of villus, and endothelium of foetal capillaries. Although the mechanism of iron transport is present in BeWo cells expressing the important iron transporters, it seems that regulation of these transporters might be different in these cells as compared to placenta. Therefore, the localisation of TfR1, DMT1 and FPN1 in BeWo cells was investigated to understand the molecular mechanism of iron transport across syncytiotrophoblasts.

Chapter 5

Localisation of iron transporter proteins in

BeWo cells

5.1 Introduction

As discussed in Chapter 1, the placenta is the only channel for transport of nutrients and exchange of gases and waste products between foetus and mother. Transport of iron is unidirectional from mother to foetus and takes place in syncytiotrophoblasts, which form the outer layer of human haemochorial placenta and are the only barrier between mother and placenta.

Previous studies have demonstrated that iron bound to transferrin in maternal serum binds to TfR1 on the apical (maternal) side of syncytiotrophoblasts (McArdle and Morgan 1982; McArdle et al. 1984). This complex is internalised into endosomes (McArdle et al. 2003) and iron is released into the cytosol of syncytiotrophoblasts possibly by DMT1 (Georgieff et al. 2000). The transport of iron across the basal membrane to the foetal circulation is not clearly understood. It is believed that iron is exported by FPN1 present on the basolateral side of syncytiotrophoblasts (Abboud and Haile 2000; Donovan et al. 2000). A number of studies have shown the expression of DMT1 (Georgieff et al. 2000; Gambling et al. 2001) and FPN1 (Donovan et al. 2000; McKie et al. 2001) on the basal membrane of syncytiotrophoblasts. Contrary to these studies, Gruper et al (2005) have shown the co-localisation of TfR1, HFE and DMT1 in the endosome of BeWo cells and have suggested an interaction between TfR1 with HFE and DMT1. However, Bastin et al. (2006) have shown localisation of HFE and FPN1 on the basal membrane and TfR1 on the apical membrane.

Natural resistance-associated macrophage protein 1 (Nramp1) is a divalent metal transporter expressed previously in phagocytes. It was hypothesized that macrophage Nramp1 may participate in the recycling of iron acquired from phagocytosed senescent erythrocytes (Soe-Lin et al 2009). Its presence and role in placental cells has not been studied before. The aim of this study is to localise the major iron transporter proteins in BeWo cells to understand the molecular mechanism of placental iron transport.

5.2 Experimental design

BeWo cells were seeded on glass coverslips until approximately 60 to 70% confluent. Cell were fixed with either paraformaldehyde or methanol and incubated with primary antibodies (anti-TfR1, Nramp1, DMT1, FPN1, ZIP14, HFE, ZO-1, Occludin, E-Cadherin) followed by incubation with fluorescent labelled secondary antibodies. The cells were visualised using a confocal microscope (Leica, TCS Sp5 AOBS, Leica, Mannheim, Germany or Zeiss), Figure 5.1.

BeWo cells grown on coverslips

Cells incubated with primary and flurescent conjugated secondary antibodies

Coverslips mounted on glass slides
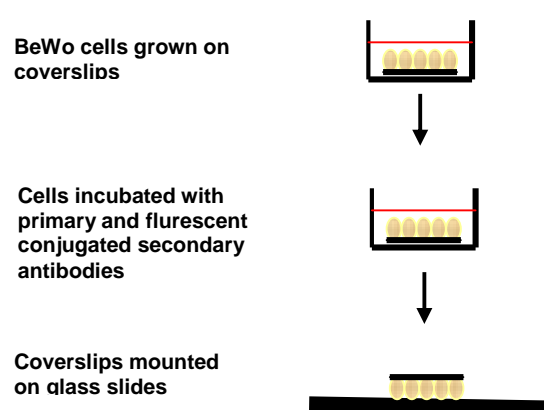
Figure 5.1 Experimental design of immunolabelling of BeWo cells

BeWo cells were seeded on coverslips and once the cells reached 60 to 70% confluency, the cells were immunolabelled with primary and secondary antibodies and the coverslips were mounted on glass slides to visualise under a confocal microscope.

5.3 Results

In order to understand the localisation of important iron transporter proteins, BeWo cells were immunolabelled for TfR1, Nramp1, DMT1, ZIP14, HFE and FPN1. Antibodies to HFE and ZIP14 available to us did not show any immunostaining. This could be due to antibodies being unsuitable for immunostaining or levels being so low that they were not detectable.

5.3.1 Localisation of TfR1 in BeWo cells

BeWo cells were grown and fixed on cover slips followed by immunolabelling for anti-TfR1 antibody (green). Cells were also incubated with AlexaFluor 594-coupled Wheat Germ Agglutinin (WGA) (red) for 15 min prior to TfR1 immunolabelling (green). WGA recognises carbohydrates present predominantly at the plasma membrane. xy-stacks were acquired by confocal microscopy with the scale bar, 5 µm. Results showed that TfR1 was co-localised with WGA on the BeWo cell membrane as shown in Figure 5.2 (c). Due to unavailability of apical and basolateral membrane markers, we could not confirm the presence of TfR1 on either side.

TfR1   WGA   Merged
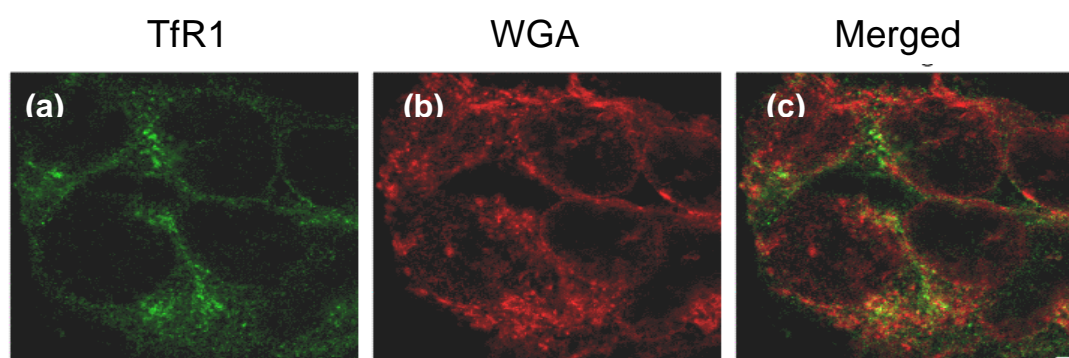
Figure 5.2 Localisation of TfR1 in BeWo cells

BeWo cells were cultured on cover slips and fixed before immunolabelling for (a) TfR1 (green) and (b) WGA (red). xy-stacks were acquired by confocal microscope (scale bar, 5 µm). (c) Merged image shows the co-localisation of TFR1 and WGA (membrane marker).

5.3.2 Co-localisation of Nramp1 with ZO-1 and Occludin in BeWo cells

Cells were seeded on glass coverslips at 70% confluence, fixed and permeabilised before immunolabelling for Nramp1 (green). Cells were also incubated with either AlexaFluor 594-coupled anti-ZO-1 (Figure 5.3) or anti-Occludin in red (Figure 5.4). Zonula Occludin (ZO-1) and Occludin are tight junction proteins present on the plasma membrane that seal together the perimeters of polarised cells. xy- and xz-stacks were acquired by confocal microscopy with the scale bar, 5 µm. Nramp1 in BeWo cells co-localised with both tight junction protein markers (yellow), Figure 5.3 (c) and 5.4 (c).
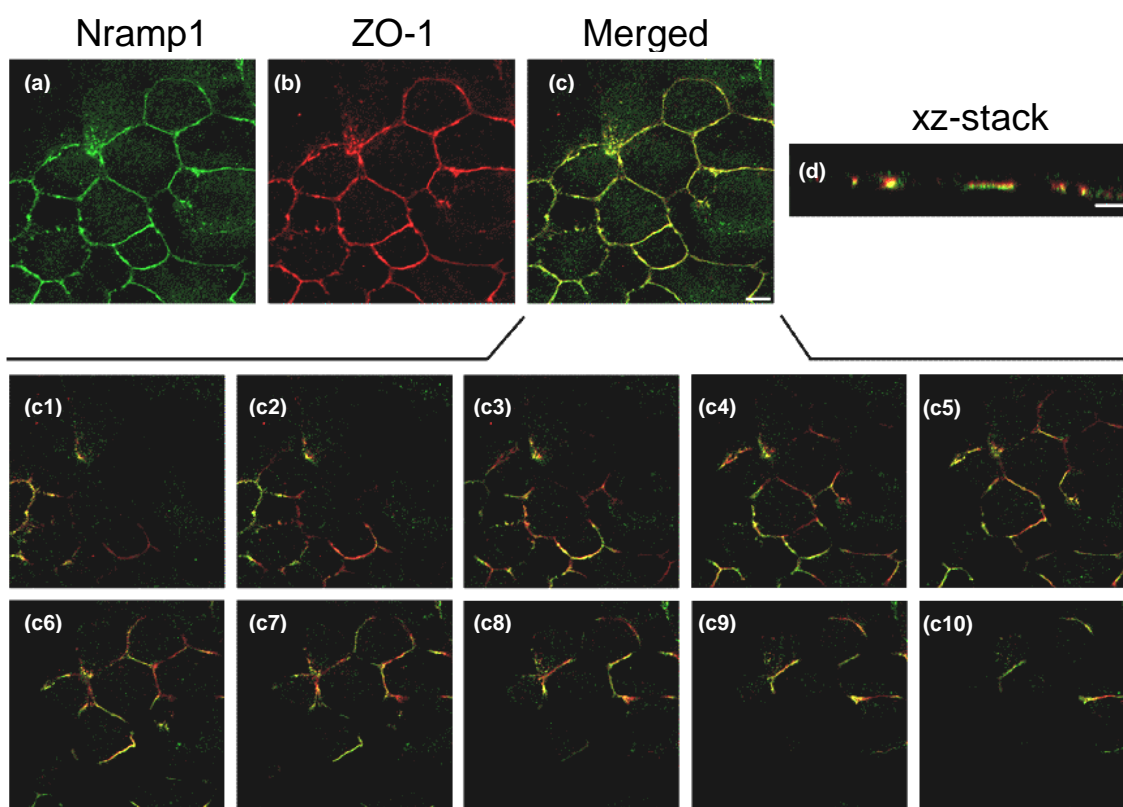
Figure 5.3 Co-localisation of Nramp1 with ZO-1 in BeWo cells

BeWo cells were fixed with 4% (w/v) buffered paraformaldehyde in PBS, and quenched with the same volume of 50 mM NH₄Cl in PBS. For (a) anti-Nramp1 (green) and (b) anti-ZO-1 (red) staining, cells were fixed and permeabilised. (c) and (c1-10) confirms sequential co-localisation of Nramp1 and ZO-1 (yellow) and (d) shows xz-view of this co-localisation.
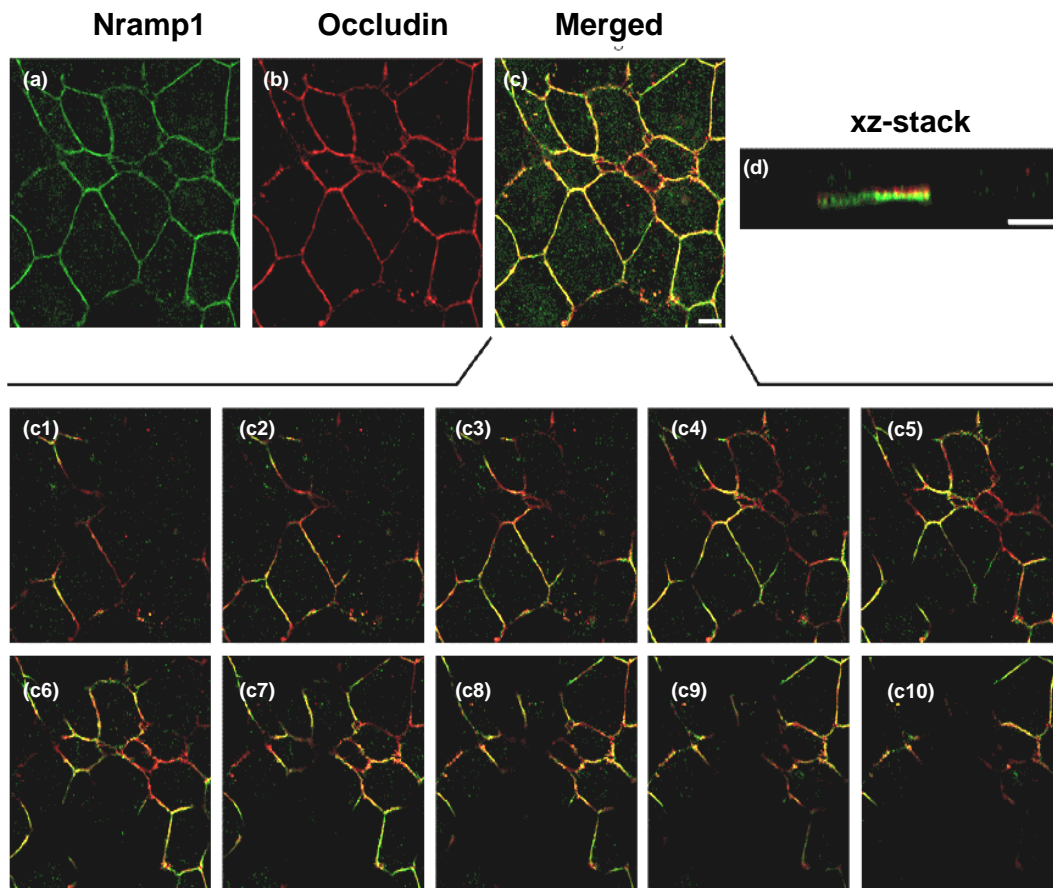
Figure 5.4 Co-localisation of Nramp1 with Occludin in BeWo cells

BeWo cells were fixed with 4% (w/v) buffered paraformaldehyde in PBS (30 min), and quenched with the same volume of 50 mM NH$_4$Cl in PBS. For (a) anti-Nramp1 (green) and (b) anti-Occludin (red) staining, cells were fixed with cold methanol and permeabilised with methanol/ethanol. (c) and (c1-10) confirms sequential co-localisation of Nramp1 and Occludin (yellow). (d) shows xz-view of co-localisation Nramp1 and Occludin.

5.3.3 Localisation of DMT1 in BeWo cells

Cells were seeded on glass cover slips at 70% confluence, fixed and permeabilised before immuno-labelling for anti-DMT1 (green), Figure 5.5. xy-stack was acquired by confocal microscopy with the scale bar, 5 μm. DMT1 in BeWo cells seemed to localise on the membrane of vesicles.

DMT1
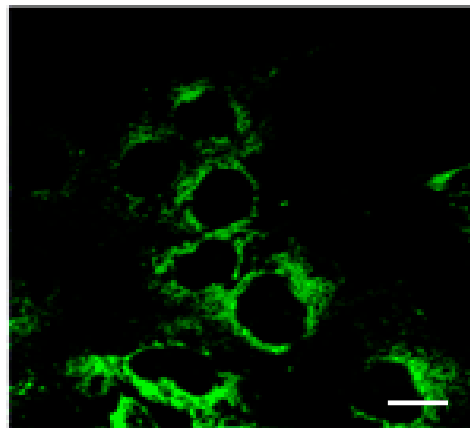
Figure 5.5 Co-localisation of DMT1 in BeWo cells

BeWo cells were seeded on cover slips with 70% confluency. Anti-DMT1 staining in green shows the localisation of DMT1 on the membrane of vesicles in BeWo cells in xy-view, bar scale 5 μm.

5.3.4 Localisation of FPN1 in BeWo cells

BeWo cells were immunolabelled with AlexaFluor 488-coupled anti-FPN1 (green) after fixation and permeabilization on cover slips. xy- and xz- views were acquired by confocal microscopy. FPN1 seemed to localise both on the membrane and in the cytosol of BeWo cells and the xz-view confirms its presence in the cytosol, Figure 5.6 (b).
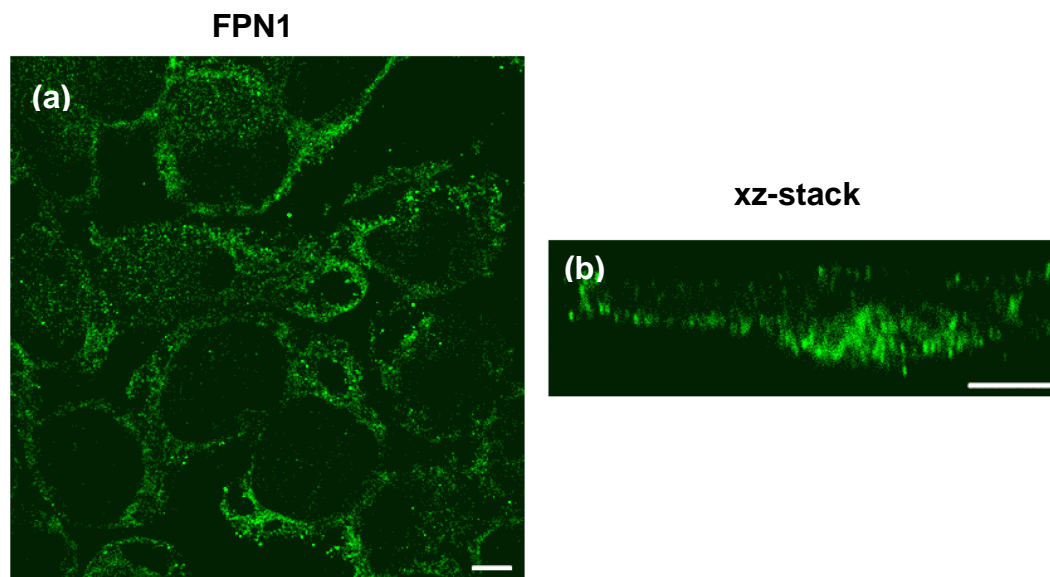
FPN1

Figure 5.6 Localisation of FPN1 in BeWo cells

BeWo cells were seeded on cover slips with 70% confluency. (a) anti-FPN1 staining in green shows the localisation of FPN1 on the membrane and cytosol of BeWo cells in xy-view. (b) shows the localisation in xz-view, bar scale 5 µm.

5.4 Discussion

In the previous chapter *TfR1*, *DMT1*, *FPN1* and *ZIP14* mRNA expression was quantified in placental tissues and BeWo cells. In this chapter the sub-cellular localisation of these important iron transporters was determined to investigate the mechanism of iron transport across syncytiotrophoblasts. Tf is recognized by specific cell membrane receptors that act as gatekeepers responsible for physiological iron uptake by most cell types (Richardson and Ponka, 1997). TfR1 is an iron sensor protein, expected to sense the extracellular concentration of holo-Tf by conventional mechanisms dependent on receptor occupancy. As mentioned in the previous chapters, diferric-Tf is taken up from the maternal serum via TfR1 (McArdle and Morgan 1982; McArdle et al. 1984). Our results have shown that TfR1 is localised on the plasma membrane in unpolarised BeWo cells. A change in placental *TfR1* mRNA expression in response to maternal Hfe status and dietary iron intake shows its role in sensing the serum transferrin bound iron (results shown in Chapter 3).

DMT1 is a mammalian transmembrane metal-ion transporter which mediates the transport of various divalent metal ions including Fe^{2+}, Cd^{2+}, Co^{2+}, Ni^{2+}, Cu^{2+}, and Ca^{2+} but with its highest affinity for iron (Gunshin et al. 1997). The data shows localisation of DMT1 inside the vesicles present in the cytoplasm of the cells. Without any lysosomal or endosomal markers, it is difficult to identify the vesicles. If we assume the vesicles are endosomes then this agrees with the role of DMT1 in transporting iron from endosome into the cytoplasm (Gruenheid et al. 1995). This finding is contrary to previous studies where

DMT1 was shown to be localised to the basal membrane of the syncytiotrophoblasts in human placental biopsies (Georgieff et al. 2000).

The data presented here demonstrate a strong co-localisation of Nramp1 on the tight junction after dual staining with anti-Nramp1 and two individual tight junction markers (ZO-1 and Occludin). Tight junctions are intracellular junctions where the cell membranes hold the two cells together. One of their functions is to maintain the polarity of cells. Tight junctions are the most apical structure of the apical complex separating the border between apical and basolateral membrane domains. Occludin was the first identified transmembrane component of tight junctions but its function is still not understood (Guo 2003; Niessen 2007). As Nramp1 is a transmembrane metal transporter, and its strong co-localisation with Occludin and ZO-1 makes it easy to understand its presence on cell junction and its involvement in intercellular iron transport but its role is still unclear and needs further investigation.

FPN1 has cytoplasmic amino acid membrane termini and 10 to 12 transmembrane domains (Abboud and Haile 2000; McKie et al. 2000; Donovan et al. 2000). It is an iron exporter present on the basal membrane of absorptive intestinal enterocytes, hepatocytes, and macrophages, all of which release iron into plasma (Abboud and Haile 2000; McKie et al. 2000; Donovan et al. 2000). Previous studies by two independent groups have demonstrated the localisation of FPN1 on the basolateral side of the placental syncytiotrophoblasts in human placental sections (Abboud and Haile 2000; Donovan et al. 2000). However, in this study FPN1 expression was identified

both on the membrane and cytoplasm of BeWo cells. The cytoplasmic localisation of FPN1 may suggest a role for FPN1 in iron transport from the cytosol to the organelles.

It is important to note that the current study was conducted in unpolarised BeWo cells *in vitro* because confocal imaging can be only done on clear glass unlike inserts, therefore we can only speculate the function of these proteins in each location. To further understand their role in placental iron transport this study should be carried out after treating BeWo cells with hepcidin and induction with iron deficiency, supplementation and hypoxia. Any response of iron transporters expression after these treatments will further help us in understanding the molecular mechanism of placental iron transport.

Chapter 6

Is ZIP14 important in placental iron transport?

6.1 Introduction

In hereditary haemochromatosis, iron overload causes transferrin saturation (TFS) resulting in an increase non-Tf-bound iron (NTBI) in serum. A number of potential candidates involved in NTBI uptake have been identified in liver. One such candidate is the transmembrane protein ZIP14 (Gao et al. 2008; Liuzzi et al. 2006). Zrt-, Irt-like proteins (ZIP) are a group of protein transporters involved in bio-metal transport into the cytosol of various cells. Mostly they are responsible for zinc transport which is involved in normal cell growth (Vallee and Falchuk 1993) and making of enzymes (Vallee and Auld 1990). It has been found that over-expression of *HFE* in HepG2 cells decreased ZIP14 level which resulted in less NTBI uptake into the cells (Gao et al. 2008). In a previous study performed in our group (unpublished data), it has been shown that expression of ZIP14 varies in response to iron levels. The role of this zinc transporter in iron homeostasis is not well understood. The presence of ZIP14 in placenta has not been reported previously.

The aim of this study is to determine *ZIP14* expression in BeWo cells and mouse placenta and to study the regulation of ZIP14 by HFE and hepcidin.

6.2 Experimental design

For *in vitro* studies BeWo cells were treated with 100µM Fe-NTA (for NTBI supplementation), 20µM DFO (for inducing iron deficiency) or 1 µM hepcidin and total RNA was extracted to determine gene expression of iron transporter and storage proteins. BeWo cells that over-express *HFE* were cultured to determine the *ZIP14* mRNA expression.

For *in vivo* experiments, to study the effect of maternal *Hfe* on *ZIP14* in placenta, WT and *Hfe* KO dams were mated with HET males. From the progeny HET pups were selected. At D18, dams were sacrificed and the placenta placental tissues were collected from WT, *Hfe* KO and HET dams. To determine the effect of foetal *Hfe* on *ZIP14*, HET dams were mated with HET males. From the progeny, WT and *Hfe* KO pups were selected and their placental and hepatic tissues were collected after the pregnant dams were sacrificed on D18**.** The experimental design is explained in detail in Chapter 3.2.

For *in vivo* studies on the effects of hepcidin treatment, on D14 of gestation WT and *Hfe* KO females were injected with either 0.15M NaCl or 10µg hepcidin dissolved in 0.15M NaCl via the intraperitoneal route every 24 hours. On D18, dams were sacrificed and their placenta used for total RNA extraction. The detailed experimental design is given in Chapter 4.2.1.

6.3 Results

6.3.1 *In vitro* studies

6.3.1.1 Effect of NTBI supplementation on iron transporter and storage gene expression in BeWo cells

BeWo cells were supplemented with NTBI in the form of Fe-NTA and mRNA expression of *TfR1*, *ZIP14*, *DMT1*, *H-Ferritin*, *L-Ferritin*, *FPN1* and zyklopen (*Zp)* was measured by RT-PCR. After iron supplementation, *ZIP14* and H-Ferritin expression were up-regulated as compared with non-treated/controlled BeWo cells. *TfR1*, *DMT1*, *FPN1* and *Zp* remained unaltered after the treatment. We were not able to detect any expression for *L-Ferritin* in BeWo cells, Figure 6.1.
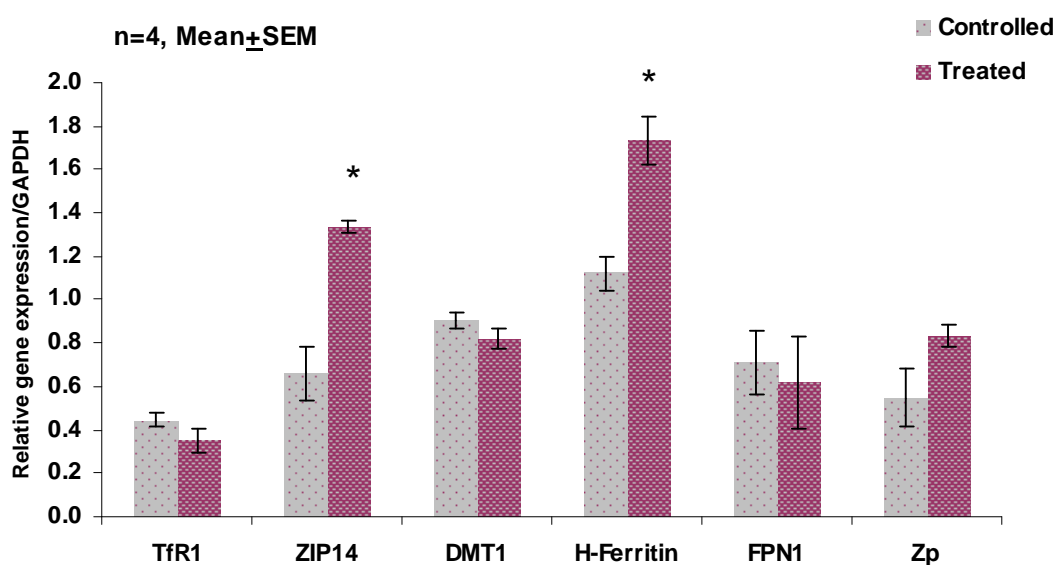
Figure 6.1 Effect of NTBI supplementation on iron transporter and storage gene expression in BeWo cells

*RNA was extracted from BeWo cells after incubation with 100µM Fe-NTA for 24 hours. mRNA expression of iron transporter and storage proteins were measured by RT-PCR. ZIP14 and H-Ferritin were down-regulated. TfR1, DMT1, FPN1 and Zp expression remained unaltered. Bar represents Mean $\pm$ SEM of 4 samples and significance difference is denoted by * with p<0.05.*

6.3.1.2 Effect of iron deficiency on iron transporter and storage gene expression in BeWo cells

Iron deficiency in BeWo cells was induced by DFO and our results have shown that *TfR1* expression was up-regulated in the treated cells. In iron deficiency, *H-Ferritin* gene expression was down-regulated and there was no significant difference in the mRNA expression of *ZIP14*, *DMT1*, *FPN1* and *Zp*, Figure 6.2.
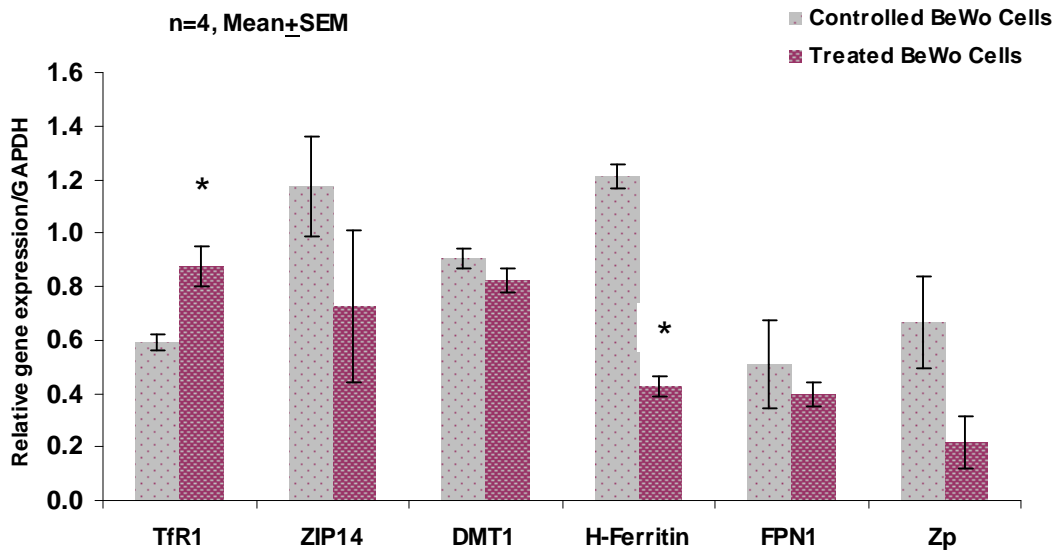
Figure 6.2 Effect of iron deficiency on iron transporter and storage gene expression in BeWo cells

*RNA was extracted from BeWo cells after induction of iron deficiency with 20µM DFO for 20 hours. mRNA expression of iron transporter and storage proteins were measured by RT-PCR. TfR1 was up-regulated after the treatment and H-Ferritin was down-regulated. ZIP14, DMT1, FPN1 and Zp expression remained unaltered. Bar represents Mean ± SEM of 4 samples and significance difference is denoted by * with p<0.05.*

6.3.1.3 Effect of hepcidin treatment on *ZIP14* mRNA expression

BeWo cells were treated with hepcidin for 2, 4, 6, 12, 24 and 48 hours and mRNA expression of *ZIP14* was measured by RT-PCR. The treatment did not alter the mRNA expression of *ZIP14* (Figure 6.3), as was the case for other iron transporters mRNA described shown in Chapter 4.3.2.2.
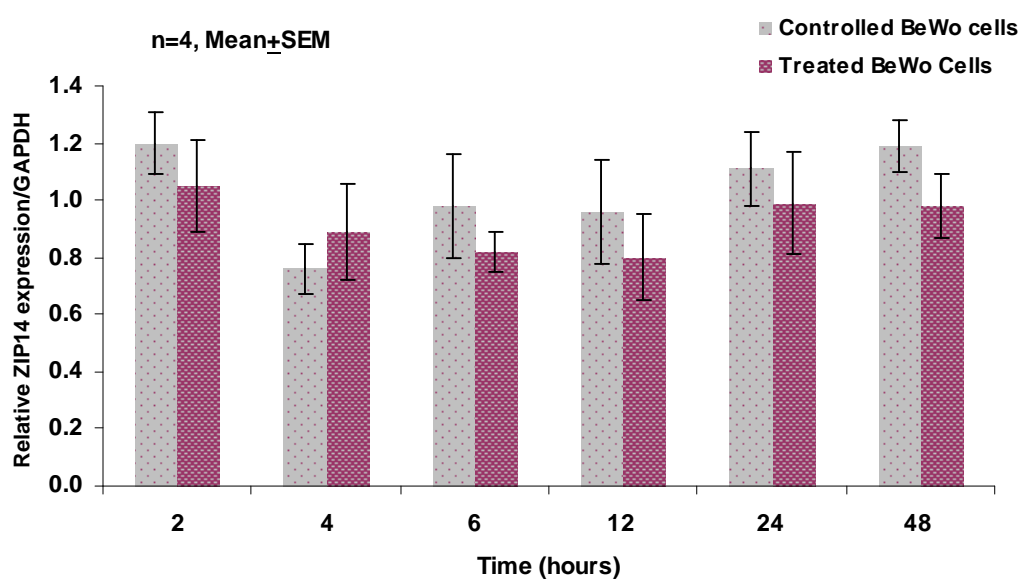
Figure 6.3 Effect of hepcidin treatment on *ZIP14* mRNA expression in BeWo cells

BeWo cells were treated with 1 μM hepcidin for 2 to 48 hours. Total RNA was isolated from BeWo cells and mRNA expression of ZIP14 was measured by RT-PCR which shows that the expression was not altered by time-dependent hepcidin treatment. Bar show mean + SEM of 4 samples.

6.3.1.4 Comparison of mRNA levels of *ZIP14* after transfection with *HFE*

BeWo cells stably transfected with *HFE* showed a reduction in the mRNA levels of *ZIP14* compared with WT BeWo cells.
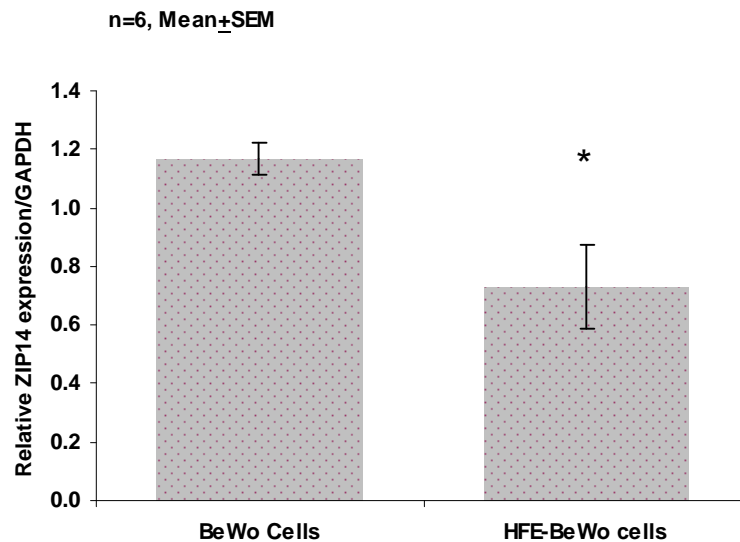
Figure 6.4 Comparison of ZIP14 mRNA levels after *HFE* transfection in BeWo cells

*ZIP14 mRNA expression was determined by RT-PCR and normalized to the internal GAPDH control in WT and stably transfected BeWo cells. ZIP14 expression was reduced significantly in the stably transfected cells. Bar graphs represent mean of 6 samples with SEM and * denotes significance difference at p<0.05.*

6.3.1.5 Effect of iron supplementation on *ZIP14* mRNA expression in *HFE* expressed BeWo cells

When WT and *HFE* transfected BeWo cells were provided NTBI in the form of Fe-NTA, ZIP14 gene expression increased significantly, Figure 6.5 (a) and (b)

(a)   **(b)**
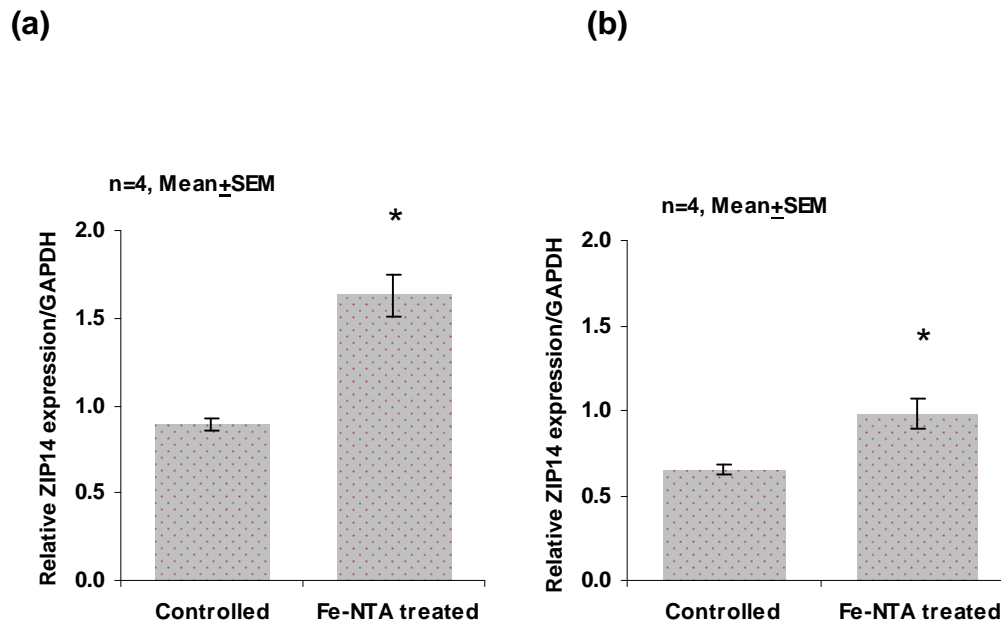
Figure 6.5 Effect of iron supplementation on ZIP14 mRNA expression

Total RNA was isolated from WT and HFE transfected BeWo cells after incubation with100µM Fe-NTA for 24 hours. ZIP14 expression was measured by RT-PCR and normalized to GAPDH. (a) In BeWo cells ZIP14 gene expression was increased after uptake of NTBI (Fe-NTA). (b) Similarly, BeWo cells transfected with HFE have increased ZIP14 expression after addition of Fe-NTA.

6.3.2 *In vivo* studies

6.3.2.1 Effect of maternal *Hfe* and dietary iron on placental mRNA expression of *ZIP14*

Maternal *Hfe* status did not seem to affect the mRNA expression of placental *ZIP14* when the pregnant dams were fed low or normal iron diets. When the dams were fed a diet with high iron content, HET pups from *Hfe* KO dams had significantly higher *ZIP14* placental gene expression as compared with HET pups from WT dams. Overall, the expression of the gene increased irrespective of the genotype of the dams when fed a high iron diet, Figure 6.6.
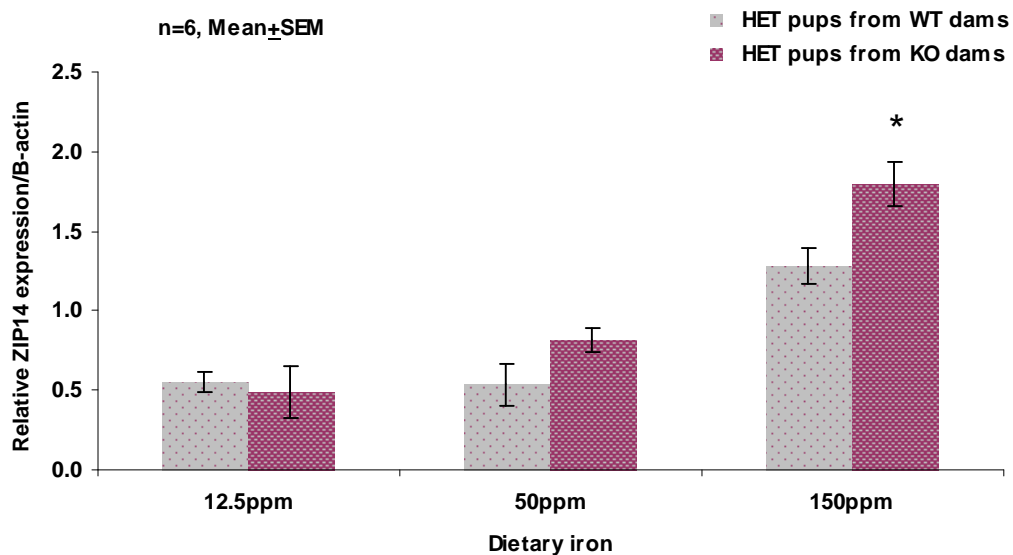
Figure 6.6 Effect of maternal genotype and dietary iron on placental *ZIP14* gene expression

*mRNA expression of placental ZIP14 was determined by RT-PCR. Only HET pups from HFE KO dams fed a high iron diet had significantly higher ZIP14 gene expression as compared with HET pups from WT dams. Bar represents Mean $\pm$ SEM of 6 samples and significance difference is denoted by * with p<0.05.*

6.3.2.2 Effect of foetal *Hfe* and dietary iron on placental mRNA expression of *ZIP14*

Foetal genotype and dietary iron of HET dams did not alter the mRNA expression of *ZIP14* in placental tissues. Overall, there was a higher trend in the *ZIP14* gene expression in *Hfe* KO pups from HET dams compared to those of WT dams, but the difference did not reach significance, Figure 6.7.
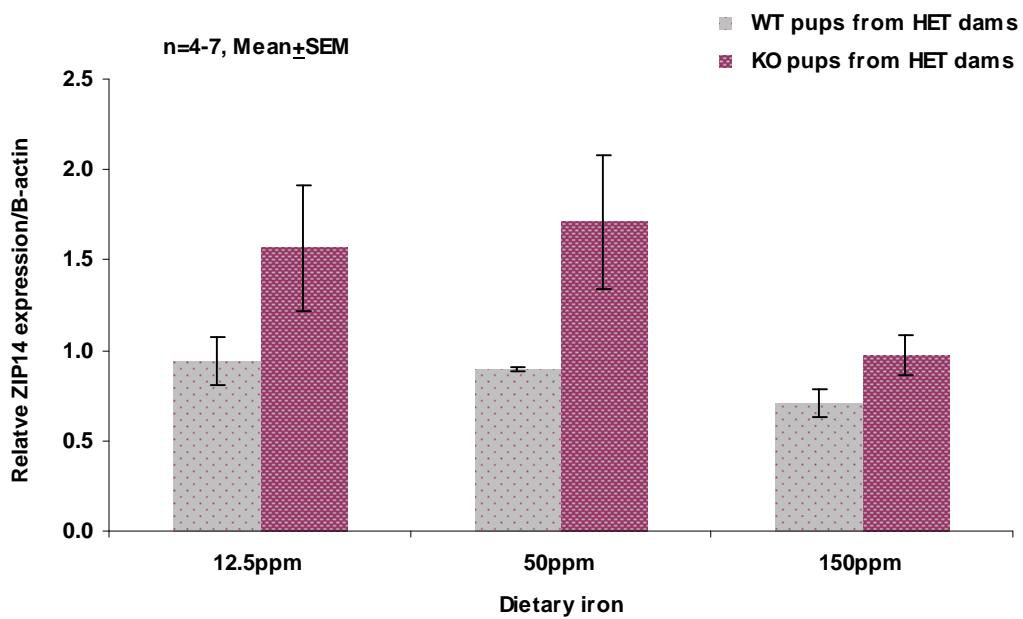
Figure 6.7 Effect of foetal genotype and dietary iron on placental *ZIP14* gene expression

The genotype of the foetus and dietary iron did not change the mRNA expression levels of ZIP14 in the placental tissues of WT and Hfe KO pups from HET dams. Bar graph shows mean ± SEM of n=4-7.

6.3.2.3 Effect of hepcidin on WT and *Hfe* KO placental *ZIP14* expression

As also shown in Chapter 4, sections 4.3.1.2 and 4.3.1.4, *ZIP14* expression has increased significantly in the placenta of WT and Hfe KO dams after hepcidin injection as compared with dams injected with saline, Figure 6.8.
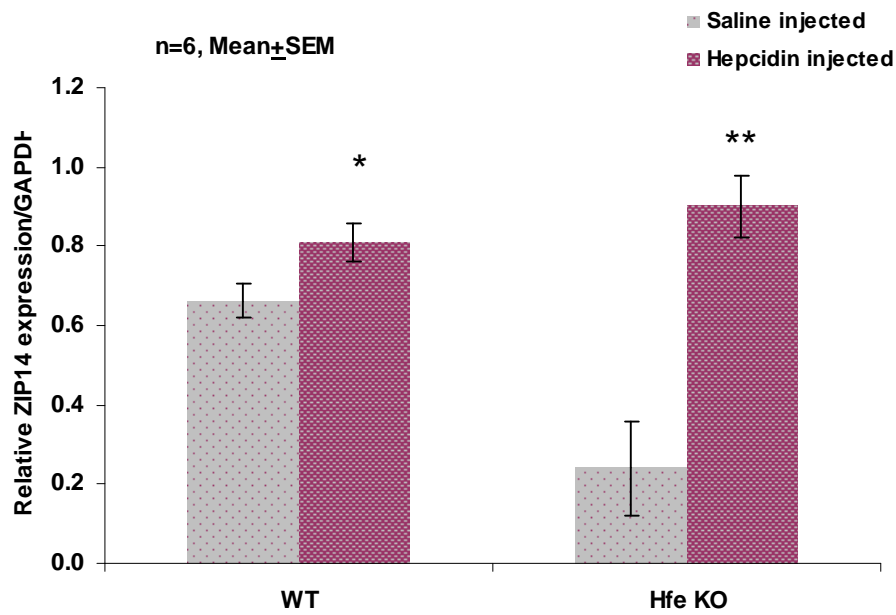
Figure 6.8 Effect of hepcidin treatment on placental *ZIP14* gene expression in WT and *Hfe* KO pregnant dams

*ZIP14 mRNA expression was analysed by RT-PCR. Hepcidin treatment increased the mRNA expression of ZIP14 in placenta of both WT and Hfe KO dams. Bars denotes mean ± SEM of 6 samples per group. * represents p < 0.05 and ** denotes p < 0.001 in hepcidin injected WT and Hfe KO mice compared to saline injected controls.*

6.4 Discussion

The developing human foetus has a huge demand for iron for its development, requiring about 250-300 mg during gestation. Iron transport is unidirectional from maternal to foetal blood. The placenta also functions as a storage depot for iron. The presence of transferrin receptors on the maternal side of the syncytiotrophoblasts plays a major role in transferrin-bound iron transport across the placenta (Johnson et al. 1980; Galbraith et al. 1980). Uptake of iron by placental syncytiotrophoblasts in the form of NTBI is not known. We used BeWo cells to determine the alternative pathways of iron uptake across syncytiotrophoblasts. These cells possess many of the key features of placenta, including the ability to polarise and secrete placental hormones.

Our results have shown that provision of NTBI resulted in increased mRNA expression of *ZIP14* and *H-Ferritin*. ZIP14, initially identified as a zinc transporter, transfection increased NTBI uptake in HEK293, HepG2 and Sf9 insect cells (Gao et al. 2008; Luizzi et al. 2006). *TfR1*, *DMT1*, *FPN1* and *Zp* expression did not alter after NTBI supplementation. We propose that *ZIP14* is involved in NTBI uptake in the cells and ferritin is involved in storing the excess iron. When the cells were made iron deficient *TfR1* expression was up-regulated as was also shown in previous studies conducted in BeWo cells (Gambling et al. 2001). However, in contrast with the *TfR1* up-regulated expression in iron deficiency, *H-Ferritin* expression was down-regulated, which is in agreement with previous findings. In order to understand the role of ZIP14 in the molecular mechanism of iron transport across placenta and its

regulation by *HFE* and hepcidin, we used BeWo cells transfected with *HFE*. Previous studies have shown that stable transfection of *HFE* in HepG2 cells reduced iron uptake compared to that of WT cells (Luizzi et al. 2006). Stable transfection of *HFE* in BeWo cells also reduced the mRNA level of *ZIP14* as compared with WT BeWo cells. When WT and *HFE* expressing BeWo cells were incubated with NTBI, up-regulation of *ZIP14* mRNA expression shows that it is regulated by iron.

Our *in vivo* results have shown that maternal *Hfe* status has affected *ZIP14* expression in placenta from *Hfe* KO dams fed a high iron diet. As discussed in Chapter 3.3.1.7 liver iron levels were high in foetuses of *Hfe* KO as compared with WT dams. This data suggests that maternal *Hfe* is controlling NTBI uptake, and is diet dependent. However, foetal genotype did not seem to play a role in NTBI transport across the placenta. Hepcidin administration did not alter the foetal liver iron levels derived from WT or *Hfe* KO dams, but increased the mRNA expression of *ZIP14* in the placenta.

Future studies to elaborate the role of ZIP14 in NTBI in placental syncytiotrophoblasts are needed.

Chapter 7

General Discussion

To determine the molecular mechanism of placental iron transport and its regulation by Hfe and hepcidin, this thesis posed the following questions:

1. How does maternal *Hfe* regulate iron transport across placenta?

2. How does foetal *Hfe* regulate maternal and foetal iron homeostasis?

3. Can hepcidin regulate placental iron transport?

4. What is the molecular mechanism of iron transport from mother to the foetus?

5. Is ZIP14 important in placental iron transport?

7.1 How does maternal *Hfe* regulate iron transport across placenta?

Knockout of functional maternal *Hfe* resulted in high iron concentration in the circulation of mothers and increased accumulation of iron in the livers when the dietary iron level was normal or high (Sections 3.3.1.1 and 3.3.12). However, when the mothers were fed an iron deficient diet, the dams maintained their body iron stores and less iron was transported to the foetus. The direct consequence of less iron transport across the placenta was low foetal body iron stores. Therefore to avoid the chances of iron deficiency anaemia in pregnant mothers and neonates and low birth weights, mothers should have good stores of iron in their livers. To further understand the transport of iron across the placenta, we measured the placental *TfR1*, *DMT1* and *FPN1* mRNA expression and found their up-regulation in placenta of HET pups derived from *Hfe* KO dams when fed normal or high iron diet. In support of this we have shown that HET pups from *Hfe* KO dams have a higher iron accumulation in their livers compared with HET pups from WT dams when the dams were fed normal or high iron diets (Section 3.3.1.7). Overall our results

show that adequate dietary iron during pregnancy plays an important role in maintaining iron homeostasis in both mother and foetus. Maternal *Hfe* expression is responsible for high iron in the maternal circulation and increased transfer of iron across the placenta.

7.2 How does foetal *Hfe* regulate maternal and foetal iron homeostasis?

Foetal *Hfe* was found to play a role in controlling iron homeostasis in both mother and foetus when the dams were fed a high iron diet. Our results have shown that the absence of *Hfe* in the foetus resulted in increased iron in the maternal circulation, high liver and spleen iron levels and more iron accumulation in foetal liver when the HET dams were fed a high iron diet (Sections 3.3.2.1, 3.3.2.2 and 3.3.2.6). Our data support previous studies showing foetal hepatic iron levels regulate iron transfer from mother to foetus. Up-regulation of DMT1+IRE expression in the placenta of *Hfe* KO pups from HET dams fed high iron diet may suggest an increase in transfer of iron to the foetus (Section 3.3.2.4). When the dietary iron intake in mother is low or normal, foetal *Hfe* has no affect in the regulation of iron homeostasis in the mother and foetus.

7.3 Can hepcidin regulate placental iron transport?

The hepcidin response is tissue or cell-specific. Our results have shown hepcidin decreasing serum iron levels in WT pregnant dams (Section 4.3.1.1) but the FPN1 expression in the placenta was up-regulated (Section 4.3.1.2). BeWo cells did not respond to hepcidin treatment. The results from the dams show that placenta plays an important role in protecting the foetus by

continuing the supply of nutrients at any cost. However, serum iron and transferrin saturation levels did not alter in *Hfe* KO pregnant dams after hepcidin treatment. Up-regulation of *ZIP14* and *DMT1+IRE* expression could indicate the uptake of iron by an alternative pathway. Localisation of Nramp1 to the cell junction shows that this protein may be involved in intercellular iron transport. FPN1 and TfR1 localisation on the membrane of BeWo cells clearly indicate their involvement in transporting the metal. A proposed model of regulation of placental iron transport by maternal and foetal HFE and hepcidin iron intake is shown in Figure 7.1.
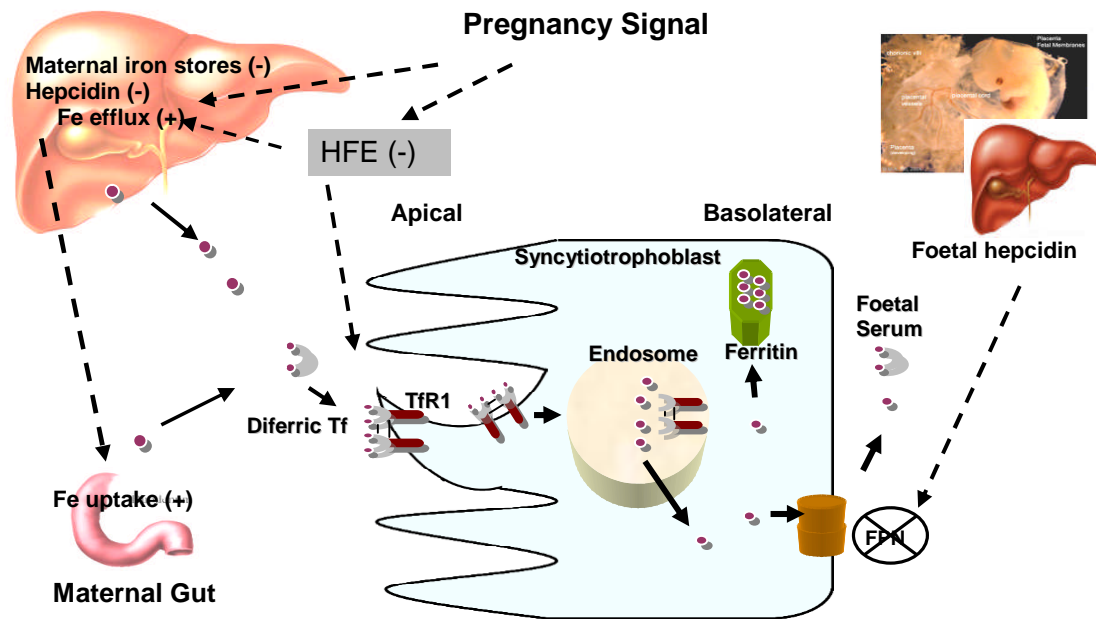
Figure 7.1 Proposed model of regulation of placental iron transport: Role of HFE and hepcidin.

A pregnancy signal (unknown) down-regulates hepcidin levels in liver during the last trimester of pregnancy. This decrease results in high duodenal iron uptake and high iron efflux from the liver into the maternal circulation. Maternal HFE can either directly or indirectly regulate iron transport across the placenta by increasing iron in the maternal circulation but this effect is diet dependent. The foetus regulates iron uptake from the placenta by regulating its liver hepcidin levels which can interact with iron exporter (FPN1). The coordinated interaction between hepcidin and FPN1 regulates foetal iron uptake from the mother, its storage in the liver and circulation in the body.

7.4 What is the molecular mechanism of iron transport from mother to the foetus?

In order to understand how iron transport is regulated across the placenta, it was crucial to determine the mechanism by which iron is transported from mother to foetus. This study demonstrated that TfR1, an iron uptake protein, was present on the cell membrane. DMT1 presence in the cell vesicles indicates that this protein is involved in iron efflux from the endosome into the cytosol of syncytiotrophoblasts as suggested before. FPN1 presence on the BeWo cell membrane and cytosol could suggest the involvement of this protein in transporting cytosol free iron to other organelles and efflux into foetal circulation.

7.5 Is ZIP14 important in placental iron transport?

Up-regulation of *ZIP14,* an NTBI transporter, after hepcidin injection during pregnancy indicates that this zinc transporter might be involved in NTBI iron transport across the placenta. This was further confirmed by its up-regulation when the BeWo cells were provided with NTBI. A proposed mechanism of placental iron transport is shown in Figure 7.2.
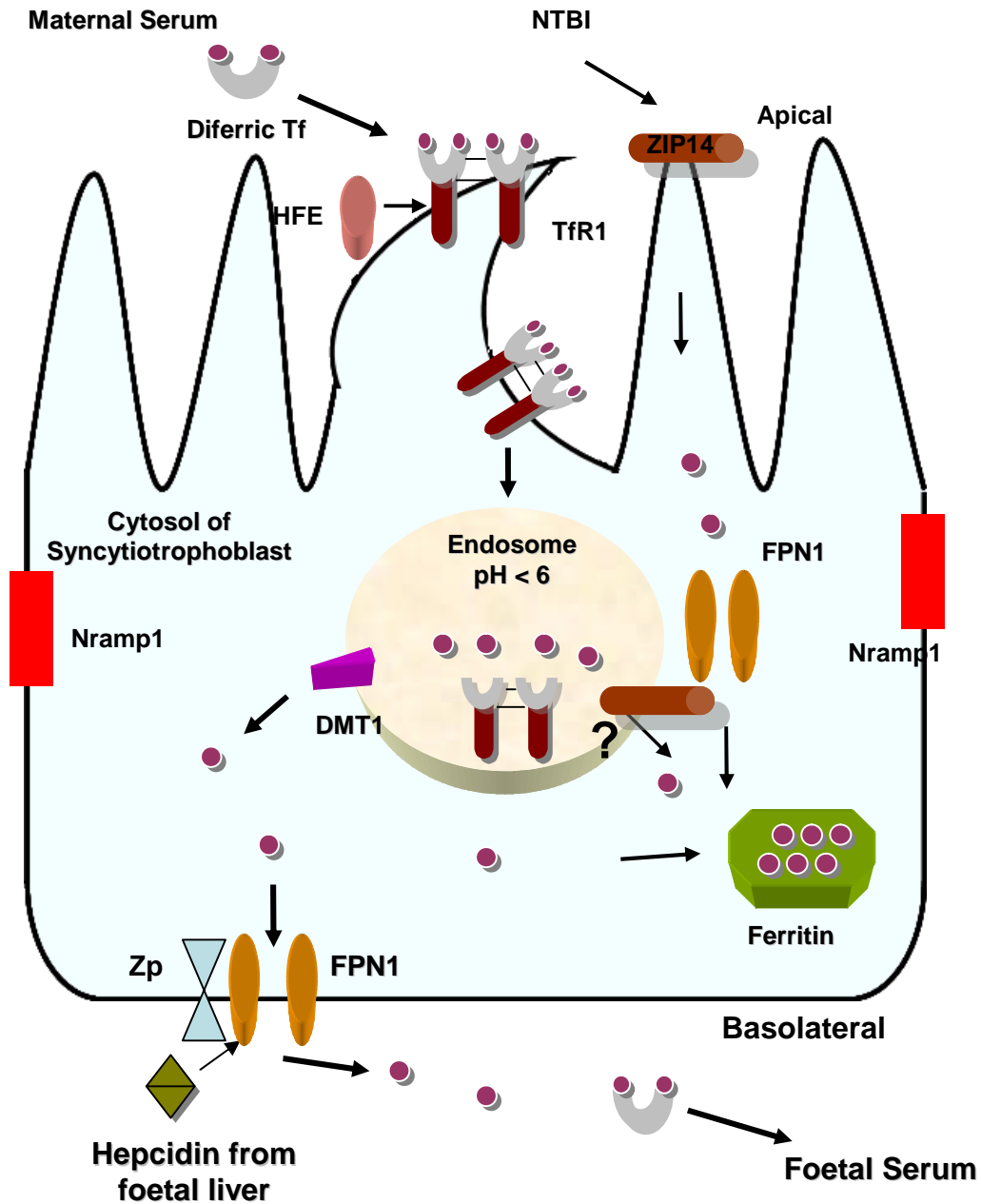
Figure 7.2 Proposed mechanism of placental iron transport

From the maternal circulation diferric-transferrin binds to TfR1 followed by its internalisation in the syncytiotrophoblasts. How iron enters the cytosol of the cells remains a mystery. In alternative pathway, iron as NTBI is taken up by ZIP14. Iron can be transported to other organelles or to be stored as ferritin, probably by FPN1. Iron is effluxed into the foetal circulation via FPN1 after oxidation by Zp.

7.6 Future work

In the present study, it was shown that hepcidin did not affect the iron transporter gene expression in BeWo cells. How hepcidin regulates iron uptake in BeWo cells is unknown. Therefore, further studies investigating the effect of hepcidin on iron uptake need to be performed. This will be done by growing BeWo cells on inserts to polarise them into apical (maternal side) and basolateral (foetal side) sides. The cells will be incubated with hepcidin from either maternal or foetal side and iron uptake using transferring-bound Fe^{55} or Fe^{59} will be measured by scintillation counting.

Localisation of DMT1 was unusual in BeWo cells. The role of DMT1 in placental iron transport in not clearly understood. To further understand the molecular mechanism of iron transport across placenta, the main iron transporter proteins (TfR1, DMT1, FPN1 and Hfe) will be localised in mice placental tissue. These proteins will be localised in BeWo cells after making them iron deficient, iron supplemented or hypoxic to determine their regulation.

Our results showed the presence of ZIP14 in mice placental tissues and BeWo cells. The localisation of ZIP14 in placental syncytiotrophoblasts is not known. Involvement of this zinc transporter in iron transport and regulation by HFE is not clearly understood. Therefore, in future studies, ZIP14 will be localised in BeWo cells or placental tissues by immunostaining using appropriate antibodies. *HFE* over-expressed BeWo cells will be provided with Fe^{55} or Fe^{59} labelled NTBI to measure iron uptake involving ZIP14. Over

expression of *HFE* resulted in decreased *ZIP14* expression so we expect

decreased NTBI uptake in BeWo cells.

Chapter 8

Bibliography

Abboud S, & Haile DJ. A Novel Mammalian Iron-regulated Protein Involved in Intracellular Iron Metabolism. *J. Biol. Chem*. 2000; 275, 199-206.

Ahmad KA, Ahmann JR, Migas MC, Waheed A, Britton RS, Bacon BR, Sly W S, & Fleming RE. Decreased liver hepcidin expression in the HFE knockout mouse. *Blood Cells Mol. Dis.* 2002; 29, 361-366.

Anderson BF, Baker HM, Norris GE, Rice DW, & Baker EN. Structure of human lactoferrin: crystallographic structure analysis and refinement at 2.8A resolution. *J. Mol. Biol.* 1989; 209, 711-734.

Anderson GJ, & Vulpe CD. Mammalian iron transport. *Cell Mol Life Sci.* 2009;*66:3241*–61*.

Andrew NC. Disorders of iron metabolism. *N. Engl. J. Med.* 1999; 341, 1986-1995.

Anita C, Chua G, Olynyk JK, Leedman PJ, & Trinder D. Nontransferrin-bound iron uptake by hepatocytes is increased in the Hfe knockout mouse model of hereditary hemochromatosis. *Blood* 2003; 11: 3872.

Bahram S, Gilfillan S, Ku¨hn LC, Moret R, Schulze JB, Lebeau A, & Schu¨mann K. Experimental hemochromatosis due to MHC class I HFE deficiency: immune status and iron metabolism. *Proceed. Nat. Acad. Sci. USA* 1999; 96: 13312–13317.

Bastin J, Drakesmith H, Ress M, Sargent I, & Townsend A. Localization of proteins of iron metabolism in the human placenta and liver. *British J. Haem.* 2006;134, 532-543.

Bergamaschi G, Bergamaschi P, Carlevati S, & Cazzola M. Transferrin receptor expression in the human placenta. *Haematologica* 1990;75, 220–223.

Bothwell TH, Charlton RW, Cook JD, & Finch CA. Iron metabolism in man. *Blackwell Sci. Oxford* 1979; 7-81.

Buus RM, & Boockfor FR. Transferrin expression by placental trophoblastic cells. Placenta. 2004;25, 45-52.

Carter AM. Animal models of human placentation—a review. *Placenta* 2007; 28 S41–S47.

Casanueva E. & Viteri FE. Iron and oxidative stress in pregnancy. *J. Nutr*. 2003;133: 1700S-1708S.

Cerneus DP, & Ende AV. Apical and basolateral transferring receptors in polarized BeWo cells recycle through separate endosomes. *J. Cell. Biol.* 1991;114,1149-1158.

Chaston T, Chung B, Mascarenhas M, Marks J, Patel B, Srai SK, & Sharp P. Evidence for differential effects of hepcidin in macrophages and intestinal epithelial cells. *Gut* 2008;57**:**374-382.

Chen H, Attieh ZK, Syed BA, Kuo YM, Stevens V, Fuqua BK, Andersen HS, Naylor CE, Evans RW, Gambling L, Danzeisen R, Haider MB, Usta J, Vulpe CD, & McArdle HJ. Identification of Zyklopen, a New Member of the Vertebrate Multicopper Ferroxidase Family, and Characterization in Rodents and Human Cells. *J. Nutr.* 2010; 140, 1728-1735.

Chen JM, Gao CJ, Chapman-Arvedson TL, & Enns CA. HFE modulates transferrin receptor 2 levels in hepatoma cells via interactions that differ from transferrin receptor 1-HFE interactions, *J. Biol. Chem.* 2007; 282, 36862–36870.

Choi JW, Im MW, & Pai SH. Serum transferrin receptor concentrations during normal pregnancy. *Clin. Chem.* 2000 46: 725–727.

Chung B, Chaston T, Marks J, Srai SK, & Sharp PA. Hepcidin Decreases Iron Transporter Expression in Vivo in Mouse Duodenum and Spleen and in Vitro in THP-1 Macrophages and Intestinal Caco-2 Cells. *J. Nutri.* 2009; 10.3945/jn.108.102905.

Cogswell ME, Parvanta I, Ickes L, Yip R, & Brittenham GM. Iron supplementation during pregnancy, anemia, and birth weight: a randomized controlled trial. *Am J Clin Nutr.* 2003;78(4):773-81**.**

Conrad ME, & Umbreit JN. Pathways of iron absorption. *Blood Cells Mol dis* 2002; 29, 336-345.

Crichton RR. Inorganic Biochemistry of iron. *Horwood, West Sussex*. 1991; 29-58.

Crowe C, Dandekar P, Fox N, Dhingra K, Bennet L, & Hanson MA. The effects of anemia on heart, placenta and body weight, and blood pressure in fetal and neonatal rats. *J. Physiol.* 1995;488, 515-519.

D, Fein E, Andriopoulos B, Pantopoulos K, & Gollan J. Alcohol metabolism-mediated oxidative stress down-regulates hepcidin transcription and leads to increased duodenal iron transporter expression. *J Biol Chem* 2006; 281:22974–22982.

Danzeisen R, & McArdle HJ**.** Copper and iron interactions in a placental cell line (BeWo) (Abstract). *Biochem Soc Trans* 1998; 26: S99.

De Domenico I, Ward DM, di Patti MC, Jeong SY, David S, Musci G, & Kaplan J. Ferroxidase activity is required for the stability of cell surface ferroportin in cells expressing GPI-ceruloplasmin. *EMBO J.* 2007*;26:2823–31.*

Donovan A, Brownlie A, Zhou Y, Shepard J, Pratt SJ, Moynihan J, Paw BH, Drejer A, Barut B, & Zapata A. Positional cloning of zebrafish ferroportin1 identifies a conserved vertebrate iron exporter. *Nature* 2000;403 776–781.

Donovan A, Lima CA, Pinkus JL, Pinkus GS, Zon LI, Robine S, et al. The iron exporter ferroportin/Slc40a1 is essential for iron homeostasis. *Cell Metabol.* 2005; 1, 191–200.

Dorak MT, Mackay RK, Relton CL, Worwood M, Parker L, & Hall AG. Hereditary hemochromatosis gene (HFE) variants are associated with birth weight and childhood leukemia risk. Pediatr Blood Cancer. 2009;15;53(7):1242-8.

Eaton BM, & Sooranna SR. In vitro modulation of L-arginine transport in trophoblast cells by glucose. *Eur J Clin Invest* 1998; 28: 1006–1010.

Eaton BM, & Sooranna SR. Transport of large neutral amino acids into BeWo cells. *Placenta* 2000; 21: 558–564.

Feder JN, Penny DM, Irrinki A, Lee VK, Lebron JA, Watson N, Tsuchihashi Z, Sigal E, Bjorkman PJ, & Schatzman RC. The hemochromatosis gene product complexes with the transferrin receptor and lowers its affinity for ligand binding. *Proc. Natl. Acad. Sci. USA.* 1998; 95, 1472-1477.

Fleming MD, Trenor CI, Su MA, Foernzler D, Beier DR, Dietrich WF, & Andrews NC. Microcytic anaemia mice have a mutation in Nramp2, a candidate iron transporter gene. *Nat. Genet.* 1997; 16, 383-386.

Fleming RE, Migas MC, Zhou X, Jiang J, Britton RS, Brunt EM, Tomatsu S, Waheed A, Bacon BR & Sly WS. Mechanism of increased iron absorption in murine model of hereditary hemochromatosis: Increased duodenal expression of the iron transporter DMT1. *Proc. Natl. Acad. Sci. USA* 1999; 96: 3143–3148.

Galbraith, G. M. P., Galbraith, R. M., and Faulk, W . P. *Placenta* 1980; 1,33-46.

Gambling L, Czopek A, Andersen HS, Holtrop G, Srai SK, et al. Fetal iron status regulates maternal iron metabolism during pregnancy in the rat. Am J Physiol Regul Integr Comp Physiol 2009;296: R1063–1070.

Gambling L, Danzeisen R, Fosset C, Andersen HS, Dunford S, Srai SK, & MCArdle HJ. Iron and copper interactions in development and the effect on pregnancy outcome. J. Nutr. 2003; 133, 1554S-6S.

Gambling L, Dunford S, Wallace DI, Zuur G, Solanky N, Srai SK, & McArdle HJ. Iron deficiency during pregnancy affects postnatal blood pressure in the rat. *J Physiol.* 2003; 5,552, 603-10.

Gambling L, Danzeisen R, Gair S, Lea RG, Charania Z, Solanky N, Joory KD, Srai SK, & McArdle HJ. Effect of iron deficiency on placental transfer of iron and expression of iron transport proteins in vivo and in vitro. *Biochem J* 2001; 15; 883-9.

Ganz T. Hepcidin and iron regulation, ten years later. *Blood* 2011; 01-258467.

Gao J, Zhao N, Knutson MD, & Enns CA. HFE inhibits non transferrin-bound iron uptake via downregulating Zip14 in HepG2 cells. *The FASEB Journal* 2008; 22: 304.

Georgieff MK, Wobken JK, Welle J, Burdo JR, & Connor JR. Identification and localization of divalent metal transporter-1 (DMT-1) in term human placenta. *Placenta.* 2000;21, 799-804.

Grantham-McGregor S, & Ani A. Review of studies on the effect of iron deficiency on cognitive development in children. *J Nutr.*2001;649S– 668S

Griffiths WJ, Sly WS, & Cox TM. Intestinal iron uptake determined by divalent metal transporter is enhanced in HFE-deficient mice with hemochromatosis. *Gastroenterol.* 2001; 1420-1429.

Gruenheid S, Cellier M, Vidal S, & Gros P. Identification and characterization of a second mouse Nramp gene. *Genomics,* 1995; *25*, 514–525.

Gruper Y, Bar J, Bachrach E & Ehrlich R. Transferrin Receptor Co-Localizes and Interacts With the Hemochromatosis Factor (HFE) and the Divalent Metal Transporter-1 (DMT1) in Trophoblast Cells. J Cell Physiol 2005; 204:901–912.

Gunshin H, Fujiwara Y, Custodio AO, DiRenzo C, Robine S, & Andrews NC. Slc11a2 is required for intestinal iron absorption and erythropoiesis but dispensable in placenta and liver. *J Clin Invest.* 2005; 115(5):1258–1266.

Gunshin H, Mackenzie B, Berger UV, Gunshin Y, Romero MF, Boron WF, Nussberger S, Gollan JL, & Hediger MA. Clonning and characterization of a mammalian proton-coupled metal-ion transporter. *Nature* 1997; 288, 482-488.

Guo WW. A dual-pathway ultrastructural model for the tight junction of rat proximal tubule epithelium. Am. J. Physiol Renal Physiol. 2003; 285: 241-257.

Hallberg L, Hulten L, & Gramatkovski E. Iron absorption from the whole diet in men: how effective is the regulation of iron absorption? *Am. J. Clin. Nutr.* 1997*;* 66:347-56.

Hallberg L. Iron balance in pregnancy. In: Gerge H (ed) Vitamins and minerals in pregnancy and lactation. Raven Press New York, 1988; 115-127.

Harris ZL, Durley AP, Man TK, & Gitlin JD. Targeted gene disruption reveals an essential role for ceruloplasmin in cellular iron efflux. *Proc Natl Acad Sci USA.* 1999;96:10812–7.

Harrison PM, & Arosio P. The ferritins: Molecular properties, iron storage function and cellular regulation. *Biochimica et Biophysica Acta* 1996; 1275, 161–203.

Harrison-Findik DD, Schafer D, Klein E & Timchenko NA. Alcohol Metabolism-mediated Oxidative Stress Down-regulates Hepcidin ranscription and Leads to Increased Duodenal Iron Transporter Expression. JBC 2006.

Harrison-Findik DD, Schafer D, Klein E, Timchenko NA, Kulaksiz H, Clemens Hunter HN, Fulton DB, Ganz T, & Vogel HJ. The solution structure of human hepcidin, a peptide hormone with antimicrobial activity that is involved in iron uptake and hereditary hemochromatosis. *J. Biol. Chem.* 2002;277, 37597-37603.

Johnson PM, Brown PJ, & Faulk WP. Reviews in Reproductiue Biology. Oxford University Press, Oxford 1980; (Finn, C. A., ed) 2; 1-40.

Johnson MB & Enns CA. Regulation of transferrin receptor 2 by transferrin: Jordan JB, Poppe L, Haniu M, Arvedson T, Syed R, Li V, Kohno H, Kim H, Schnier PD, Miranda LP, Cheetham J, & Sasu BJ. Hepcidin revisited, disulfide connectivity, dynamics, and structure. *J. Biol. Chem.* 2009;284:24155–67.

Jordanov J, Courtois-Verniquet F, Neuburger M, & Douce R. Structural investigations by extended X-ray absorption fine structure spectroscopy of the iron center of mitochondrial aconitase in higher plant cells. *J. Biol. Chem.* 1992; 267, 16775-16778.

Kanevsky VYu, Pozdnyakova LP, Katukov VYu, & Severin SE. Isolation of the transferrin receptor from human placenta. *Biochem. Mol. Biol. Int.*1997; 42, 309−314.

Kawabata H, Fleming RE, Gui D, Moon SY, Saitoh T, O'Kelly J. Expression of hepcidin is down-regulated in TfR2 mutant mice manifesting a phenotype of hereditary hemochromatosis. *Blood* 2005; 105, 376–381.

Kawabata H, Yang R, Hirama T, Vuong PT, Kawano S, Gombart AF, & Koeffler HP. Molecular cloning of transferrin receptor 2. A new member of the transferrin receptor-like family, *J. Biol. Chem.* 1999; 274**,** 20826–20832.

Kosman DJ. Fet3p, ceruloplasmin and the role of copper in iron metabolism*. Adv Protein Chem.* 2002*;*60*:*221–69*.*

Krause A, Neitz S, & Magert HJ, et al. LEAP-1, a novel highly disulphide-bonded human peptide, exhibits antimicrobial activity. *FEBS Lett.* 2000;480, 147-150.

Laftah AH, Ramesh B, Simpson RJ, Solanky N, Bahram S, Schu¨mann K, Debnam ES, & Srai KS. Effect of hepcidin on intestinal iron absorption in mice. *Blood* 2004 103: 3940-3944.

Lee PL, Gelbart T, West C, Halloran C, & Beutler E. The human Nramp2 gene: characterization of the gene structure, alternative splicing, promoter region and polymorphisms. *Blood Cells mol. Dis.* 1998; 24, 199-215.

Liu XB, Hill P, & Haile DJ. Role of the ferroportin iron-responsive element in iron and nitric oxide dependent gene regulation. *Blood Cells, Molecules, and Diseases* 2002; 29, 315–326.

Liuzzi JP, & Cousins RJ. Mammalian zinc transporters. *Annu. Rev. Nutr.* 2004; 24:151–72

Liuzzi JP, Aydemir F, Nam H, Knutson MD, & Cousins RJ. Zip14 (Slc39a14) mediates non-transferrin-bound iron uptake into cells. *Proc Natl Acad Sci USA.* 2006; 103(37): 13612–13617.

Luckwood JF, & Sherman AR. Spleen natural killer cells from iron-deficient rats pubs manifest an altered ability to be stimulated by interferam. *J. Nutr.* 1988; 118, 1558-1563.

Ludwiczek S, Theurl I, Muckenthaler MU, Jakab M, Mair SM, Theurl M, Kiss J, Paulmichl M, Hentze MW, Ritter M, & Weiss G. Ca^{2+} channel blockers reverse

iron overload by a new mechanism via divalent metal transporter-1. *Nat Med* 2007*;*13*(4):*448*-*454*.*

Mackenzie B, Shawki A, Ghio AJ, Stonehuerner JD, Zhao L, Ghadersohi S, Garrick LM, & Garrick MD. Calcium-channel blockers do not affect iron transport mediated by divalent metal-ion transporter-1. *Blood* 2010; 115, 4148-4149.

McArdle HJ, Douglas AJ, Bowen BJ, & Morgan EH. The mechanism of iron uptake by the rat placenta. *J. Cell physiology* 1985;124(3):446-50.

McCord JM. Iron, free radicals, and oxidative injury. *Semin Hematol* 1998; 35: 5–12.

McGregor JA. The genetic and functional characterisation of iron metabolism genes in health and disease. *London: University of London* 2006.

McKie AT, Barrow D, Latunde-Dada GO, Rolfs A, Sager G, & Mudaly. An iron-regulated ferric reductase associated with the absorption of dietary iron. *Science* 2001; 291:1755-1759.

McKie AT, Marciani P, Rolfs A, Brennan KW, & Barrow, D. A novel duodenal iron-regulated transporter, IREG1, implicated in the basolateral transfer of iron to the circulation. *Molecular Cell* 2000; 5, 299–309.

McKnight GS, Lee DC, Hemmaplardh D, Finch CA, & Palmiter RD. Transferrin gene expression. Effects of nutritional iron deficiency. Effects of nutritional iron deficiency. *J. Biol. Chem.* 1980; 255, 144-147.

Milman N. Iron and pregnancy—a delicate balance. *Ann Hematol.* 2006;85:559–565.

Moore KL, & Persaud TVN. The Developing Human: Clinically Oriented Embryology, 6th Ed., *Saunders, Philadelphia.* 1998

Mura C, Le GG, Jacolot S, & Ferec C. Transcriptional regulation of the human HFE gene indicates high liver expression and erythropoiesis coregulation. *FASEB J.* 2004;58, 373-382.

Nemeth E, Preza GC, Jung CL, Kaplan J, Warning AJ, & Ganz T. The N-terminus of hepcidin is essential for its interaction with ferroportin: structure-function study. *Blood.* 2006; 107, 328-333.

Nemeth E, Roetto A, Garozzo G, Ganz T, & Camaschella C. Hepcidin is decreased in TFR2 hemochromatosis*. Blood* 2005; 105, 1803–1806.

Nemeth E, Roetto A, Garozzo G, Ganz T, & Camaschella C. Hepcidin is decreased in TFR2 hemochromatosis*. Blood* 2005; 105, 1803–1806.

Nemeth E, Tuttle MS, Powelson J, Vaughn MB, Donovan A, Ward DM. Hepcidin regulates cellular iron efflux by binding to ferroportin and inducing its internalization. *Science* 2004: 306, 2090–2093.

Nicholas G, Viatte L, Lou DQ, Bennoun M, Beaumont C, Kahn A, Andrews N C, & Vaulont S. Constitutive hepcidin expression prevents iron overload in a mouse model of haemochromatosis. *Nat. Genet.* 2003; 34, 97-101.

Nicolas G, Bennoun M, Porteu A, et al. Severe iron deficiency anemia in transgenic mice expressing liver hepcidin. *Proc. Natl. Acad. Sci. USA.* 2002;99, 4596-4601.

Niessen CM. Tight Junctions/Adherens Junctions: Basic Structure and Function. *Journal of Investigative Dermatology* (2007) 127, 2525–2532.

O'Brien KO, Zavaleta N, Abrams SA, Caulfield LE. Maternal iron status influences iron transfer to the fetus during the third trimester of pregnancy. *Am J Clin Nutr.* 2003;77:924.

Orberger G, Fuchs H, Geyer R, Gessner R, Köttgen E, & Tauber R. Structural and functional stability of the mature transferrin receptor from human placenta. Arch Biochem Biophys 2001; 386(1):79-88.

Oudit GY, Trivieri MG, Khaper N, Liu PP, & Backx PH. Role of L-type Ca^{2+} channels in iron transport and iron-overload cardiomyopathy. *J Mol Med* 2006; 84:349–364.

Park CH, Valore EV, Warning AJ, & Ganz T. Hepcidin, a urinary antimicrobial peptide, exhibits antimicrobial activity. FEBS Lett. 2001;480, 147-150.

Parkkila S, Waheed A, Britton RS, Bacon BR, Zhou XY, Tomatsu S, Fleming R E, & Sly WS. Association of the transferrin receptor in human placenta with HFE, the protein defective in hereditary haemochromatosis. *Proc. Natl. Acad. Sci. U.S.A.* 1997a;94, 13198-13202.

Parkkila S, Waheed A, Britton RS, Feder JN, Tsuchihashi Z, Schatzman RC, Bacon BR, & Sly WS. Immunohistochemistry of HLA-H, the protein defective in patients with hereditary haemochromatosis, reveals unique pattern of expression in gastrointestinal tract. *Proc. Natl. Acad. Sci. U.S.A.* 1997b;94, 2534-2539.

Pattillo RA, & Gey GO. The establishment of a cell line of human hormone-synthesizing trophoblastic cells in vitro. *Cancer Res* 1968; 28: 1231–1236.

Pepe GJ, & Albrecht ED. Actions of placenta and fetal adrenal steroid hormones in primate pregnancy. *Endocrine Rev.* 1995;16, 608-648.

Petry CD, Wobken JD, McKay H, Eaton MA, Seybold VS, Johnson DE, & Georgieff MK. Placental transferrin receptor in diabetic pregnancies with

increased fetal iron demand. *American Journal of Physiology* 1994;267, E507–E514.

Pigeon C, Ilyin G, Courselaud B, Leroyer P, Turlin B, Brisot P, & Loreal O. A new mouse liver peptide hormone with antimicrobial peptide hepcidin, is overexpressed during iron overload. *J. Biol. Che.* 2001;276, 7811-7819.

Ponka P, Beaumont C, & Richardson DR. Function and regulation of transferrin and ferritin. *Semin. Hematol.* 1998; 35, 35-54.

Rehu M, Punnonen K, Ostland V, Heinonen S, Westerman M, Pulkki K, Sankilampi U. Maternal serum hepcidin is low at term and independent of cord blood iron status. *European J. Haemat.:* 2010; 85, 345–352.

Richardson DR, & Ponka P. The molecular mechanisms of the metabolism and transport of iron in normal and neoplastic cells. *Biochem. Biophys. Acta.* 1997; 1331,1-40.

Rivera, S., Nemeth, E., Gabayan, V., Lopez, M. A., Farshidi, D., & Ganz, T. Blood. 2005;106, 2196-2199.

Roetto A, Totaro A, Cazzola M, Cicilano M, Bosio S, D'Ascola G, Carella M, Zelante L, Kelly AL, Coz TM, Gasparini P & Camaschella C. Juvenile hemochromatosis locus maps to chromosome1q. *Am J Hum Genet* 1999; **64**: 1388–1393.

Rossant J, & Cross JC. Placental development: lessons from mouse mutants. *Nat Rev Genet* 2001;2**:** 538–548.

Rouault TA, & Cooperman S. Brain Iron Metabolism. *Semin Pediatr Neurol.* 2006; 13:142-148.

Schmidt PJ, Toran PT, Giannetti AM, Bjorkman PJ, & Anfrews NC. The Transferrin Receptor Modulates Hfe-Dependent Regulation of Hepcidin Expression. *Cell Metab.* 2008; 7, 205-214.

Schneider H. The role of the placenta in nutrition of the human fetus. *Am. J. Obstet. Gynecol.* 1991;164, 967–973.

Sharp P, & Kaila SKS. Molecular mechanisms involved in intestinal iron absorption. *World J. Gastroentrol.* 2007; 13, 4716-4724.

Sloan N, EA Jordan, & Winikoff B. Does Iron Supplementation Make a Difference? MotherCare Working Paper 15. Arlington, VA: John Snow, Inc. 1992.

Soewondo S. The effect of iron deficiency and mental stimulation on Indonesian children's cognitive performance and development. *Kobe. J. Med. Sci.* 1995;41, 1-17.

Tabuchi M, Tanaka N, Nishida-Kitayama J, Ohno H, & Kishi F. Alternative splicing regulates the subcellular localisation of divalent metal transporter 1 isoforms. *Mol. Biol. Cell.* 2000; 13. 4371-4387.

Taylor KM, & Nicholson RI. The LZT proteins; the new LIV-1 subfamily of zinc transporters. *Biochim. Biophys. Acta* 2003; 1611, 16-30.

Taylor RN, Newman ED, & Chen S. Forskolin and methotrexate induce an intermediate trophoblast phenotype in cultured human choriocarcinoma cells. *Am. J. Obstet. Gyneol.* 1991;164: 204-210.

Theil E. Ferritin: structure, gene regulation, and cellular function in animals, plants, and microorganisms. *Annual review of biochemistry* 1987; 56 (1): 289–315.

Trinder D, Morgan E, & Baker E. The mechanisms of iron uptake by fetal rat hepatocytes in culture. *Hepatology* 1986; 6(5):852-8.

Turkewitz P, & Harrison SC. Concentration of transferrin receptor in human placental coated vesicles. *J. Cell Biol.* 1989;108, 2127-2135.

Uppsten M, Davis J, Rubin H, Uhlin U. Crystal structure of the biologically active form of class Ib ribonucleotide reductase small subunit from Mycobacterium tuberculosis. *FEBS Lett.* 2004; 569, 117-122.

Vallee BL & Auld DS. Zinc coordination, function, and structure of zinc enzymes and other proteins. *Biochem* 1990; 29, 5647-59.

Vallee BL, Falchuk KH. The biochemical basis of zinc physiology. *Physiol Rev.* 1993;73, 79–118.

Van der Ende A, du Maine A, Simmons CF, Schwartz AL, & Strous GJ. Iron metabolism in BeWo chorion carcinoma cells. Transferrin-mediated uptake and release of iron. *J Biol Chem* 1987; 262: 8910–8916.

Van Eijk HG, & de Jong G. The physiology of iron, transferrin, and ferritin. *Biological Trace Element Research* 1992; 35,13-24.

Vanderpuye OA, Kelley LK, & Smith CH. Transferrin receptors in the basal plasma membrane of the human placental syncytiotrophoblasts. *Placenta.* 1986;7, 391-403.

Vardhana PA, & Illsley NP. Transepithelial glucose transport and metabolism in BeWo choriocarcinoma cells. *Placenta* 2002;23: 653–660.

Verrijt CE, Kroos MJ, Van Noort WL, Van Eijk HG, & Van Dijk JP. Binding of human isotransferrin variants to microvillous and basal membrane vesicles from human term placenta. *Placenta* 1997;18, 71–77.

Viatte L, Nicolas G, Lou DQ, Bennoun M, Lesbordes-Brion JC, Canonne-Hergaux F, Schönig K, Bujard H, Kahn A, Andrews NC, & Vaulont S. Chronic hepcidin induction causes hyposideremia and alters the pattern of cellular iron accumulation in hemochromatotic mice. *Blood* 2006; 107(7):2952-8.

Vujic Spasic M, Kiss J, Herrmann T, Galy B, Martinache S, Stolte J, Grone HJ, Stremmel W, Hentze MW, & Muckenthaler MU. Hfe acts in hepatocytes to prevent hemochromatosis. *Cell Metab.* 2008;7(2):173–178.

Vulpe CD, Kuo Y-M, Libina N, Askwith C, Murphy TL, Cowley L, Gitschier J, & Anderson G. Hephaestin, a ceruloplasmin homologue implicated in intestinal iron transport, is defective in the sla mouse. *Nat Genet.* 1999*;*21*:*195–9*.*

Waheed A, Parkkila S, Zhou XY, et al. Hereditary hemochromatosis: effect of C282Y and H63D mutations on association with beta-2-microglobulin, intracellular processing, and cell surface expression of the HFE protein in COS-7 cells. *Proc Natl Acad Sci USA* 1997; 94: 12384–12389.

Wallace DF, Summerville L, Lusby PE, & Subramaniam VN. First phenotypic description of transferrin receptor 2 knockout mouse, and the role of hepcidin. *Gut* 2005; 54, 980–986.

Watkins JA, Altazan JD, Elder P, Li CY, Nunez MT, & Cui XX. Kinetic characterization of reductant dependent processes in iron mobilization from endocytic vesicles. *Biochemistry* 1992; 31, 5820–5830.

Whittaker PG, Lind T, & William JG. Iron absorption during normal human pregnancy: a study using stable isotopes. *Br. J. Nutr.* 1991;65: 457-463.

WHO2009
http://www.who.int/nutrition/publications/micronutrients/weekly_iron_folicacid.pdf

Winfield ME. Electron transfer within and between haemoprotein molecules. *J. Mol. Biol.* 1965; 12, 600-611.

World Health Organization. Maternal mortality ratio and rates. 1991 Document WHO/MCH/MSM/91.6.

World Health Organization. The prevalence of anaemia in women: A tabulation of available information. 1992 Document WHO/MCH/MCM/92.2.

Yip R. Iron supplementation during pregnancy: is it effective? *American J. Clini. Nutri.* 1996; 63, 853-855.

Zhang AS, Xiong S, Tsukamoto H, & Enns CA. Localization of iron metabolism-related mRNAs in rat liver indicate that HFE is expressed predominantly in hepatocytes. *Blood* 2004; 103, 1509–1514.

Zhang DL, Senecal T, Ghosh MC, Ollivierre-Wilson H, Tu T, & Rouault TA. Hepcidin regulates ferroportin expression and intracellular iron homeostasis of erythroblasts. *Blood.* 2011; 8;118(10):2868-77.

Zhou XY, Tomatsu S, Fleming RE, Parkilla S, Waheed A, Jiang J, Fei Y, Brunt EM, Ruddy DA, Prass CE, Schatzman RC, Oneill R, Britton RS, Bacon BR, & Sly WS. HFE gene knockout produces mouse model of hereditary hemochromatosis. *Proc. Natl. Acad. Sci. USA.* 1998;95,2493-2497.

Appendix

Data presented in Figure 3.3 (a)

Serum iron levels (µg/dL) of WT pregnant dams

Diet	n	Mean	SD	SEM	p value with 50ppm	p value with 150ppm
12.5ppm	4	39.87	6.22	3.11	0.1031	0.0124
50ppm	5	72.16	33.55	15.00		0.2075
150ppm	4	104.42	36.03	18.02		

Serum iron levels (µg/dL) of KO pregnant dams

Diet	n	Mean	SD	SEM	p value with 50ppm	p value with 150ppm
12.5ppm	2	38.79	30.48	21.55	0.1059	0.0002
50ppm	4	108.82	41.27	20.63		0.0065
150ppm	5	181.53	11.14	4.98		

Data presented in Figure 3.3 (b)

Transferrin saturation (%) of WT pregnant dams

Diet	n	Mean	SD	SEM	p value with 50ppm	p value with 150ppm
12.5ppm	4	14.13	1.86	0.93	0.2608	0.0134
50ppm	5	20.68	6.26	3.13		0.9638
150ppm	4	24.41	4.10	2.40		

Tranferrin saturation (%) of KO pregnant dams

Diet	n	Mean	SD	SEM	p value with 50ppm	p value with 150ppm
12.5ppm	2	38.67	18.34	10.59	0.7032	0.6491
50ppm	3	39.00	7.03	4.06		0.01
150ppm	5	42.34	4.34	1.94		

Data presented in Figure 3.12 (a)

Serum iron levels (µg/dL) of HET pregnant dams

Diet	n	Mean	SD	SEM	p value with 50ppm	p value with 150ppm
12.5ppm	4	45.26	32.11	16.06	0.1425	0.0294
50ppm	5	77.25	26.18	11.71		0.2142
150ppm	5	100.80	28.94	12.94		

Data Presented in Figure 3.12 (b)

Transferrin saturation (%) of HET pregnant dams

Diet	n	Mean	SD	SEM	p value with 50ppm	p value with 150ppm
12.5ppm	4	28.00	14.26	7.13	0.6348	0.2853
50ppm	5	24.59	5.53	2.47		0.0192
150ppm	5	42.34	4.34	1.94		